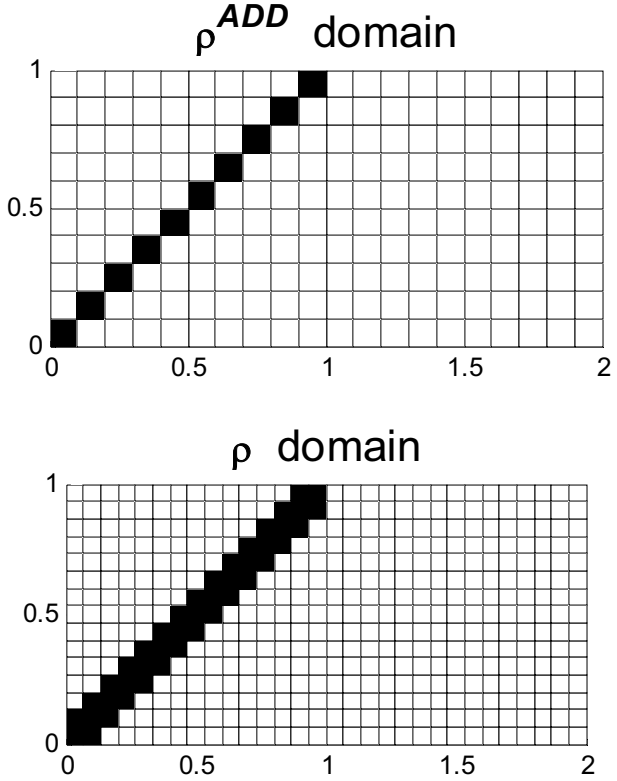

รูปที่ 6-5 การแปลงระหว่างกริด ADD และกริดของเอลิเมนต์พื้น $\rho^0 = \mathbf{0.25}$

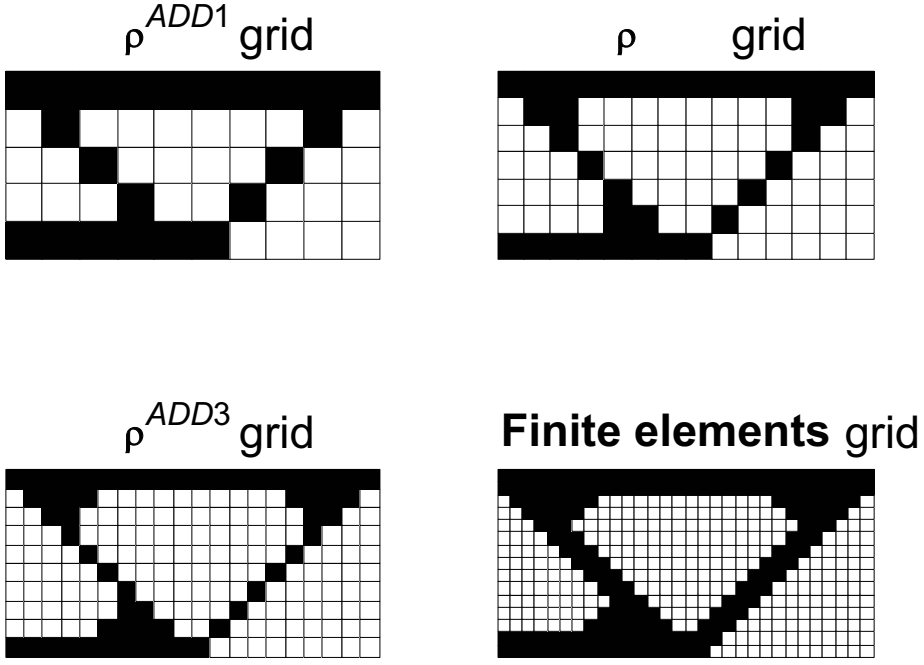

รูปที่ 6-6 การแปลงของตัวแปรออกแบบหลายระดับความชัด

6.4 ปัญหาทดสอบ

เพื่อทดสอบประสิทธิภาพของเทคนิคตัวแปรหลายระดับความชัด ได้ทำการตั้งปัญหาการออกแบบ 5 ปัญหาเพื่อเปรียบเทียบสมรรถนะในการค้นหาคำตอบของวิธีการที่นำเสนอ โดเมนออกแบบของปัญหาทั้ง 5 แสดงในรูปที่ 6-7 ถึง 6-11 ปัญหาออกแบบมีดังต่อไปนี้

OPT1

$$\min : \left(\frac{m}{m_{\max}}\right)^{w_1}\left(\frac{c}{c_{\max}}\right)^{w_2}$$

เมื่อ m = มวลของโครงสร้าง

c = ความอ่อนตัวของโครงสร้างเนื่องจากแรงกระทำภายนอก $\mathbf{F}$

w_1 และ w_2 คือเลขยกกำลังถ่วงน้ำหนักสำหรับมวลและความอ่อนตัวของโครงสร้าง

รูปที่ 6-7 แสดงโดเมนออกแบบของ OPT1 โครงสร้างทำจากวัสดุที่มีคุณสมบัติดังนี้ $E = 200\times10^9$ N/m^2 และ $\nu = 0.3$ เมื่อ $L = 2$ m และ $H = 1$ m แบบจำลองไฟไนท์เอลิเมนต์ที่ใช้คือเมมเบรนแบบ 4 จุดต่อ ค่าของ ρ^0 คือ 0.25 ความหนาของเอลิเมนต์ที่ i^{th} หมายถึงความหนาของแผ่นโครงสร้าง 0.00001 m ถ้า $\rho_i^e = 0$ นอกเหนือจากนั้นความหนาของแผ่นคือ 1 ค่าพารามิเตอร์ $m_{\max}$ คือมวลของโครงสร้างเมื่อ $\boldsymbol{\rho}^e = \mathbf{1}$ ค่าของ $c_{\max}$ คือค่าความอ่อนตัวของโครงสร้างเมื่อ $\boldsymbol{\rho}^e = \mathbf{0}$ เลขยกกำลังของมวลและความอ่อนตัวมีค่าเป็น $w_1 = 1$ และ $w_2 = 1$

รูปที่ 6-8 และ 6-9 แสดงโครงสร้างสำหรับปัญหาการออกแบบ OPT2 และ OPT3 ตามลำดับ เงื่อนไขต่างๆของปัญหาการหาโทโปโลยีเหมาะสมสุด OPT2 และ OPT3 ใช้เงื่อนไขเดียวกันกับปัญหา OPT1 ถ้าไม่ระบุเป็นอย่างอื่น ค่า h สำหรับสะพาน 2 มิติมีค่าเป็น 1/15 m

OPT4

$$\min : \left(\frac{m}{m_{\max}}\right)^{w_1}\left(\frac{\lambda}{\lambda_{\max}}\right)^{w_2}$$

เมื่อ m = มวลของโครงสร้าง

λ = ค่าไอเกนค่าแรกของโครงสร้าง

w_1 และ w_2 คือเลขยกกำลังของมวลและค่าไอเกนตามลำดับ

โดเมนการออกแบบของปัญหาทดสอบ OPT4 แสดงในรูปที่ 6-10 ส่วนพารามิเตอร์ $m_{\max}$ และ $\lambda_{\max}$ คือค่ามวลและค่าไอเกนของโครงสร้างเมื่อ $\boldsymbol{\rho}^e = \mathbf{1}$ เงื่อนไขต่างๆที่ใช้ใน OPT4 มีค่าเช่นเดียวกับ OPT3 ถ้าไม่มีการระบุเป็นอย่างอื่น ค่าเลขยกกำลังสำหรับมวลและค่าไอเกนมีค่าเป็น $w_1 = 2$ และ $w_2 = 1$ ตามลำดับ

OPT5

$$\min : \left(\frac{m}{m_{\max}}\right)^{w_1}\left(\frac{c_1}{c_{1,\max}}\right)^{w_2}\left(\frac{c_2}{c_{2,\max}}\right)^{w_3}$$

เมื่อ m = มวลของโครงสร้าง

c_1 = ความอ่อนตัวของโครงสร้างเนื่องจากแรงกระทำภายนอก $\mathbf{F}_1$

c_2 = ความอ่อนตัวของโครงสร้างเนื่องจากแรงกระทำภายนอก $\mathbf{F}_2$

w_1, w_2 และ w_3 คือค่าเลขยกกำลังของมวลและความอ่อนตัวของโครงสร้างเนื่องจากแรงภายนอกกรณีของ $\mathbf{F}_1$ และ $\mathbf{F}_2$ ตามลำดับ

ในปัญหาทดสอบนี้ โครงสร้างรับภาระสองชุดที่แตกต่างกันคือ $\mathbf{F}_1$ และ $\mathbf{F}_2$ ส่วนโดเมนการออกแบบแสดงในรูปที่ 6-11 เงื่อนไขการออกแบบอื่นๆมีค่าเช่นเดียวกันกับเงื่อนไขของ OPT1 พารามิเตอร์ $m_{\max}$ คือมวลของโครงสร้างเมื่อ $\boldsymbol{\rho}^e = \mathbf{1}$ ค่าของ $c_{1,\max}$ และ $c_{2,\max}$ คือค่าความอ่อนตัวของโครงสร้างเนื่องจากกรณีของภาระ $\mathbf{F}_1$ และ $\mathbf{F}_2$ ตามลำดับเมื่อ$\boldsymbol{\rho}^e = \mathbf{0}$ ค่าของเลขยกกำลังคือ $w_1 = 5$, $w_2 = 1$ และ $w_3 = 1$

กริดของไฟไนท์เอลิเมนต์มีความละเอียดเป็น 30×15 เอลิเมนต์ ใช้กริดของตัวแปรออกแบบ 3 ระดับซึ่งมีความละเอียดเป็น 10×5, 14×7 และ 20×10 เอลิเมนต์ ดังแสดงในรูปที่ 6-6 เทคนิคการซ่อมโครโมโซมที่นำเสนอใน [86] ถูกดำเนินการในกรณีที่ผลเฉลยโทโปโลยีถูกแยกออกมากกว่าหนึ่งชิ้น

เพื่อสามารถระบุจำนวนรอบของการคำนวณให้กับกริดของตัวแปรออกแบบที่หลากหลาย ทำการหาค่าเหมาะสมสุดของปัญหาการออกแบบ OPT1 5 ครั้ง โดยใช้ กริด 10×5 ใช้จำนวนรอบของการคำนวณ 120 รอบและขนาดของ n_s คือ 5 รูปที่ 6-12 แสดงประวัติการค้นหาค่าเหมาะสมสุดดังกล่าว เราสามารถสังเกตได้ว่า ในรอบของการคำนวณต้นๆ ค่าฟังก์ชันเป้าหมายลดลงอย่างรวดเร็ว จากนั้นหลังจากรอบการคำนวณที่ 20 การหาคำตอบของ SA จะมีพัฒนาการน้อยมาก รูปที่ 6-13 แสดงประวัติการหาค่าเหมาะสมสุดของ OPT1 โดยใช้กริด 14×7 5 ครั้ง การหาผลเฉลยในกรณีนี้จะคงที่ที่รอบของการคำนวณที่ 40-60 โดยประมาณ รูปที่ 6-14 แสดงประวัติการหาค่าเหมาะสมสุดของ OPT1 โดยใช้ SA และกริดของตัวแปรออกแบบ 20×10 5 ครั้ง จากการสังเกตค่าฟังก์ชันเป้าหมายจะคงที่เมื่อถึงจำนวนรอบที่ 120 โดยประมาณ จากการทดสอบนี้พบว่า ยิ่งระดับความชัดหรือระดับความละเอียดของตัวแปรออกแบบมีค่าสูงมาก SA ยิ่งใช้จำนวนรอบของการคำนวณมากเพื่อสามารถเข้าถึงจุดเหมาะสมสุดได้ อย่างไรก็ตามเป็นที่ทราบกันดีว่าการใช้ตัวแปรที่ระดับความชัดสูงกว่าย่อมส่งผลให้ได้โทโปโลยีที่ดีกว่าถ้าวิธีหาค่าเหมาะสมสุดมีประสิทธิภาพมากพอ

จากการศึกษาขั้นต้นนี้ทำให้ได้จำนวนรอบของการคำนวณสูงสุดของแต่ละกริดของตัวแปรออกแบบ ADD การทดลองขั้นต่อไปมีเงื่อนไขในการรันการหาค่าเหมาะสมสุดดังรายละเอียดในตารางที่ 6-1 ตัวแปรออกแบบ DSV1, DSV2 และ DSV3 ใช้กริด ADD หนึ่งระดับความชัด ในขณะที่ DSV4, DSV5 และ DSV6 คือตัวแปรออกแบบหลายระดับความชัดดังรายละเอียด เพื่อให้ง่ายในการอธิบาย SA ที่ใช้ตัวแปรชุด DSV*i* จะเรียกว่า SA*i* ดังแสดงในตาราง

SA แต่ละวิธีถูกใช้หาผลเฉลยเหมาะสมสุดของปัญหาต่างๆ 5 ครั้ง จำนวนผลเฉลยลูก (children) ในแต่ละรอบการคำนวณมีค่าเป็น $n_s = 5$ เมื่อรัน SA ครบรอบของการคำนวณสูงสุดแล้ว $\mathbf{x}_{best}$ ในรอบของการคำนวณสุดท้ายถือว่าเป็นผลเฉลยเหมาะสมสุด

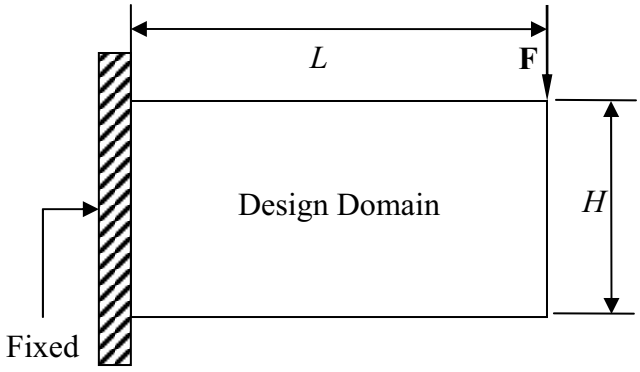

รูปที่ 6-7 คานยื่น

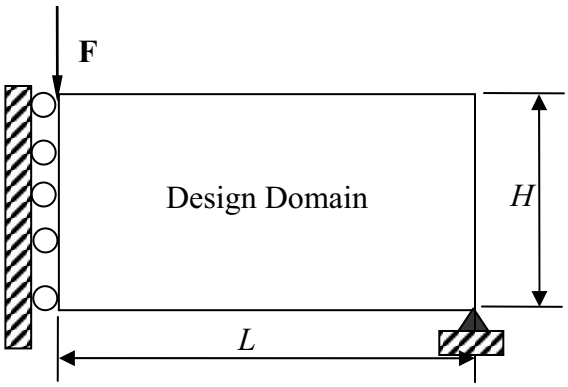

รูปที่ 6-8 คาน MBB

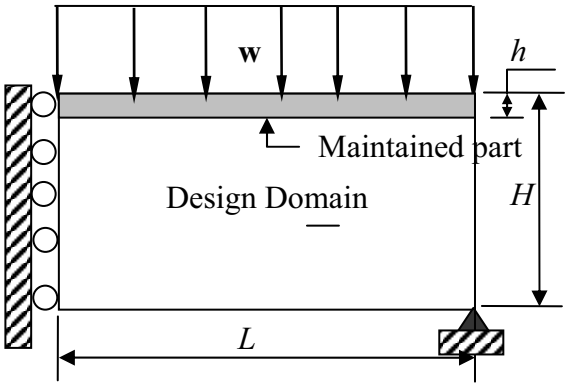

รูปที่ 6-9 สะพานในสองมิติ

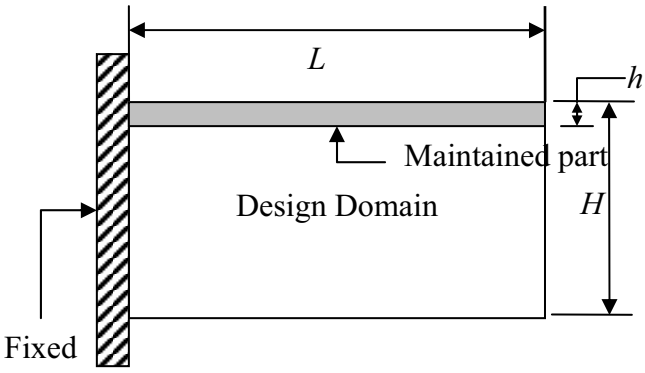

รูปที่ 6-10 คานยื่นสำหรับ OPT4

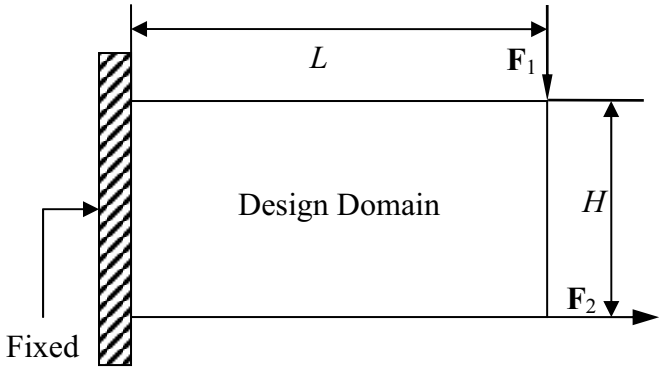

รูปที่ 6-11 คานยื่นสำหรับรับภาระสองกรณี OPT5

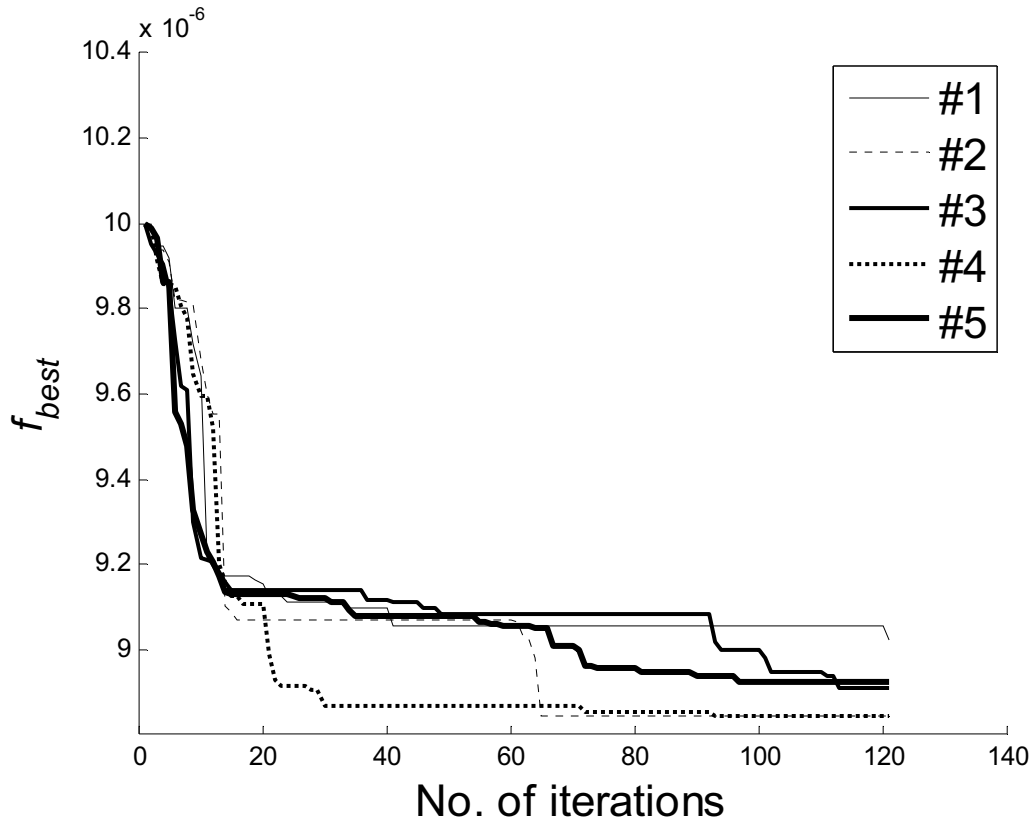

รูปที่ 6-12 ประวัติการค้นหาผลเฉลยของ OPT1 ที่ใช้ความละเอียดของกริดเป็น 10×5

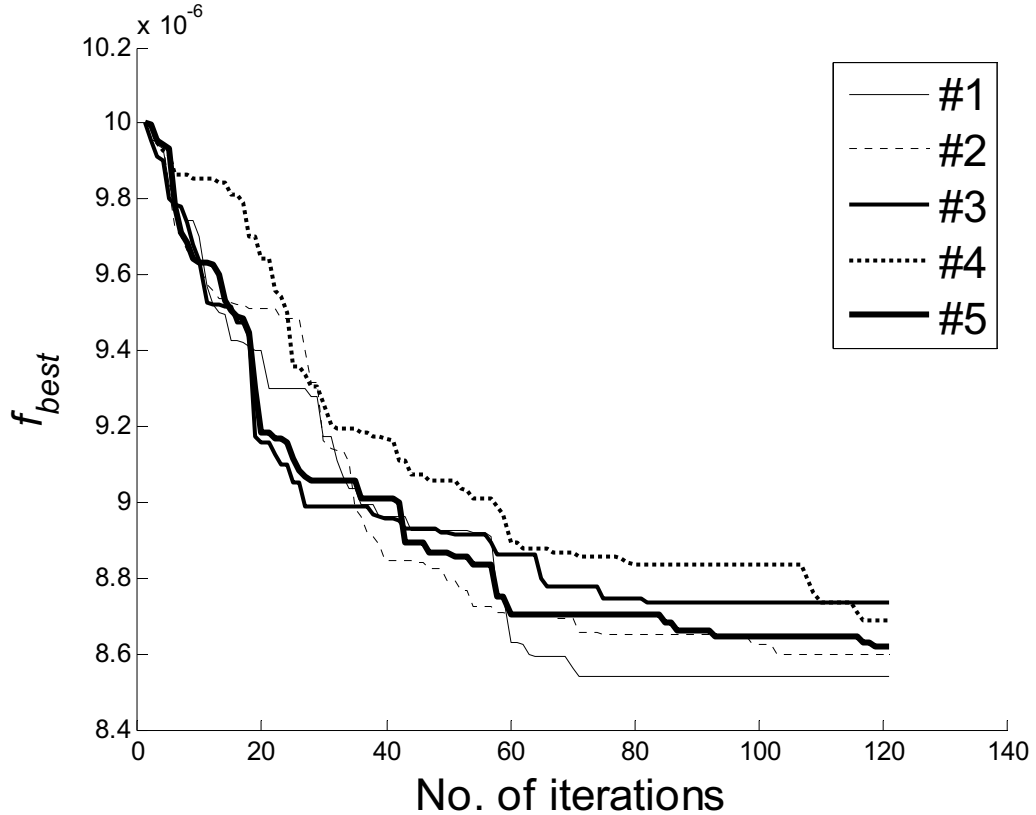

รูปที่ 6-13 ประวัติการค้นหาผลเฉลยของ OPT1 ที่ใช้ความละเอียดของกริดเป็น 14×7

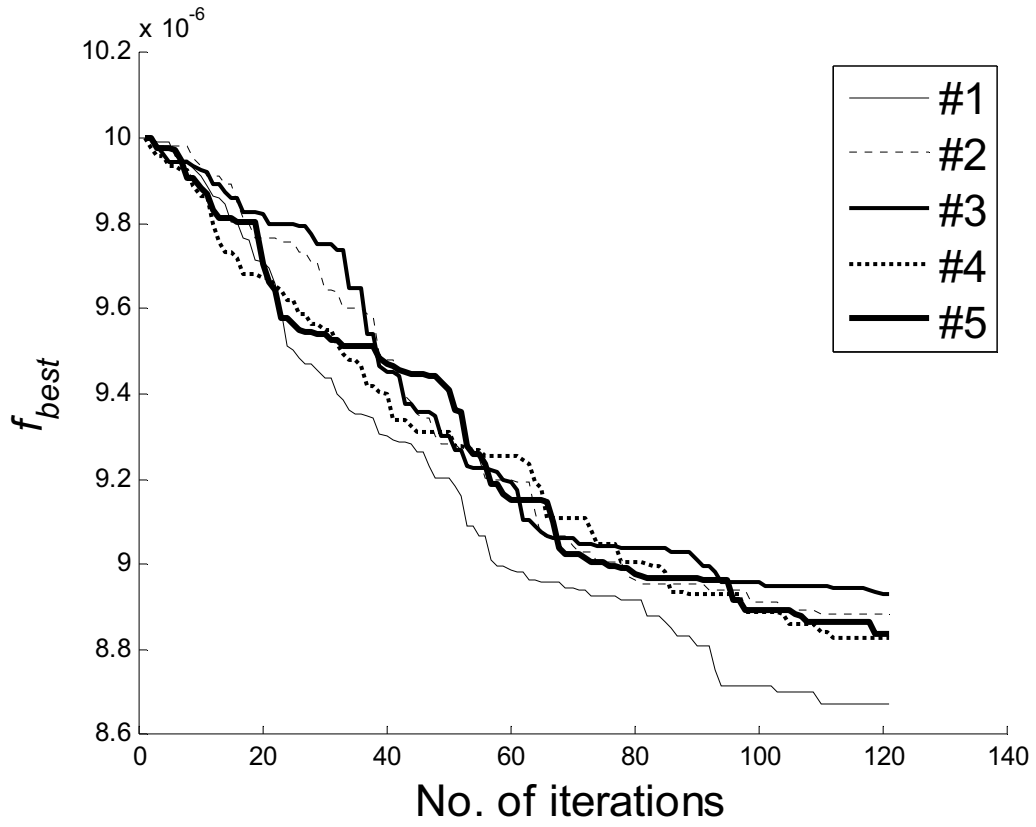

รูปที่ 6-14 ประวัติการค้นหาผลเฉลยของ OPT1 ที่ใช้ความละเอียดของกริดเป็น 20×10

ตารางที่ 6-1 เงื่อนไขการออกแบบ

DSV	**ADD grid resolutions**	**No. of iterations**	**Population size**	**SA strategies**
DSV1	10×5	120	10	SA1
DSV2	14×7	120	10	SA2
DSV3	20×10	120	10	SA3
DSV4	10×5,14×7	40,80	10	SA4
DSV5	10×5,20×10	40,80	10	SA5
DSV6	10×5,14×7,20×10	20,40,60	10	SA6

6.5 ผลการหาค่าเหมาะสมสุดและการเปรียบเทียบสมรรถนะ

รูปที่ 6-15 แสดงโทโปโลยีผลการออกแบบของปัญหาทดสอบ OPT1 ผลการเปรียบเทียบค่าฟังก์ชันเป้าหมายของวิธีต่างๆแสดงในรูปที่ 6-16 รูปที่ 6-17 แสดงโทโปโลยีของโครงสร้างที่ได้จากวิธี SIMP และ OCM ที่อัตราส่วนของมวลต่อมวลเริ่มต้นเป็น r = 0.4 0.5 และ 0.6 จากรูปที่ 6-16 ชุดตัวแปรออกแบบที่ดีที่สุดคือ DSV6 ส่วนชุดตัวแปรที่ดีที่สุดอันดับสองคือ DVS4 กรณีศึกษานี้แสดงให้เห็นว่า การใช้งานตัวแปรออกแบบหลายระดับความชัดช่วยเพิ่มสมรรถนะในการหาคำตอบเหมาะสมสุดของ SA โทโปโลยีที่ได้จากการใช้ DSV6 สามารถเปรียบเทียบได้กับโทโปโลยีที่ได้จากวิธี SIMP

รูปที่ 6-18 แสดงโทโปโลยีผลการออกแบบของปัญหาทดสอบ OPT2 ที่ได้จากการใช้ SA หลากหลายวิธี ผลการเปรียบเทียบค่าฟังก์ชันเป้าหมายของวิธีต่างๆแสดงในรูปที่ 6-19 รูปที่ 6-20 แสดงโทโปโลยีของโครงสร้างที่ได้จากวิธี SIMP และ OCM ที่อัตราส่วนของมวลต่อมวลเริ่มต้นเป็น r = 0.4 0.5 และ 0.6 จากรูปที่ 6-19 ชุดตัวแปรออกแบบที่ดีที่สุดคือ DSV6 ส่วนชุดตัวแปรที่ดีที่สุดอันดับสองคือ DVS4 ในขณะที่ชุดตัวแปรออกแบบที่ดีที่สุดอันดับที่สามได้แก่ DSV5 โทโปโลยีที่ได้จากการใช้ตัวแปรออกแบบหลายระดับความชัดสามารถเปรียบเทียบได้กับโทโปโลยีที่ได้จากวิธี SIMP

รูปที่ 6-21 แสดงโทโปโลยีผลการออกแบบของปัญหาทดสอบ OPT3 ผลการเปรียบเทียบค่าฟังก์ชันเป้าหมายของวิธีต่างๆแสดงในรูปที่ 6-22 รูปที่ 6-23 แสดงโทโปโลยีของโครงสร้างที่ได้จากวิธี SIMP และ OCM ที่อัตราส่วนของมวลต่อมวลเริ่มต้นเป็น r = 0.4 0.5 และ 0.6 จากรูปที่ 6-22 ชุดตัวแปรออกแบบที่ดีที่สุดคือ DSV5 ส่วนชุดตัวแปรที่ดีที่สุดอันดับสองคือ DVS4 และ DSV6

รูปที่ 6-24 แสดงโทโปโลยีผลการออกแบบของปัญหาทดสอบ OPT4 ที่ได้จากการใช้ SA หลากหลายวิธี ผลการเปรียบเทียบค่าฟังก์ชันเป้าหมายของวิธีต่างๆแสดงในรูปที่ 6-25 รูปที่ 6-26 แสดงโทโปโลยีของโครงสร้างที่ได้จากวิธี SIMP และ OCM ที่อัตราส่วนของมวลต่อมวลเริ่มต้นเป็น r = 0.4 0.5 และ 0.6 จากรูปที่ 6-25 ชุดตัวแปรออกแบบที่ดีที่สุดคือ DSV6 ส่วนชุดตัวแปรที่ดีที่สุดอันดับสองคือ DVS4 โทโปโลยีที่ได้จากการใช้ตัวแปรออกแบบหลายระดับความชัดสามารถเปรียบเทียบได้กับโทโปโลยีที่ได้จากวิธี SIMP

รูปที่ 6-27 แสดงโทโปโลยีผลการออกแบบของปัญหาทดสอบ OPT2 ที่ได้จากการใช้ SA หลากหลายวิธี ผลการเปรียบเทียบค่าฟังก์ชันเป้าหมายของวิธีต่างๆแสดงในรูปที่ 6-28 รูปที่ 6-29 แสดงโทโปโลยีของโครงสร้างที่ได้จากวิธี SIMP และ OCM ที่อัตราส่วนของมวลต่อมวลเริ่มต้นเป็น r = 0.4 0.5 และ 0.6 จากรูปที่ 6-28 ชุดตัวแปรออกแบบที่ดีที่สุดคือ DSV6 ส่วนชุดตัวแปรที่ดีที่สุดอันดับสองคือ DVS5 โทโปโลยีที่ได้จากการใช้ตัวแปรออกแบบหลายระดับความชัดสามารถเปรียบเทียบได้กับโทโปโลยีที่ได้จากวิธี SIMP

โดยรวมแล้ว วิธีที่ดีที่สุดคือ SA6 ซึ่งใช้ตัวแปรออกแบบ DSV6 ซึ่งมีกริดตัวแปรออกแบบสามระดับความละเอียด จากการศึกษานี้พบว่าการประยุกต์ใช้ตัวแปรออกแบบหลายระดับความชัดส่งผลให้วิธีวิวัฒนาอย่างเช่น SA มีประสิทธิภาพในการหาผลเฉลยเหมาะสมสุดมากขึ้น อย่างไรก็ตามตัวแปรออกแบบหลายระดับความชัดยังมีจุดที่ต้องปรับปรุงอีกมาก เช่น การได้มาซึ่งจำนวนรอบของการคำนวณสำหรับแต่ละกริดของตัวแปรออกแบบจำเป็นต้องทดสอบก่อนจึงจะสามารถตั้งค่าที่เหมาะสมได้

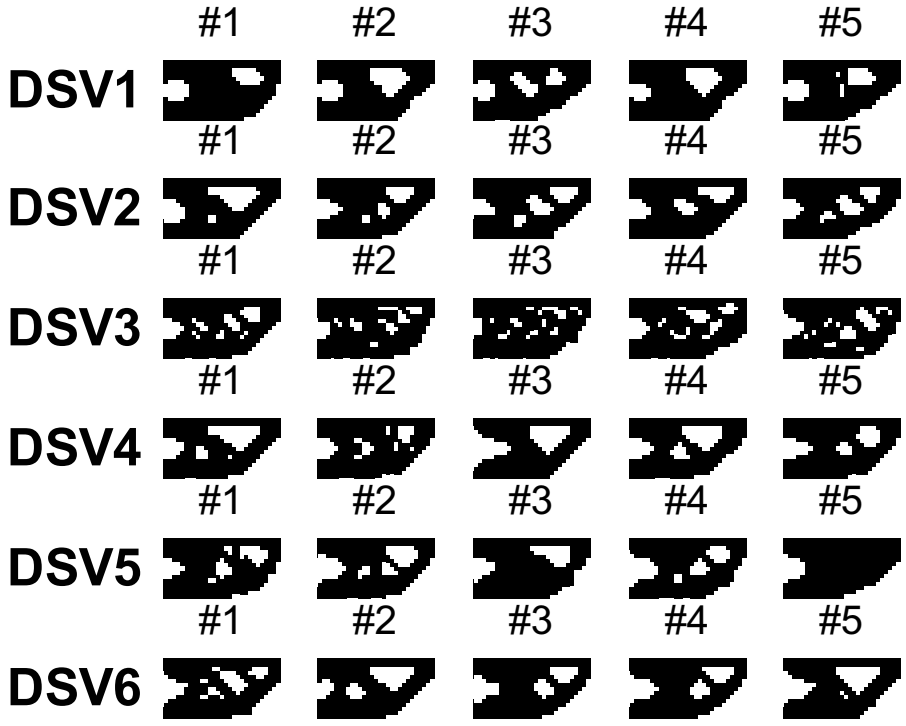

รูปที่ 6-15 ผลเฉลยเหมาะสมสุดของ OPT1

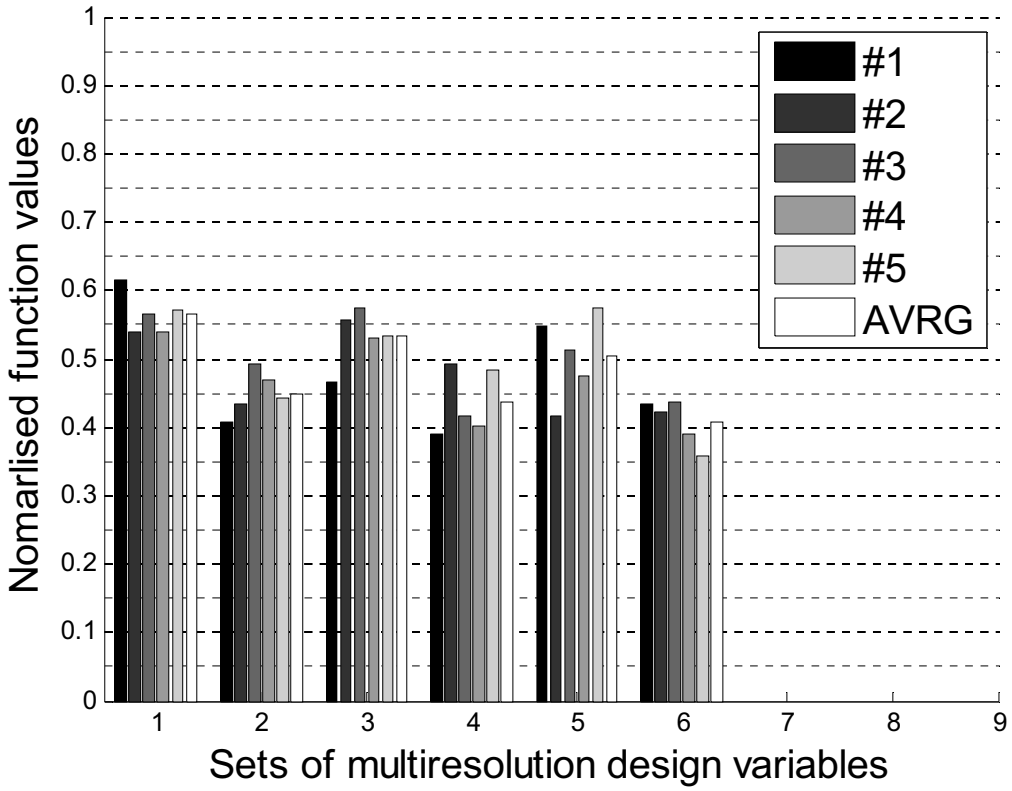

รูปที่ 6-16 เปรียบเทียบค่าฟังก์ชันเป้าหมายของ OPT1

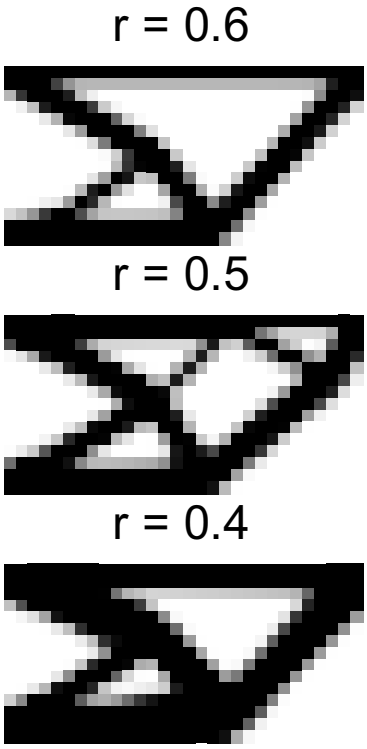

รูปที่ 6-17 โทโปโลยีจาก SIMP

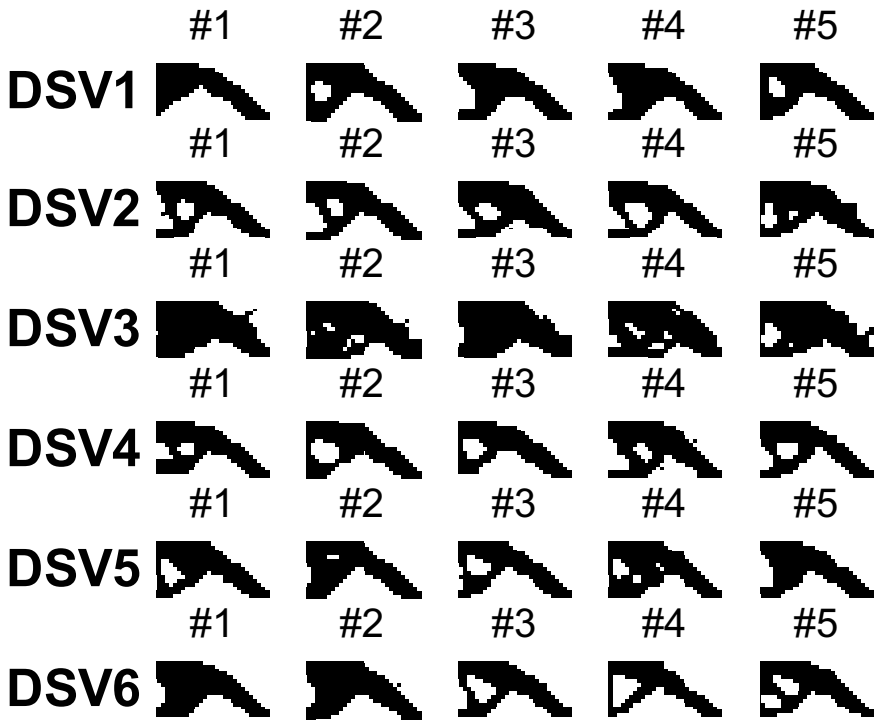

รูปที่ 6-18 ผลเฉลยเหมาะสมสุดของ OPT2

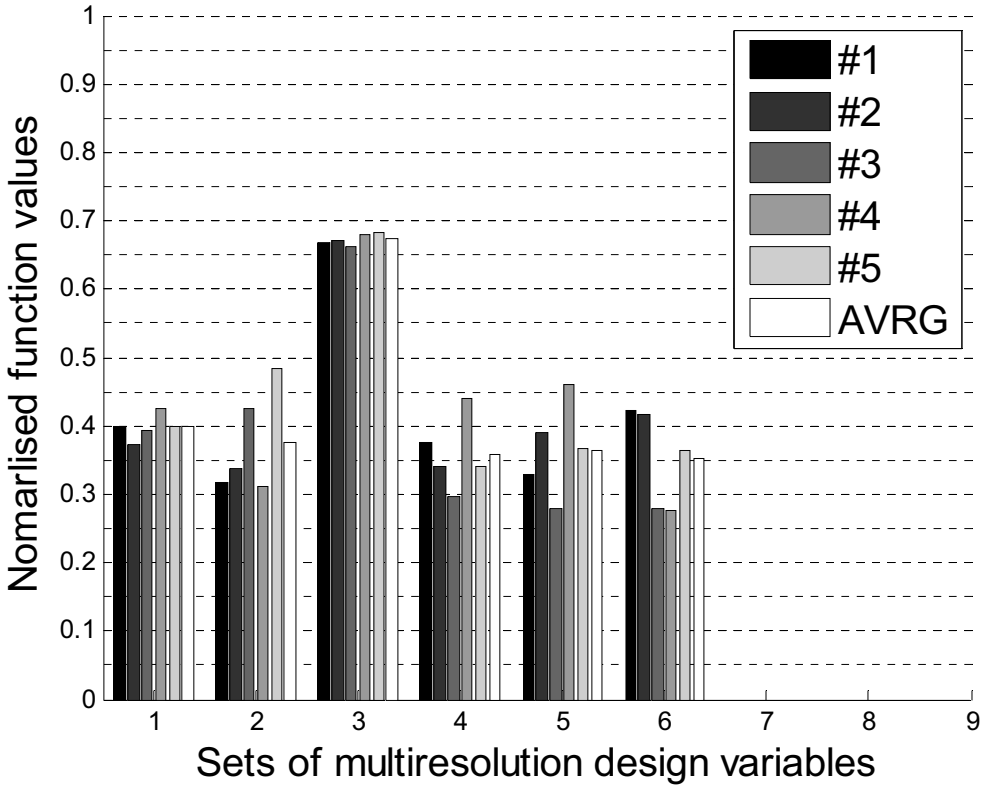

รูปที่ 6-19 เปรียบเทียบค่าฟังก์ชันเป้าหมายของ OPT2

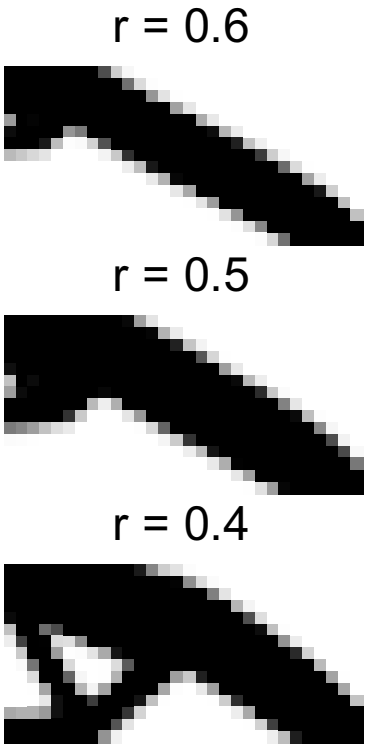

รูปที่ 6-20 โทโปโลยีจาก SIMP

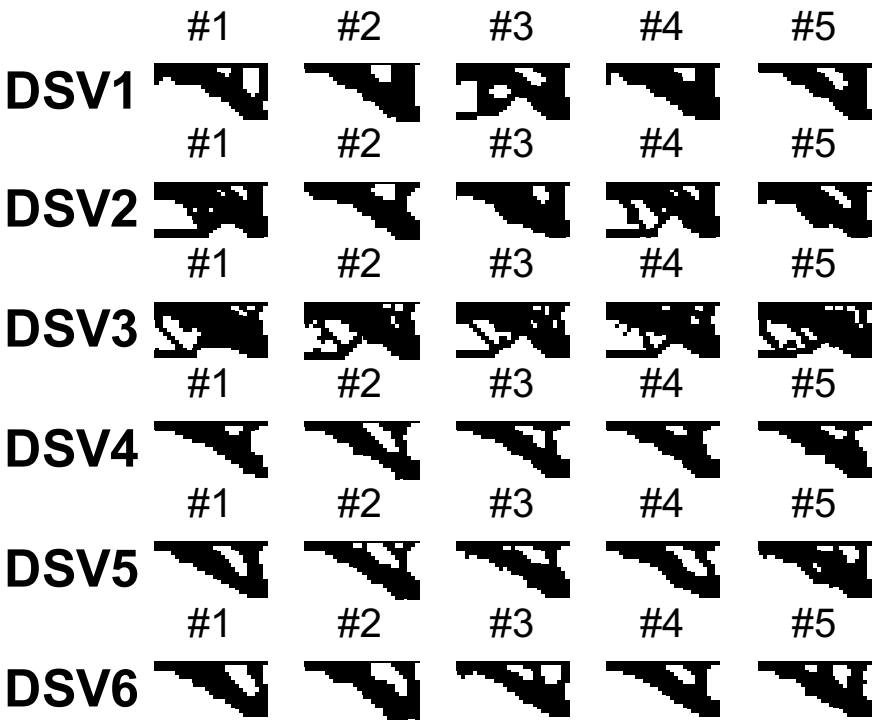

รูปที่ 6-21 ผลเฉลยเหมาะสมสุดของ OPT3

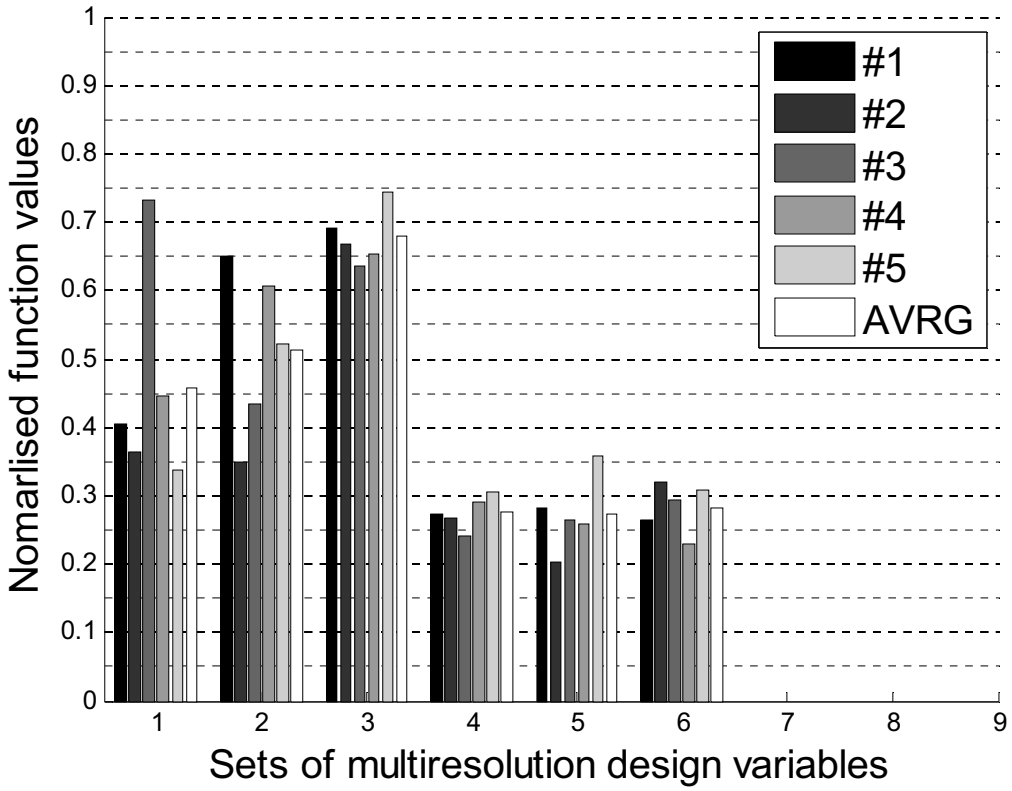

รูปที่ 6-22 เปรียบเทียบค่าฟังก์ชันเป้าหมายของ OPT3

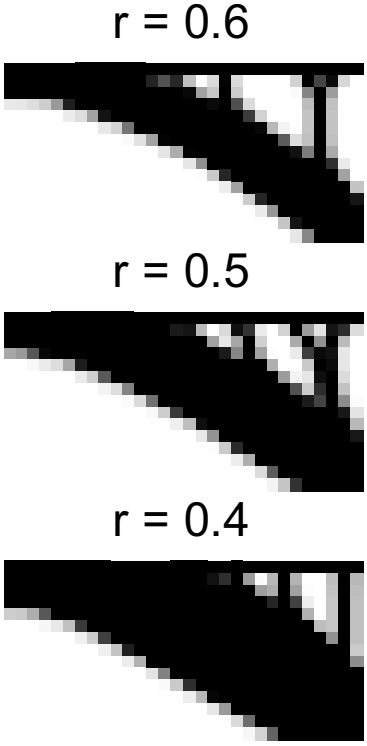

รูปที่ 6-23 โทโปโลยีจาก SIMP

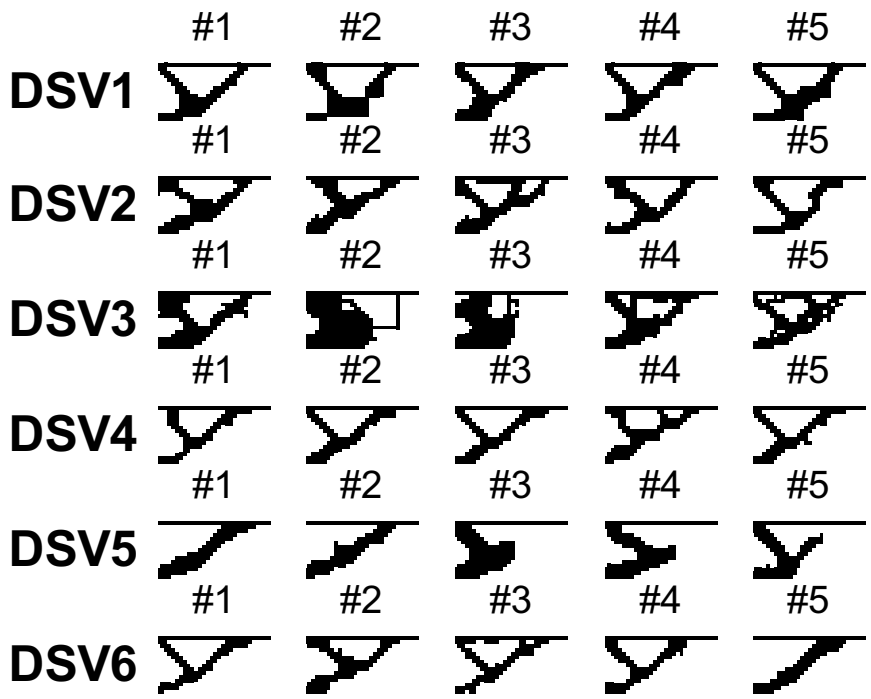

รูปที่ 6-24 ผลเฉลยเหมาะสมสุดของ OPT4

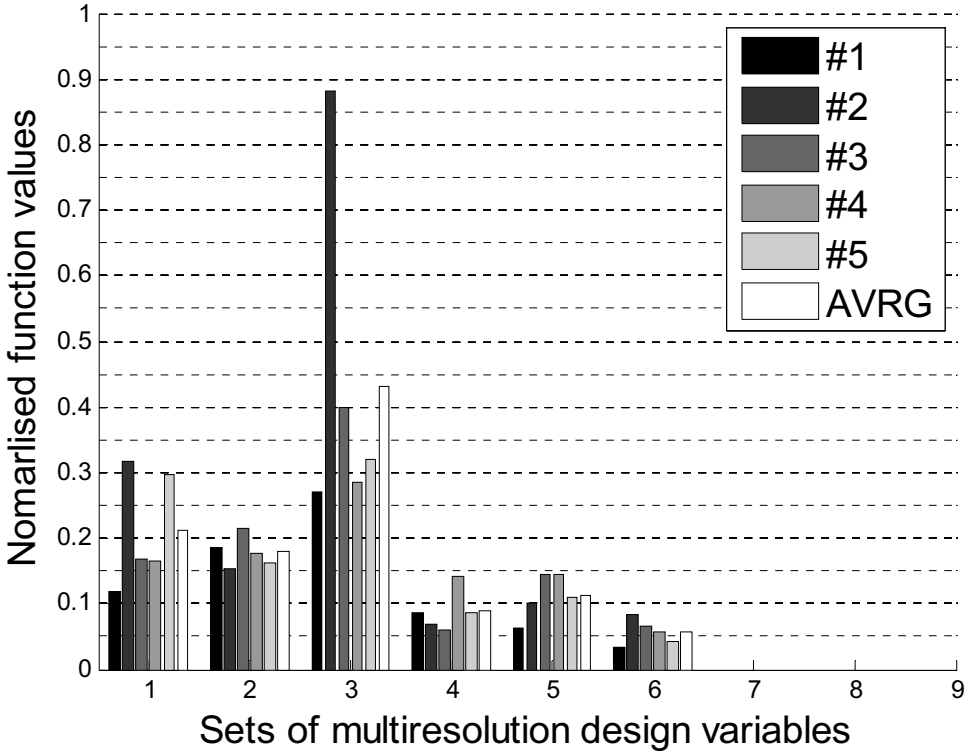

รูปที่ 6-25 เปรียบเทียบค่าฟังก์ชันเป้าหมายของ OPT4

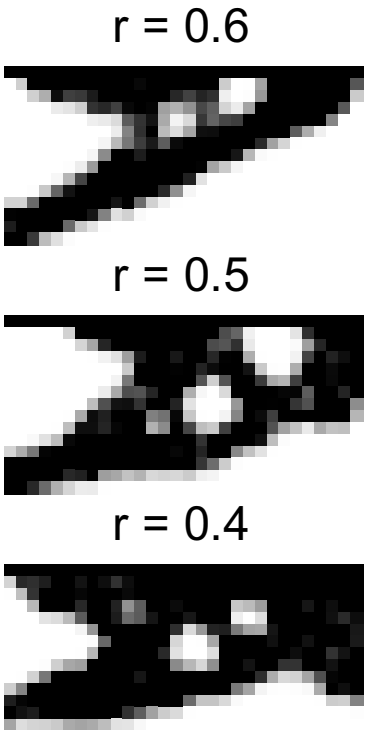

รูปที่ 6-26 โทโปโลยีจาก SIMP

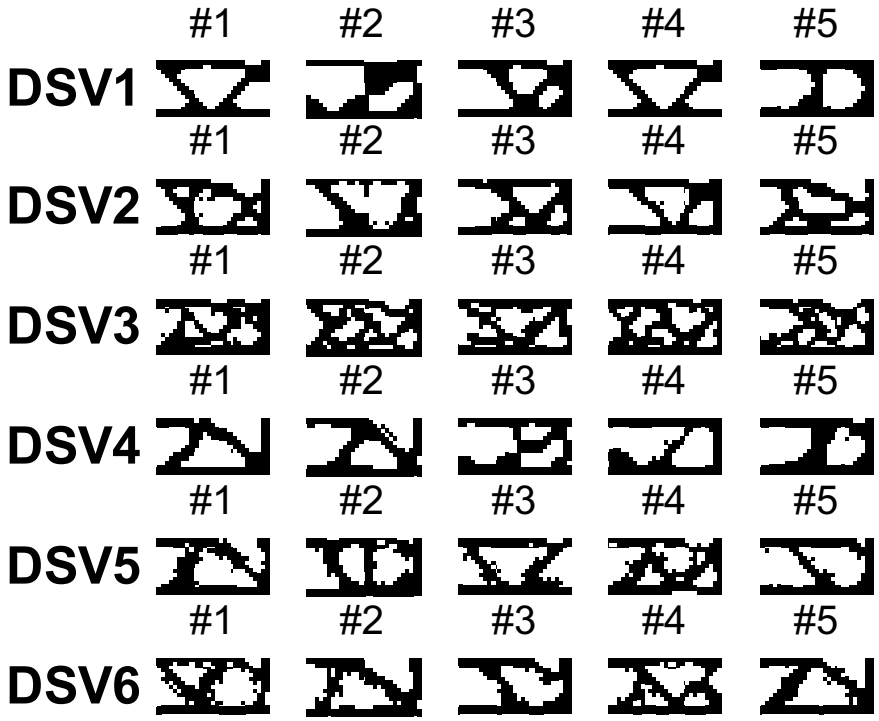

รูปที่ 6-27 ผลเฉลยเหมาะสมสุดของ OPT5

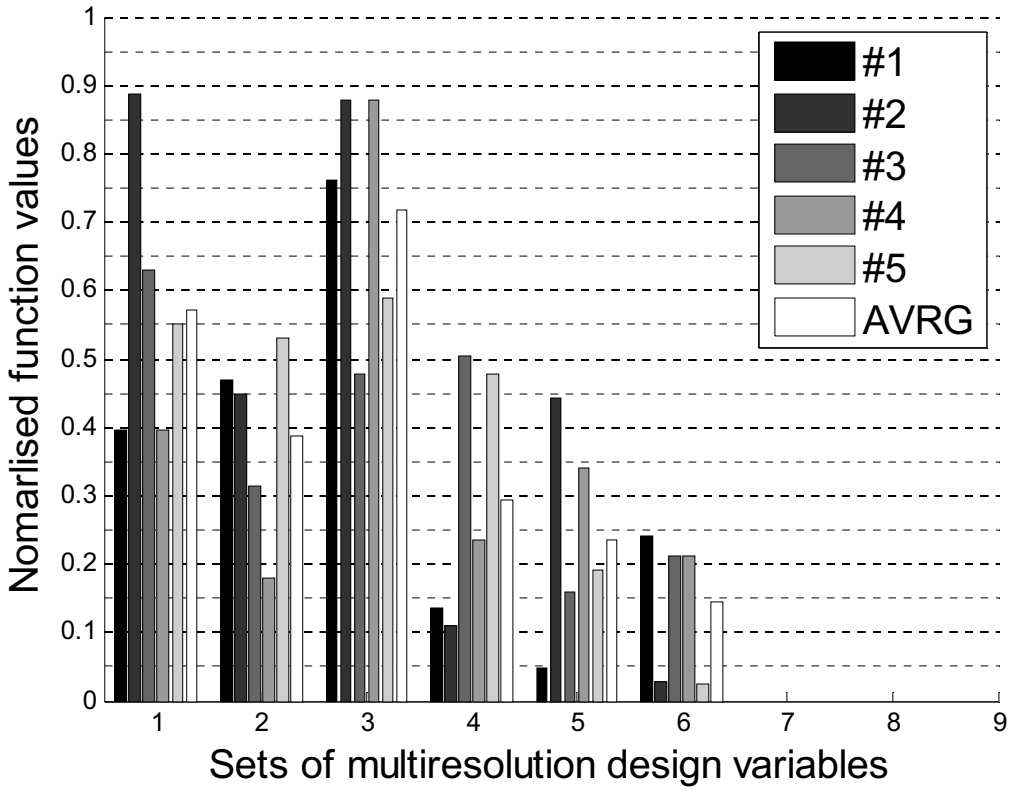

รูปที่ 6-28 เปรียบเทียบค่าฟังก์ชันเป้าหมายของ OPT5

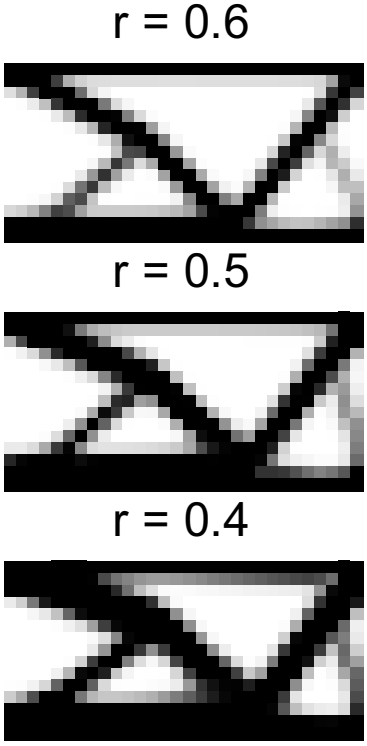

รูปที่ 6-29 โทโปโลยีจาก SIMP

สรุป วิจารณ์ และงานในอนาคต
Conclusions Discussion and Future work

องค์ความรู้ที่ได้จากงานวิจัยนี้มีหลายส่วนดังนี้

การพัฒนาขั้นตอนวิธีวิวัฒนาการแบบหลายเป้าหมายวิธีใหม่ (PBIL) ที่มีสมรรถนะสูงสุดในบรรดาขั้นตอนวิธีวิวัฒนาการแบบหลายเป้าหมายที่ใช้เลขฐานสองเป็นตัวแปรออกแบบ PBIL จัดว่าเป็นวิธีวิวัฒนาการแบบหลายเป้าหมายที่ให้ความหลากหลายของผลเฉลยของพาเรโตมากที่สุดวิธีหนึ่ง

การประยุกต์ใช้ขั้นตอนวิธีวิวัฒนาการหลากหลายวิธีในการออกแบบเหมาะสมสุดแบบหลายฟังก์ชันเป้าหมายของระบบโครงข่ายท่อประปา ผลจากการศึกษาพบว่าการใช้วิธีวิวัฒนาการหาผลเฉลยพาเรโตจะได้ผลเฉลยส่วนใหญ่ดีกว่าโครงข่ายท่อที่ใช้ในปัจจุบันของอำเภอเมืองยโสธร วิธีวิวัฒนาการที่ใช้จำนวนจริงเป็นตัวแปรออกแบบจะมีสมรรถนะสูงกว่าวิธีที่ใช้เลขฐานสอง วิธีวิวัฒนาการที่ใช้จำนวนจริงเป็นตัวแปรออกแบบที่จัดว่าสามารถใช้ในงานจริงได้อย่างมีประสิทธิภาพคือ MPSO SPEA2 และ NSGAII ในกรณีเฉพาะกลุ่มของวิธีที่ใช้เลขฐานสอง PBIL คือวิธีที่ดีที่สุดรองลงมาคือ PAES ขั้นตอนวิธีวิวัฒนาการสามารถใช้ได้กับทั้งการออกแบบโครงข่ายใหม่และการออกแบบปรับปรุงโครงข่ายเดิมที่มีอยู่แล้ว

การประยุกต์ใช้ขั้นตอนวิธีวิวัฒนาการแบบหลายเป้าหมายกับปัญหาการหาโทโปโลยีเหมาะสมสุดของโครงสร้างสามารถทำได้และจากการทดสอบเบื้องต้นพบว่า PBIL เป็นวิธีที่ดีที่สุด และผลเฉลยที่ได้สามารถเปรียบเทียบกับผลเฉลยที่ได้จากวิธีหาค่าเหมาะสมสุดที่ใช้อนุพันธ์ในการหาคำตอบ

การประยุกต์ใช้ตัวแปรออกแบบหลายระดับความชัดช่วยเพิ่มสมรรถนะในการหาผลเฉลยของขั้นตอนวิธีวิวัฒนาการแบบเป้าหมายเดียวเช่น SA ได้อย่างมีประสิทธิผล อย่างไรก็ตาม วิธีการดังกล่าวไม่สามารถเพิ่มสมรรถนะในการค้นหาผลเฉลยเหมาะสมสุดของพาเรโตของขั้นตอนวิธีวิวัฒนาการแบบหลายเป้าหมายได้อย่างชัดเจน และยังเป็นประเด็นสำหรับการวิจัยในสาขาวิชานี้ต่อไป

งานที่จะทำต่อในอนาคตคือการประยุกต์ใช้ขั้นตอนวิธีวิวัฒนาการแบบหลายเป้าหมายกับการออกแบบที่ใช้งานจริงในโรงงานอุตสาหกรรม การเพิ่มสมรรถนะของวิธีวิวัฒนาการโดยการใช้การประมาณค่าพื้นผิวตอบสนอง (response surface model) และการประมาณค่าเกรเดียน (approximate gradient) จากกลุ่มประชากร

เอกสารอ้างอิง

[1] Marler RT, Arora JS. Survey of multi-objective optimization methods for engineering. *Struct. Multidisc. Optim*. 2004; 26: 369 – 395

[2] Coello CC, Romero CEM. Evolutionary Algorithms and Multiple Objective Optimization. Multicriteria Optimization. Ehrgott, Matthias; Gandibleux, Xavier (Eds.). 2002: 277-331

[3] Grandhi RV, Bharatram G. Multiobjective optimization of large-scale structures. AIAA 1993; 31(7):1329-1337

[4] Benage WA, and Dhingra AK. Single and Multiobjective Structural Optimization in Discrete-continuous Variables Using Simiulated Annealing. *International Journal of Numerical Methods in Engineering*. 1994; 38: 2753-2773

[5] Messac A, Ismail-Yahaya A, Mattson CA. The normalized normal constraint method for generating the Pareto frontier. Structural and Multidisciplinary Optimization. 2003; 25(2): 86-98

[6] Bureerat S, Cooper JE. Evolutionary methods for the optimisation of engineering systems. IEE Colloquium Optimisation in Control: Methods and Applications, IEE, London, UK. 1998, pp. 1/1-1/10

[7] Deb K, Goel T. Multi-objective evolutionary algorithms for engineering shape design. KanGAL Report No. 200003, Dept. of Mechanical Engineering, Indian Institute of Technology

[8] Coello CC. A short tutorial on evolutionary multiobjective optimization. Dept. of Electrical Engineering, Av. Instituto Politecnico Nacional No. 2508, Col. San Pedro Zacatenco

[9] Zitzler E, Laumanns M, Bleuler S. A tutorial on evolutionary multiobjective optimization. Computer Engineering and Network Laboratory, ETH, Zurich

[10] Knowles JD, Corne DW. Approximating the non-dominated front using the pareto archive evolution strategy. Evolutionary Computation. 2000; 8(2): 149-172

[11] Fonseca CM, Fleming PJ. Genetic algorithms for multiobjective optimization: Formulation, discussion and generalization. In: Proc. Of the 5th Inter. Conf. on GAs, 1993, pp. 416-423

[12] Horn J, Nafpliotis N, Goldberg DE. A niched pareto genetic algorithm for multiobjective optimization. In: The 1st IEEE Conf. on Evolutionary Computation, 1994, pp. 82-87

[13] Srinivas N, Deb K. Multiobjective optimization using non-dominated genetic algorithms. Evolutionary Computation. 1994; 2(3):221-248

[14] Deb K, Pratap A, Agarwal S, Meyarivan T. A Fast and elitist multiobjective genetic algorithm: NSGAII. IEEE Trans. On Evolutionary Computation 2002; 6(2): 182-197

[15] Zitzler E, Thiele L. Multiobjective evolutionary algorithms: A comparative case study and the strength pareto approach. IEEE Trans. On Evolutionary Computation. 1999; 3(4): 257-271

[16] Zitzler E, Laumanns M, Thiele L. SPEA2: Improving the strength pareto evolutionary algorithm for multiobjective optimization. In: Evolutionary Methods for Design, Optimization and Control, Barcelona, Spain, 2002

[17] Knowles J, Corne D. The Pareto archived evolution strategy: a new baseline algorithm for Pareto multiobjective optimization. Congress on Evolutionary Computation, 1999

[18] Coello CC, Pulido GT. A Micro-genetic algorithm for multiobjective optimization. Lecture Notes in Computer Science. 2001; 1993/2001: 126

[19] Zitzler E, Deb K, Thiele L. Comparison of multiobjective evolutionary algorithms: empirical results. Evolutionary Computation 2000; 8(2):173-195

[20] Zitzler E, Thiele L, Laumanns M, Fonseca CM, Fonseca VG. Performance assessment of multiobjective optmizers: an analysis and review. IEEE trans. on Evolutionary Computation. 2003; 7(2): 117-132

[21] Coello CAC (2002) List of references on evolutionary multi-objective optimization (journal papers only). www.jeo.org/emo/EMOOjournals.html

[22] Suppapitnarm A, Seffen KA, Parks GT, Clarkson PJ. A simulated annealing algorithm for multiobjective optimization. Engineering Optimization. 2000

[23] Nam D, Park CH. Multiobjective simulated annealing: a comparative study to evolutionary algorithms. Department of Electrical Engineering, KAIST, Korea

[24] Schaffer JD. Multiobjective optimization with vector evaluated genetic algorithms. In: GAs and their Application: Proc. of 1st Inter Conf. on GAs, 1985, pp. 93-100

[25] Camponogara E, Talukdar SN. A genetic algorithm for constrained and multi-objective optimization. Technical Report, Engineering Design Research Center, Carnegie Mellon University, 1988
[26] Ivvan S, Pena V, Rionda SB, Aguirre AH. Multiobjective Shape Optimization Using Estimation Distribution Algorithms and Correlated Information. Evolutionary Multi-Criterion Optimization. In: EMO2005, 2005, pp. 664-676
[27] Farina M, Amato P. Linked interpolation-optimization strategies for multicriteria optimization problems. Soft computing. 2005; 9: 54-65
[28] Shan S, Wang GG. An efficient pareto set identification approach for multi-objective optimization on black-box functions. University of Manitoba, 2004
[29] Cheng FY, Li D. Fuzzy set theory with genetic algorithms in constrained structural optimization. In: ASCE Proceeding of US-Japan Joint Seminar on Structural Optimization, New York, USA, 1997, pp. 55-66
[30] Fawaz Z, Xu YG, Behdinan K. Hybrid evolutionary algorithm and application to structural optimization. Struct. Multidisc. Optim. 2005; 30: 219 – 226
[31] Bendsoe MP, Sigmund O. *Topology Optimization: Theory, Methods and Applications*. Springer, Berlin, 2003
[32] Min SJ, Nishiwaki S, Kikuchi N. Unified Topology Design of Static and Vibrating Structures Using Multiobjective Optimization, *Computers and Structures*; 75: 93-116
[33] Shyh-Chang Wu, Ting-Yu Chen. Multiobjective optimal topology design of structures Computational Mechanics. 1998; 21(6): 483 – 492
[34] Parsons R, Canfield SL. Developing genetic programming techniques for the design of compliant mechanisms. Struct. Multidisc. Optim. 2002; 24:1 78 – 86
[35] Kane C, Jouve F, Schoenauer M. Structural topology optimization in linear and nonlinear elasticity using genetic algorithms, *21st ASME Design Automatic Conf.*, Boston, 1995
[36] Kane C, Schoenauer M. Topological optimum design using genetic algorithms, *Control & Cybernetics*. 1996; 25(5)
[37] Chapman CD, Jakiela MJ. Genetic algorithm-based structural topology design with compliance and topology simplification considerations. *ASME Journal of Mechanical Design*. 1996; 118(1): 89-98
[38] Kunakote T Bureerat S. Structural topology optimisation using evolutionary algorithms. *17th ME-NETT* 2003, Thailand (in Thai)
[39] S. Bureerat and T. Kunakote. 2006. Topological design of structures using population-based optimisation methods. Inverse Problems in Science and Engineering, 14:589-607.
[40] Bureerat S, Limtragool J. Performance enhancement of evolutionary search for topology optimization. Finite Element in Analysis and Design, 42: 547-566.
[41] Kunakote T. Topology optimization using evolutionary algorithms: comparison of the evolutionary methods and checkerboard suppression technique. Master thesis, Khon Kaen University, 2004
[42] Sigmund O. A 99 line topology optimization code written in MATLAB. *Struct. Multidisc. Optim*. 2001; 21: 120 – 127
[43] Bureerat S, Kunakote T. A Simple Checkerboard Suppression Technique for Topology Optimisation Using Simulated Annealing. *17th ME-NETT* 2003, Thailand
[44] Chu DN, Xie YM, Hira A, Steven GP. Evolutionary Structural Optimization for Problems with Stiffness Constraints. *Finite Element in Analysis and Design* 1996; 21: 239-251
[45] Krog LA, Olhoff N. Optimum Topology and Reinforcement Design of Disk and Plate Structures with Multiple Stiffness and Eigenfrequency Objectives. *Computers and Structures*; 72: 535-563
[46] Pederson NL. Maximization of eigenfrequencies using topology optimization. Struct. Multidisc Optim. 2000; 20: 2-11
[47] Bureerat S, Limtragool J. Structural compliance minimisation using evolutionary algorithms with surface spline interpolation, in: 18th ME-NETT Conf., Khon Kaen, Thailand, 2004, pp. 319 - 324.
[48] Neves MM et al. Generalized Topology Design of Structures with a Buckling Load Criterion. *Structural Optimization*; 10(2): 71-78

[49] Wang SY, Tai K. Graph representation for structural topology optimization using genetic algorithms. in: Computers and Structures, Vol. 82, 2004, pp. 1609-1622.
[50] Jakiela M, Chapman C, Duda J, Adewuya A, Saitou K. Continuum structural topology design with genetic algorithms. J. Comp. Methods in App. Mech. and Eng. 2002; 86(2): 339–356
[51] Abebe AJ, Solomatine DP. Application of global optimization to the design of pipe networks." *Proc. 3rd Int. Conf. Hydrodynamics, Copenhagen*, 1998
[52] Jeppson RW. *Analysis of Flow in Pipe Networks*, Ann Arbor Science, Michigan. 1976
[53] Rosado IJR, Agustin JLB. Reliability and costs optimization for distribution of networks expansion using an evolutionary algorthm. *IEEE Trans. On Power Sys.* 2001; 10(1): 111-118.
[54] Walski TM. The wrong paradigm – why water distribution optimization doesn't work. J. of water resources planning and management. 2001; July-August: 203
[55] Prasad TD, Park NS. Multiobjective genetic algorithms for design of water distribution networks." J. of Water resource planning and management. 2004; Jan-Feb: 73-82.
[56] Sriworamas K, Bureerat S, Permkamol V. A Population-Based Approach for Discrete Optimisation: Applications to Multi-Objective Optimisation of Pipe Network System. การประชุมวิชาการ นวัตกรรมทางวิศวกรรมสำหรับการจัดการทรัพยากรอย่างยั่งยืน คณะวิศวกรรมศาสตร์ มหาวิทยาลัยขอนแก่น, 2003
[57] Farmani R, Walters GA, Savic DA. Trade-off between total cost and reliability for anytown network J. of Water resource planning and management. 2005; May-June: 161-171.
[58] Ramírez-Rosado IJ, Bernal-Agustín JL. Reliability and cost optimization for distribution networks expansion using an evolutionary algorithm. IEEE Trans on Power Systems, 2001; 16(1)
[59] Vamvakeridou-Lyroudia LS. Fuzzy multiobjective optimization of water distribution networks. J. of Water Resources Planning and Management. 2005; 131(6): 467-476
[60] Cunha M de C, Sousa J. Water Distribution Design Optimization: simulated annealing approach. J. Water Resour. Plng. and Mgmt. 1999; 125(4): 215-221
[61] Schaffer, J.D.: Multiobjective Optimization with Vector Evaluated Genetic Algorithms. In: GAs and their Application: Proc. of 1st Inter Conf. on GAs (1985) 93-100
[62] Reyes-Sierra, M., Coello Coello, C.A.: Multi-Objective Particle Swarm Optimizers: A Survey of the State-of-the-Art. Int. J. of Computational Intelligence Research, 2:3 (2006) 287-308
[63] S. Bureerat and K. Sriworamas. 2007. Population-Based Incremental Learning for Multiobjective Optimisation. Advances in Soft Computing, 39:223-232.
[64] Bureerat S, Introduction to Optimisation, Lecture notes, Dept. of Mechanical Engineering, Khon Kaen University, Thailand, 2008
[65] Baluja, S.: Population-Based Incremental Learning: a Method for Integrating Genetic Search Based Function Optimization and Competitive Learning, Technical Report CMU_CS_95_163, Carnegie Mellon University (1994)
[66] Siwadol Kanyakam and Sujin Bureerat 2007 Passive Vibration Suppression of a Walking Tractor Handlebar Structure Using Multiobjective PBIL, CEC 2007, Singapore, pp. 4162-4169
[67] M. A. Villalobos-Arias, G. T. Pulido and C. A. C. Coello, "A proposal to use stripes to maintain diversity in a multi-objective particle swarm optimizer ," in Swarm Intelligence Symposium, 2005, Proceeding IEEE, June 2005, pp. 22-29.
[68] Deb, K., Pratap, A., Agarwal, S., Meyarivan, T.: A Fast and Elitist Multiobjective Genetic Algorithm: NSGAII. IEEE Trans. On Evolutionary Computation 6(2) (2002) 182-197
[69] Zitzler, E., Laumanns, M., Thiele, L.: SPEA2: Improving the Strength Pareto Evolutionary Algorithm for Multiobjective Optimization, In: Evolutionary Methods for Design, Optimization and Control, Barcelona, Spain (2002)
[70] Srisomporn S and Bureerat S., Geometrical Design of Plate-Fin Heat Sinks Using Hybridization of RSM and MOEA, IEEE Trans on Components and Packaging Technologies, 2008
[71] Deb, K., Pratap, A., Meyarivan, T.: Constrained Test Problems for Multi-Objective Evolutionary Optimization, KanGAL Report No. 200002, Kanpur Genetic Algorithms Laboraotry (KanGAL), Indian Institute of Technology, Kanpur, India
[72] Bureerat S, Kunakote T and Limtragool J. Structural Topology Optimisation Using Design Variable Filtering, TISD2006, Khon Kaen

[73] T. Kunakote and S. Bureerat. 2006. Topological Design of Structures with Stress Constraints. The 20th Conference of Mechanical Engineering Network of Thailand, October
[74] Kunakote T and Bureerat S, Topology Optimisation of a Plate Structure Using Multiobjective Population-Based Incremental Learning, TISD2008, Khon Kaen, Thailand
[75] Sujin Bureerat and Jumlong Limtragool, Structural Topology Optimisation Using Simulated Annealing with Multiresolution Design Variables, Finite Element in Analysis and Design, in-press, 2008
[76] Boonapan A, Bureerat S, Limtragool J, Inban S. Multi-level design of an automotive part. 19th Conference of Mechanical Engineering Network of Thailand, Phuket, Thailand 2005; 172-177 (in THAI)
[77] Yildiz AR, Kaya N, Ozturk F, Alanku O. Optimal design of vehicle components using topology design and optimization. Int. J. Vehicle Design 2004; 34:387-398.
[78] Bureerat S, Boonapan A, Kunakote T, Limtragool J. Design of compliance mechanisms using topology optimisation. 19th Conference of Mechanical Engineering Network of Thailand, Phuket, Thailand 2005; 421-427.
[79] Luo Z, Chen L, Yang J, Zhang Y, Abdel-Malek K. Compliance mechanism design using multi-objective topology optimization scheme of continuum structures. Struct Multidisc Optim 2005; 30:142 – 154.
[80] Suzuki K, Kikuchi N. A homogenization method for shape and topology optimization. Comp. Meth. Appl. Mech. Engrng. 1991; 93:291-318.
[81] Xie YM, Steven GP. Evolutionary Structural Optimization, Berlin: Springer-Verlag, 1997
[82] Fujii D, Kikuchi N. Improvement of numerical instabilities in topology optimization using the SLP method. Structural and Multidisciplinary Optimization 2000; 19:113-121.
[83] Wang SY, Tai K. Graph representation for structural topology optimization using genetic algorithms. Computers and Structures 2004; 82:1609-1622.
[84] Jakiela M, Chapman C, Duda J, Adewuya A, Saitou K. Continuum structural topology design with genetic algorithms. J. Comput. Methods Appl. Mech. Eng. 2000; 86:339–356.
[85] Woon SY, Tong L, Querin OM, Steven GP. Effective optimisation of continuum topologies through a multi-GA system. Computer Methods in Applied Mechanics and Engineering 2005; 194:3416-3437.
[86] Madeiraa JA, Rodriguesa HC, Pina H. Multiobjective topology optimization of structures using genetic algorithms with chromosome repairing. Struct Multidisc Optim. 2006; 32:31–39.
[87] Patrick YS, Manoochehri S. Generating optimal configurations in structural design using simulated annealing. International Journal for Numerical Methods in Engineering 1997; 40:1053-1069.
[88] Cui GY, Tai K, Wang BP. Topology optimization for maximum natural frequency using simulated annealing and morphological representation. AIAA Journal 2002; 40(3): 586-589
[89] Kirkpatrik S, Gelatt Jr. CD, Vecchi MP. Optimization by simulated annealing. J. Science 1983; 220:671-680.
[90] Benage WA, Dhingra AK. Single and multiobjective structural optimization in discrete-continuous variables using simulated annealing. International Journal of Numerical Methods in Engineering 1994; 38:2753-2773.

Output จากโครงการวิจัย

ผลลัพธ์ที่ได้จากโครงการวิจัยนี้มีดังนี้

1. ผลงานตีพิมพ์ในวารสารวิชาการนานาชาติ

   S. Bureerat and K. Sriworamas. 2007. Population-Based Incremental Learning for Multiobjective Optimisation. *Advances in Soft Computing*, 39:223-232.

   S. Bureerat and J. Limtragool. 2008. Structural Topology Optimisation Using Simulated Annealing with Multiresolution Design Variables. *Finite Element in Analysis and Design*, in-press

2. การนำผลงานวิจัยไปใช้ประโยชน์

   - เชิงสาธารณะ ปัจจุบันยังไม่มีการนำผลการวิจัยไปใช้ประโยชน์อย่างเป็นรูปธรรม แต่ในอนาคตจะมีการเผยแพร่รายงานผลการออกแบบและปรับปรุงระบบโครงข่ายท่อประปาด้วยขั้นตอนวิธีวิวัฒนาการแบบหลายเป้าหมายไปสู่การใช้งานจริง
   - เชิงวิชาการ นักวิจัยใหม่ทางด้านการออกแบบโครงข่ายท่อประปา ปัจจุบันกำลังศึกษาระดับปริญญาเอก ที่ภาควิชาวิศวกรรมโยธา มหาวิทยาลัยอุบลราชธานี
   - เชิงวิชาการ ได้บรรจุวิธี PBIL ที่พัฒนาขึ้นมาในวิชาที่ผู้วิจัยสอนที่ ภาควิชาวิศวกรรมเครื่องกล มหาวิทยาลัยขอนแก่น คือ วิชา Mechanical System Optimization สำหรับนักศึกษาระดับบัณฑิตศึกษา และ Introduction to Optimization สำหรับนักศึกษาปริญญาตรี

3. อื่นๆ

   S. Kanyakam and S. Bureerat. 2007. Passive Vibration Suppression of a Walking Tractor Handlebar Structure Using Multiobjective PBIL. *CEC 2007*, Singapore, pp. 4162-4169

   T. Kunakote and S. Bureerat. 2008. Topology Optimisation of a Plate Structure Using Multiobjective Population-Based Incremental Learning. *TISD2008*, Khon Kaen, Thailand

ภาคผนวก

ARTICLE IN PRESS

Finite Elements in Analysis and Design ▮▮▮ (▮▮▮▮) ▮▮▮–▮▮▮

Contents lists available at ScienceDirect

Finite Elements in Analysis and Design

journal homepage: www.elsevier.com/locate/finel

Structural topology optimisation using simulated annealing with multiresolution design variables

Sujin Bureerat*, Jumlong Limtragool

Department of Mechanical Engineering, Faculty of Engineering, Khon Kaen University, Khon Kaen 40002, Thailand

ARTICLE INFO

Article history:
Received 18 August 2007
Received in revised form 3 April 2008
Accepted 26 April 2008

Keywords:
Topology optimisation
Simulated annealing
Multiresolution design variables
Approximate density distribution
Checkerboard suppression

ABSTRACT

The use of evolutionary algorithms for structural topology optimisation is said to be ineffective due to a considerably large number of topological design variables. However, such a problem can be alleviated by using additional numerical techniques. This paper presents the applications of simulated annealing (SA) for solving structural topology optimisation. The numerical technique termed multiresolution design variables (MRDV) is proposed as a numerical tool to enhance the searching performance of SA when dealing with topology optimisation. The approximate density distribution (ADD) and chromosome repairing techniques are employed to deal with checkerboard patterns and multiple disconnected areas on the structural topologies. The SA strategies using various sets of MRDV are implemented to solve a number of structural topology optimisation problems. The results obtained from the various optimisation strategies are illustrated and compared. The effect of using many resolutions of design variables on SA's searching performance is investigated. It is shown that the technique of MRDV is a powerful tool for the performance enhancement of SA when solving structural topology optimisation. The structural topologies obtained from employing the presented approach are comparable to those obtained from the classical gradient-based method.

1. Introduction

Topology optimisation is an effective design tool for a variety of engineering applications. For example, it can be used in the conceptual design stage of structural, mechanical and automotive components, e.g. in [1,2]. Also, it is applicable to the synthesis of compliance mechanisms [3,4]. Much research work has been made towards this design technology as mentioned in [5]. The design process is usually carried out by using an optimiser for problem solving and finite element (FE) analysis for function evaluation. The well-established approaches for topology optimisation are solid isotropic material with penalisation (SIMP) [5], homogenisation method [6], and evolutionary structural optimisation [7].

The most preferable optimisers for the topological design problem are gradient-based methods such as optimality criteria method (OCM) [8], the method of moving asymptotes (MMA) [5] and sequential linear programming (SLP) [9]. There have been some attempts to use evolutionary algorithms (EAs) for this type of optimisation problem [10,11] and it was found that their search performances are incomparable to the gradient-based methods. This is because most if not all of topology optimisation problems have a great many design variables. Since the EAs somewhat base their searching strategies on randomisation, they are not as powerful when solving such a large-scale design problem.

As a result, a number of numerical strategies have been developed and employed so that the search performance of EAs for both single and multiobjective topology optimisations is improved, such as in [12–15]. Using an approximate density distribution (ADD) technique as presented in [16] was found to be powerful and effective for single objective design cases. It is a simple trick used for reducing a number of design variables whilst slightly affecting a topological design domain. It can also be used for suppression of checkerboard patterns on the resulting topologies [3]. Furthermore, from the numerical investigation in [16,17], it has been shown that the mutation-based optimisation methods such as simulated annealing (SA) are more efficient than the other EAs when solving large-scale topological design problems with single objective functions. The results obtained from using such methods can even be compared to the optimum results from the gradient-based approaches, although they still require more function evaluations. With an improved searching performance, using EAs for topology optimisation would be advantageous since they can deal with unconventional topological design problems, which may be difficult or even impossible to be solved by using the gradient-based optimisers.

* Corresponding author.
E-mail address: sujbur@kku.ac.th (S. Bureerat).

0168-874X/$ - see front matter © 2008 Elsevier B.V. All rights reserved.
doi:10.1016/j.finel.2008.04.002

Please cite this article as: S. Bureerat, J. Limtragool, Structural topology optimisation using simulated annealing with multiresolution design variables, Finite Elem. Anal. Des. (2008), doi: 10.1016/j.finel.2008.04.002

This paper presents the applications of SA for solving structural topology optimisation. It is said to be the extension of the work presented in [16]. The numerical technique named MRDV is developed as a numerical tool to enhance the searching performance of SA. The chromosome repairing technique presented in [15] is employed to repair a design solution that leads to multiple disconnected areas. The SA strategies using various sets of MRDV are implemented to solve a number of structural topology optimisation problems. The results obtained from the various SA strategies are illustrated and compared. The effect of using many resolutions of design variables on SA's searching performance is examined. It is shown that the technique of MRDV is a powerful tool for the performance enhancement of SA when solving structural topology optimisation.

2. Simulated annealing

SA can sometimes be classified as an EA. The method can be seen as mimicking the random behaviour of molecules during an annealing process, which involves slow cooling from a high temperature. As the temperature cools, the atoms line themselves up and form a crystal, which is the state of minimum energy in the system. By using SA, almost all kinds of design variables including binary codes can be applied. The search procedure of SA starts with an initial solution, which will be called the parent. The parent is then mutated in some manner leading to a set of children or offspring. The best offspring is said to be a candidate to challenge its parent. For minimisation, if the candidate has a lower objective value than that of the parent, the parent is replaced by the candidate. In cases where the candidate has a higher objective function value than its parent, it still has a chance to replace the parent if accepted by a Boltzmann probability. Since on each loop the worse candidate may replace its parent, the best solution and the parent may not be the same solution. Therefore, the best individual on each loop should be kept along with a parent ensuring that the best solution of the search is not lost. The best solution can also be used in the mutation strategy of SA.

The SA algorithm used for minimisation in this paper can be detailed as

1. Initialisation: initial solution $\mathbf{x}_{\text{parent}}=\mathbf{x}_{\text{best}}$, $f_{\text{parent}}=f_{\text{best}}$, initial temperature T.
2. Generate n_s design solutions $\{\mathbf{x}_1^1,\mathbf{x}_2^1,\ldots,\mathbf{x}_{n_s}^1\}$ and their corresponding function values $\{f_1^1,f_2^1,\ldots,f_{n_s}^1\}$ by mutating on $\mathbf{x}_{\text{parent}}$.
3. Generate n_s design solutions $\{\mathbf{x}_1^2,\mathbf{x}_2^2,\ldots,\mathbf{x}_{n_s}^2\}$ and their corresponding function values $\{f_1^2,f_2^2,\ldots,f_{n_s}^2\}$ by mutating on $\mathbf{x}_{\text{best}}$.
4. Find $f_{\text{candidate}}=\min(\{f_i^1\}\cup\{f_i^2\})$ and its corresponding design solution $\mathbf{x}_{\text{candidate}}$.
5. If $f_{\text{candidate}}\leqslant f_{\text{parent}}$:
   5.1. Set $\mathbf{x}_{\text{parent}}=\mathbf{x}_{\text{candidate}}$, $f_{\text{parent}}=f_{\text{candidate}}$
   5.2. If $f_{\text{candidate}}\leqslant f_{\text{best}}$, $\mathbf{x}_{\text{best}}=\mathbf{x}_{\text{candidate}}$, $f_{\text{best}}=f_{\text{candidate}}$
   5.3. Go to step 7.
6. If $f_{\text{candidate}}>f_{\text{parent}}$, find $P_B=\exp(\frac{f_{\text{parent}}-f_{\text{candidate}}}{T})$, and generate a random number *rand*.
   6.1. If *rand* $\leqslant P_B$, set $\mathbf{x}_{\text{parent}}=\mathbf{x}_{\text{candidate}}$, $f_{\text{parent}}=f_{\text{candidate}}$ and $\mathbf{x}_{\text{best}}$ and f_{best} are not changed. Go to step 7.
   6.2. If *rand* $>P_B$, $\mathbf{x}_{\text{parent}}$, f_{parent}, $\mathbf{x}_{\text{best}}$ and f_{best} are not changed. Go to step 7.
7. Reduce the temperature T if the condition is fulfilled.
8. If the termination criterion is met, stop the procedure. Otherwise, go to step 2.

On each iteration n_s individuals are created by mutating on $\mathbf{x}_{\text{parent}}$ and other n_s individuals are obtained from mutating on $\mathbf{x}_{\text{best}}$. The solutions $\mathbf{x}_{\text{best}}$ and $\mathbf{x}_{\text{parent}}$ are the same initially but they can be different during the optimisation process. The parameter *rand* $\in[0,1]$ is a uniform random number sampled every time the computational step 6 is operated. The reduction of temperature can be scheduled by a designer. The use of SA for structural topology optimisation has been studied by several researchers e.g. in [16–19]. For more details of SA algorithms, see [16] and [18–22].

3. Multi-resolution design variables

A topological design process of continuous structural systems can be carried out by using FE analysis for function evaluation and a numerical optimiser for solving the design problem. Fig. 1 demonstrates the process of topology optimisation. The design domain is a predefined region used to form a structural topology. There are some parts of the structure that are not changed during the optimisation process. There can also be some predefined voids on the domain. The domain is then discretised into a number of FEs, which are called ground elements. Topological design variables are parameters that can be used to define a topology, e.g. elements' pseudo-densities and thicknesses. Having obtained the optimum solution, the elements that have low density values form holes while the elements with high density values represent material existent on the structure. One of the greatest difficulties when using this approach is that the resulting topology is full of checkerboard patterns when a low order FE model is implemented [5]. A number of numerical techniques have been developed to deal with such a problem and one of them is the ADD technique [16].

ADD is a simple numerical technique exploiting surface spline interpolation for approximating the values of FE densities from the known density distribution on another grid domain. The grid of design variables can be achieved by discretising the design domain with a resolution different from the FEs grid resolution. Fig. 2 shows a rectangular design domain being meshed into n ground FEs whereas the design variables have m elements. Let $\mathbf{r}_j^0$ be the position vectors of the m centre points of the design variable grids (plus signs) and $\mathbf{r}_k^v$ be the position vectors of the centre points of the n ground elements (`o' signs). By using radial-basis function interpolation, the densities at the centre points of the ground FEs $\boldsymbol{\rho}$ can be computed from the given density values at the design variables' centre points, $\boldsymbol{\rho}^{\text{ADD}}$, as

$$\boldsymbol{\rho}=\mathbf{C}\mathbf{A}^{-1}\boldsymbol{\rho}^{\text{ADD}}=\mathbf{T}\boldsymbol{\rho}^{\text{ADD}} \tag{1}$$

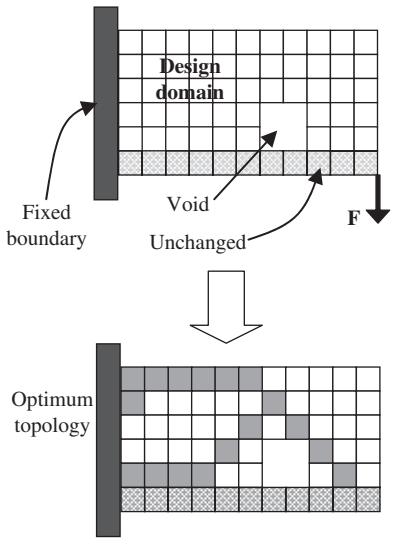

Fig. 1. Topology optimisation.

Please cite this article as: S. Bureerat, J. Limtragool, Structural topology optimisation using simulated annealing with multiresolution design variables, Finite Elem. Anal. Des. (2008), doi: 10.1016/j.finel.2008.04.002

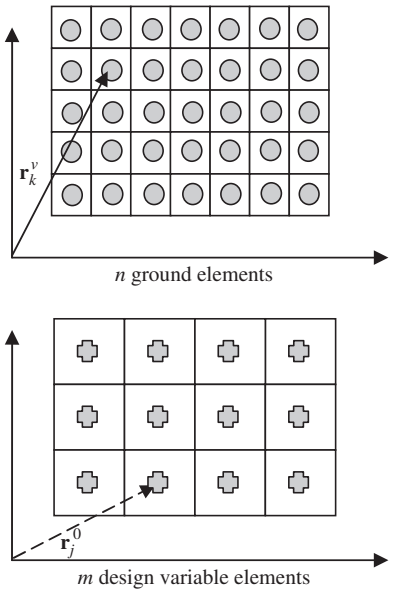

Fig. 2. Ground finite elements and design variable grid.

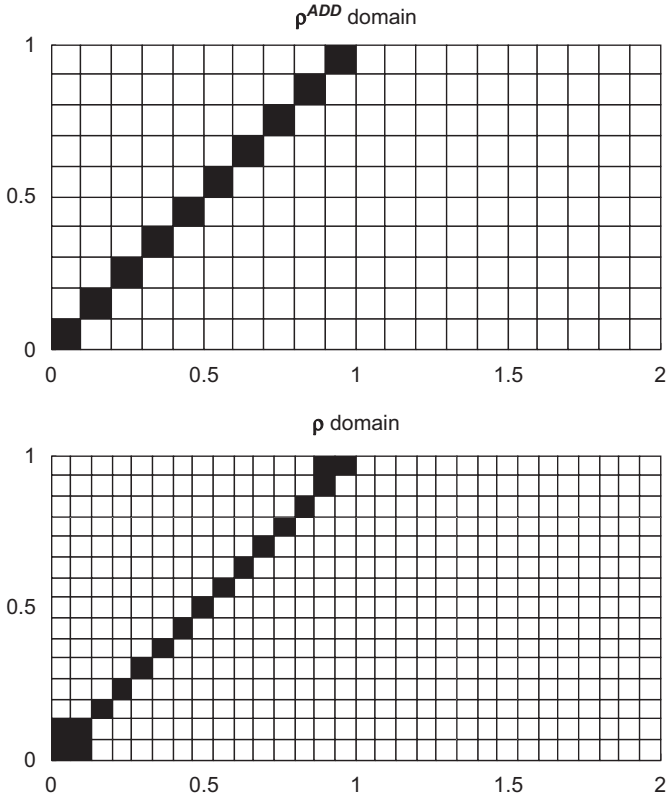

Fig. 3. Mapping between ADD grid and ground element densities $\boldsymbol{\rho}^0 = \mathbf{0.05}$.

where

$$\mathbf{A} = [a_{ij}]_{m\times m} = [f(d(\mathbf{r}_i^0, \mathbf{r}_j^0))] = [f(d_{ij})]$$

$$\mathbf{C} = [c_{kj}]_{n\times m} = [f(d(\mathbf{r}_k^v, \mathbf{r}_j^0))] = [f(d_{kj})]$$

and

$$d(\mathbf{r}_i, \mathbf{r}_j) = \sqrt{(\mathbf{r}_i - \mathbf{r}_j)^{\mathrm{T}}(\mathbf{r}_i - \mathbf{r}_j)}.$$

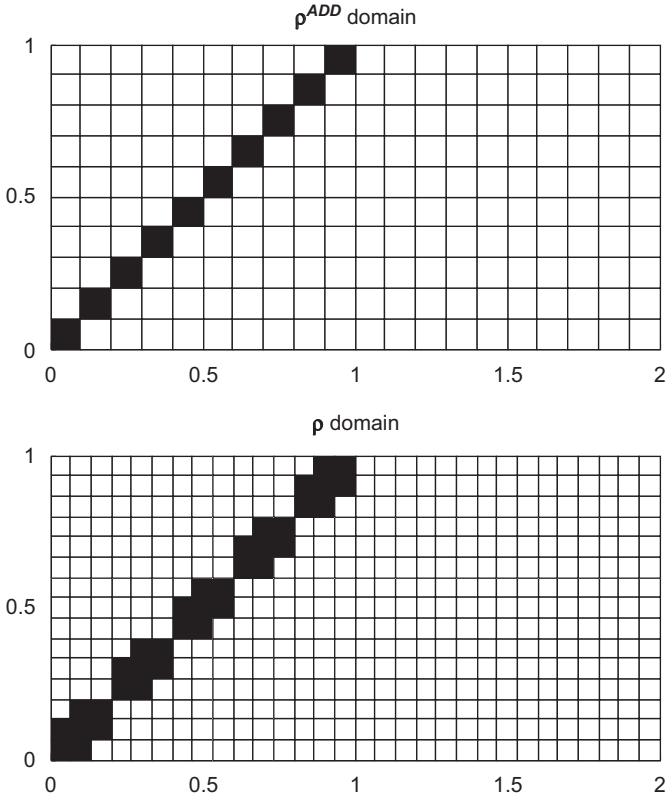

Fig. 4. Mapping between ADD grid and ground element densities $\boldsymbol{\rho}^0 = \mathbf{0.15}$.

Here we use the function $f(x) = x$. The resolution of the design variables (or ADD grid) must be lower than that of the ground elements. The process can be seen as the densities of the ground elements being filtered by the densities value on the design variables grid, thus, it is sometimes called a ground elements filter. For more details see Refs. [3,16].

In order to prevent intermediate densities on the resulting topology, binary design variables are used and the transformation in Eq. (1) needs to be modified. The components of $\boldsymbol{\rho}$ in (1) are refined to be $\boldsymbol{\rho}^e$ as

$$\rho_i^e = \begin{cases} 0, & \rho_i + \rho^0 \leqslant 0.5 \\ 1, & \rho_i + \rho^0 > 0.5 \end{cases} \tag{2}$$

where $\rho^0 \in (0, 0.5)$ is a constant value to be specified.

Eq. (2) can be expressed in a matrix form as

$$\boldsymbol{\rho}^e = round(\mathbf{T}\boldsymbol{\rho}^{\mathrm{ADD}} + \boldsymbol{\rho}^0) \tag{3}$$

where $\boldsymbol{\rho}^0$ is a vector sized $n \times 1$ with all the elements being ρ^0, and the function $round(x)$ is used to round off the real number x to its nearest integer.

Figs. 3–5 demonstrate the mapping of densities from the ADD domain to the densities of the FEs where the density values in the ADD domain form a checkerboard pattern. Note that the density values in both ADD and FE domains are set to be either ones (black elements) or zeros (white elements). The ADD domain has 20 × 10 elements while the FE grid has 30 × 15 elements. In Fig. 3, the value of ρ^0 is set to be 0.05 while it is set to be 0.15 and 0.25 for the transformation shown in Figs. 4 and 5, respectively. It can be seen that the transformation in Figs. 3 and 4 cannot totally suppress checkerboard patterns (or one-node connected part) whereas the transformation in Fig. 5 results in no checkerboards. This implies that the proper value of ρ^0 needs to be determined in the pre-process.

Please cite this article as: S. Bureerat, J. Limtragool, Structural topology optimisation using simulated annealing with multiresolution design variables, Finite Elem. Anal. Des. (2008), doi: 10.1016/j.finel.2008.04.002

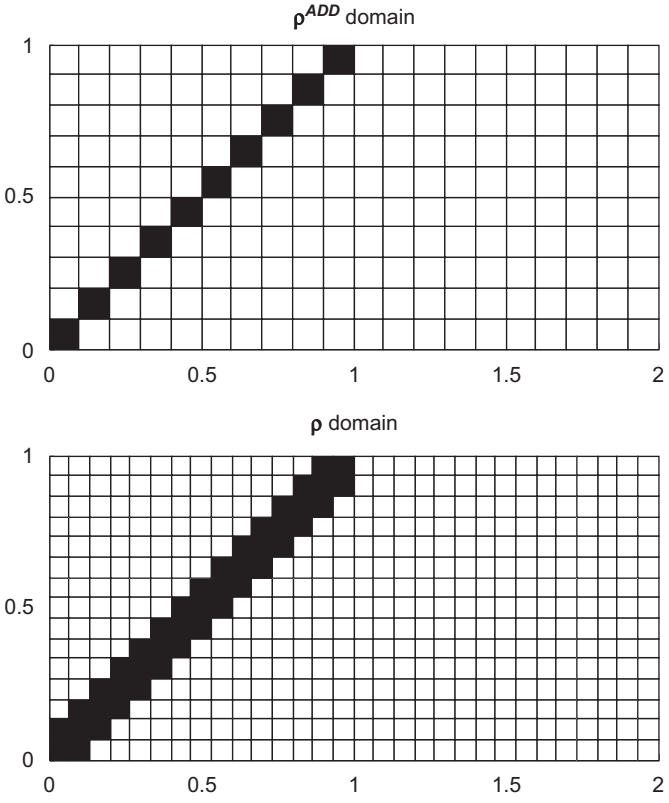

Fig. 5. Mapping between ADD grid and ground element densities $\boldsymbol{\rho}^0 = \mathbf{0.25}$.

As mentioned in [16] that the ADD technique is not only capable of preventing checkerboards on a structural topology but it also reduces the number of design variables. With the decreased number of design variables, the design results obtained from using the EAs are improved. However, it has also been shown that the higher resolution of topological design variables always results in the better structural topology if the optimiser is powerful enough. Due to this observation, the work in this paper presents the use of multiple resolutions of the ADD design variables in one optimisation run. The design strategy is to start with using the lowest resolution ADD design variables in the early iterations. Then, as the optimisation process continues, the resolution of the design variables increases. Such a design strategy is achievable by using the transformation equations (1) and (3). The use of Eq. (1) is for changing the resolution of the design variables during the optimisation process while Eq. (3) is used for checkerboard suppression.

Fig. 6 demonstrates the idea of how the MRDV work. The figure displays four different grid resolutions on the same rectangular design domain. The first and lowest resolution grid (defined as $\boldsymbol{\rho}^{\mathrm{ADD1}}$) is an ADD grid with 10×5 elements. The second ADD grid ($\boldsymbol{\rho}^{\mathrm{ADD2}}$) is the second set of ADD design variables, which has 14×7 elements. The third grid ($\boldsymbol{\rho}^{\mathrm{ADD3}}$) with 20×10 elements is also an ADD grid whereas the fourth grid having 30×15 elements is created for ground FEs ($\boldsymbol{\rho}^{e}$). The transformation between the grids can be achieved by using the transformation matrix in (1). For example, with the known vector $\boldsymbol{\rho}^{\mathrm{ADD1}}$, the values of $\boldsymbol{\rho}^{\mathrm{ADD2}}$ on the second ADD grid can be estimated as

$$\boldsymbol{\rho}^{\mathrm{ADD2}}_{98\times 1} = \mathbf{T}^{12}_{98\times 50}\boldsymbol{\rho}^{\mathrm{ADD1}}_{50\times 1} \tag{4}$$

where $\mathbf{T}^{12}$ is a transformation matrix sized 98×50.

Similarly, the values of element density on the third ADD design domain can be computed as

$$\boldsymbol{\rho}^{\mathrm{ADD3}}_{200\times 1} = \mathbf{T}^{23}_{200\times 98}\boldsymbol{\rho}^{\mathrm{ADD2}}_{98\times 1} \tag{5}$$

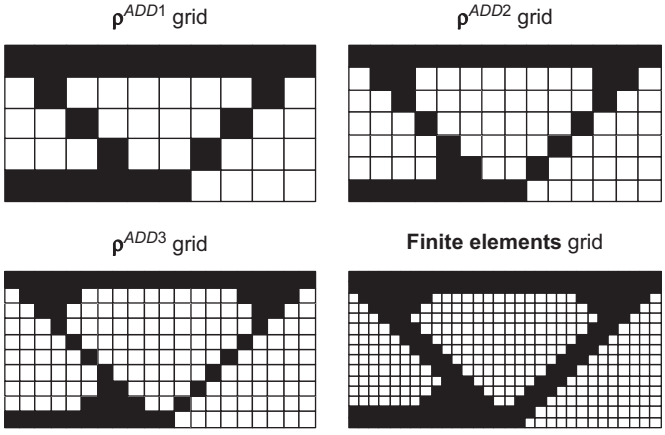

Fig. 6. Transformation of multiresolution design variables.

or

$$\boldsymbol{\rho}^{\mathrm{ADD3}}_{200\times 1} = \mathbf{T}^{23}_{200\times 98}(\mathbf{T}^{12}_{98\times 50}\boldsymbol{\rho}^{\mathrm{ADD1}}_{50\times 1}). \tag{6}$$

The last transformation is carried out to find the values of ground FE density, which can be computed as

$$\boldsymbol{\rho}^{e}_{300\times 1} = round(\mathbf{T}_{300\times 200}\boldsymbol{\rho}^{\mathrm{ADD3}}_{200\times 1} + \boldsymbol{\rho}^{0}). \tag{7}$$

The pre-process is required for computing the ADD and ground element grids as well as all the transformation matrices and the value of ρ^0. Fig. 6 shows the transformations from $\boldsymbol{\rho}^{\mathrm{ADD1}}$ to $\boldsymbol{\rho}^{\mathrm{ADD2}}$, and then from $\boldsymbol{\rho}^{\mathrm{ADD2}}$ to $\boldsymbol{\rho}^{\mathrm{ADD3}}$ and finally from $\boldsymbol{\rho}^{\mathrm{ADD3}}$ to $\boldsymbol{\rho}^{e}$. A particular binary design solution is defined on the $\boldsymbol{\rho}^{\mathrm{ADD1}}$ design domain. It is then transformed to the second and third ADD domains as shown in the figure. The last stage is the transformation of density values from the third design domain to the ground element domain where $\boldsymbol{\rho}^0 = \mathbf{0.25}$. It can be seen that checkerboard-like topologies can occur on the ADD design domains but they disappear on the FE grid by using the transformation (3).

For topology optimisation using SA, the search procedure starts with the lowest resolution ADD design variables (here is $\boldsymbol{\rho}^{\mathrm{ADD1}}$). As the searching process continues for a number of iterations, it is expected that the SA algorithm using such low resolution design variables can quickly find the design solutions close to the optimum. The higher resolution of design variables $\boldsymbol{\rho}^{\mathrm{ADD2}}$ is then applied so as to refine the optimum results obtained from using $\boldsymbol{\rho}^{\mathrm{ADD1}}$. As the optimisation process continues, the resolution of design variables is increased. The procedure is terminated when the termination condition is met. In the pre-processing step, a designer needs to define how many grid resolutions of the ADD design variables should be used. The resolution of each grid level and the resolution of ground FEs are also predetermined. Apart from that, the number of iteration and population size for each level of ADD design variables must be assigned in the initial stage. The searching performance depends on the aforementioned parameters and the evolutionary optimiser being used. Since the ADD design variables are encoded as binary strings, mutation of a vector of design variables can be achieved in such a way that a randomly selected bit position is changed to `1' if its current value is `0' or vice versa. This is said to be a common mutation for binary codes [16], which can be applied to any ADD grid resolution.

4. Test problems

In order to examine the efficiency and effectiveness of the proposed numerical strategy, five topology optimisation problems are

Please cite this article as: S. Bureerat, J. Limtragool, Structural topology optimisation using simulated annealing with multiresolution design variables, Finite Elem. Anal. Des. (2008), doi: 10.1016/j.finel.2008.04.002

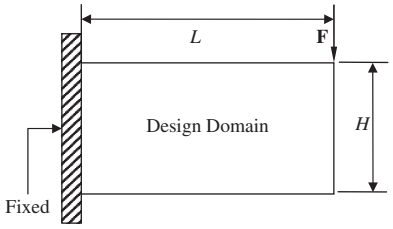

Fig. 7. Cantilever plate.

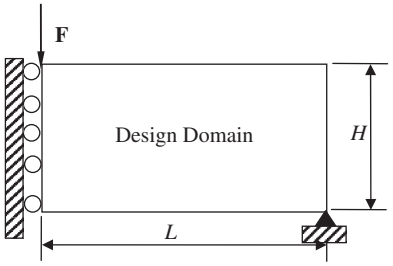

Fig. 8. MBB beam.

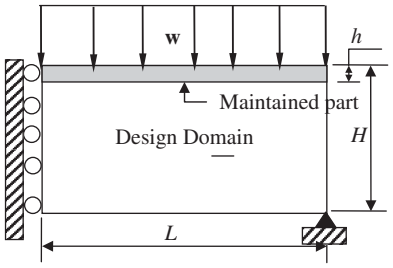

Fig. 9. 2D bridge.

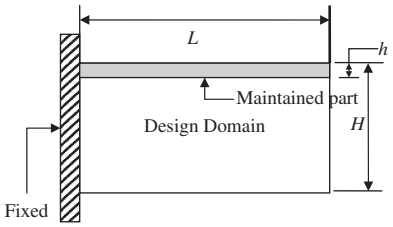

Fig. 10. Cantilever plate for dynamic stiffness maximisation.

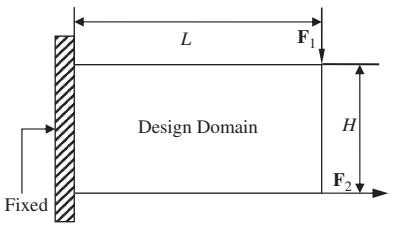

Fig. 11. Cantilever plate with two load-cases.

assigned and used for performance comparison. The structural design domains used for the five design problems are illustrated in Figs. 7–11. The problems are detailed as follows:

OPT1

$$\min : \left(\frac{m}{m_{\max}}\right)^{w_1}\left(\frac{c}{c_{\max}}\right)^{w_2}$$

where m is the structural mass, c the structural compliance due to the applied load $\mathbf{F}$ and w_1 and w_2 are the degrees of importance for the mass and compliance, respectively.

Fig. 7 shows the structure used for the test problem OPT1. The structure is made up of a material with $E=200\times10^9$ N/m^2 and $\nu=0.3$ where $L=2$ m and $H=1$ m. The elements' densities here mean the elements' thicknesses since the four-node membrane FE model is employed. The value of ρ^0 is set to be 0.25. The thickness value of the ith element is decoded to be 0.00001 if $\rho_i^e=0$; otherwise, it is set to be 1 (from thousands of FE analyses in the optimisation process, the stiffness matrix is always invertible although the difference between maximum and minimum thicknesses is large). The parameter $m_{\max}$ is a structural mass where the vector $\boldsymbol{\rho}^e$ is full of ones ($\boldsymbol{\rho}^e=\mathbf{1}$). The value $c_{\max}$ is a structural compliance where the vector $\boldsymbol{\rho}^e$ is full of zeros ($\boldsymbol{\rho}^e=\mathbf{0}$). The degrees of importance for mass and compliance are set as: $w_1=1$ and $w_2=1$.

Figs. 8 and 9 show an MBB beam and 2D bridge used for the test problems OPT2 and OPT3, respectively. The optimisation problems, FE model, structural material and dimensions used in OPT2 and OPT3 are similar to those applied in OPT1 where the dimension h of the 2D bridge is set to be $\frac{1}{15}$ m.

OPT4

$$\min : \left(\frac{m}{m_{\max}}\right)^{w_1}\left(\frac{\lambda}{\lambda_{\max}}\right)^{w_2}$$

where m is the structural mass, λ is the first eigenvalue from solving free vibration of a structure and w_1 and w_2 are the degrees of importance for the mass and eigenvalue, respectively.

The design domain of OPT4 is displayed in Fig. 10. The parameters $m_{\max}$ and $\lambda_{\max}$ are the structural mass and eigenvalue at which all of the elements' densities are equal to ones ($\boldsymbol{\rho}^e=\mathbf{1}$). The FE model, structural material, and dimensions are similar to those used in OPT1. The dimension h is set to be $\frac{1}{15}$ m. The degrees of importance for structural mass and eigenvalue are assigned as: $w_1=2$ and $w_2=1$.

OPT5

$$\min : \left(\frac{m}{m_{\max}}\right)^{w_1}\left(\frac{c_1}{c_{1,\max}}\right)^{w_2}\left(\frac{c_2}{c_{2,\max}}\right)^{w_3}$$

where m is the structural mass, c_1 the structural compliance due to the applied load case $\mathbf{F}_1$, c_2 the structural compliance due to the applied load case $\mathbf{F}_2$ and w_1, w_2 and w_3 are the degrees of importance for the mass and compliances due to the load cases $\mathbf{F}_1$ and $\mathbf{F}_2$, respectively.

This test problem has two applied load cases, $\mathbf{F}_1$ and $\mathbf{F}_2$, as shown in Fig. 11. The FE model, design domain, structural material and dimensions are similar to those used in OPT1. The parameter $m_{\max}$ is a structural mass where $\boldsymbol{\rho}^e=\mathbf{1}$. The values $c_{1,\max}$ and $c_{2,\max}$ are structural compliances due to $\mathbf{F}_1$ and $\mathbf{F}_2$, respectively, where $\boldsymbol{\rho}^e=\mathbf{0}$. The degrees of importance for mass and compliances are set as: $w_1=5$, $w_2=1$ and $w_3=1$.

The first three design problems are said to be compliance minimisation while the fourth topological design problem can be classified as the maximisation of structural dynamic stiffness. The last problem is the minimisation of structural compliance due to two applied load cases. FE grid resolution is set to be 30×15 elements. There are three different resolutions of ADD design variables grid used in this study, 10×5, 14×7 and 20×10 as displayed in Fig. 6. As the mutation operator used with SA can result in multiple disconnected parts on a topology, the chromosome repairing technique presented in [15] is therefore employed to deal with this undesirable occurrence. The function evaluation starts with defining thickness values on the ADD domain. They are then transformed to be FE thicknesses by using the process detailed in Section 3. The chromosome repairing operator is also activated in cases where the resulting topology has many disconnected parts.

Please cite this article as: S. Bureerat, J. Limtragool, Structural topology optimisation using simulated annealing with multiresolution design variables, Finite Elem. Anal. Des. (2008), doi: 10.1016/j.finel.2008.04.002

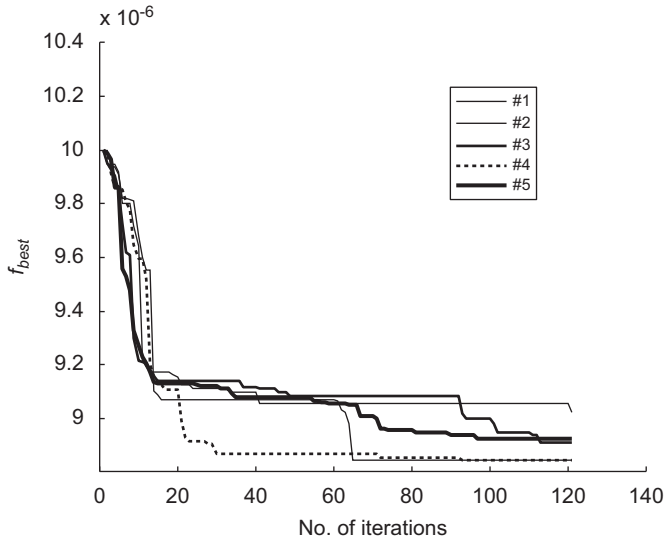

Fig. 12. Search history of OPT1 using design variables with 10×5 grid resolution.

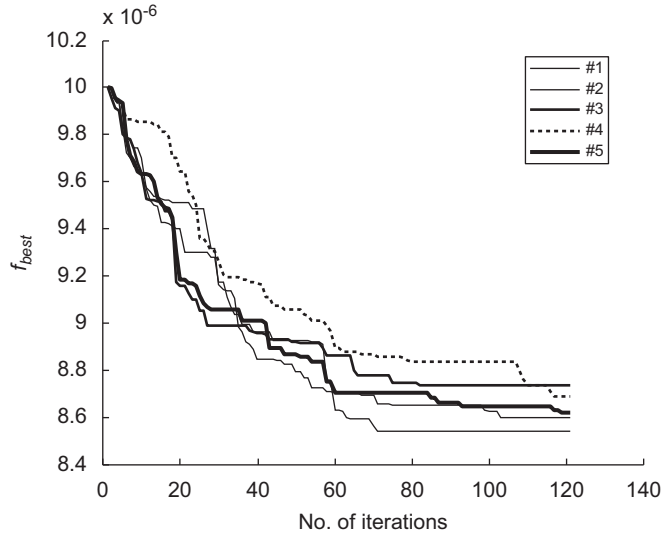

Fig. 13. Search history of OPT1 using design variables with 14×7 grid resolution.

In order to examine the impact of different resolutions of the ADD design variables on the searching performance, a primary investigation is made. Fig. 12 displays the search history of using SA with the 10×5 ADD grid for solving OPT1 five times. The total number of iterations is set to be 120 while five individuals are created from mutating on $\mathbf{x}_{\text{parent}}$ and another five individuals are obtained from mutating on $\mathbf{x}_{\text{best}}$. From the five search histories, it can be seen that the objective function value decreases rapidly in the early iterations (say 20 iterations). Afterwards, it remains rather constant or slightly decreased as the optimisation process carries on. The five search histories of using SA with the ADD grid of 14×7 elements are plotted in Fig. 13. Similarly to Fig. 12, it can be observed that the objective function value reduces rapidly in the early iterations (say 40–60 iterations) and then remains rather constant or slightly reduced. For the search histories of using SA with the 20×10 ADD grid for solving OPT1 five times, the search histories tend to be similar to the first two cases but it seems that 120 iterations are insufficient for these high resolution design variables. From this comparison, it can be said that the higher resolution needs more iterations to reach or become close to the optimum. However, the higher resolution design variables provide wider design space and can lead to a better topology.

Table 1
Design conditions

DSV	ADD grid resolutions	No. of iterations	Population size	SA strategies
DSV1	10×5	120	10	SA1
DSV2	14×7	120	10	SA2
DSV3	20×10	120	10	SA3
DSV4	10×5, 14×7	40,80	10	SA4
DSV5	10×5, 20×10	40,80	10	SA5
DSV6	10×5, 14×7, 20×10	20,40,60	10	SA6

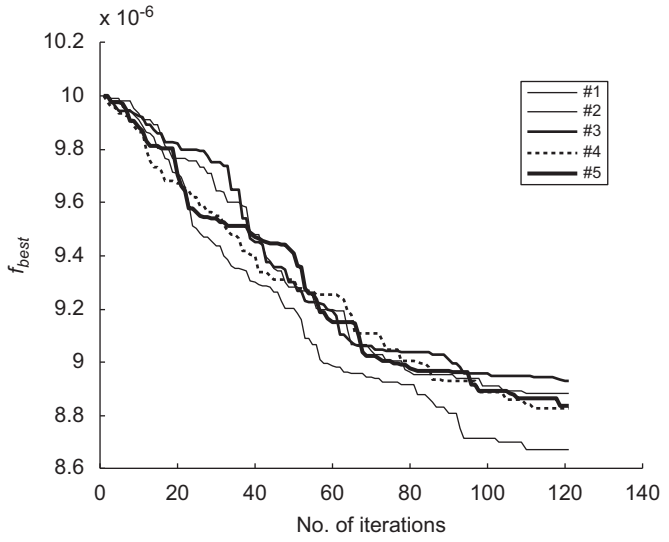

Fig. 14. Search history of OPT1 using design variables with 20×10 grid resolution.

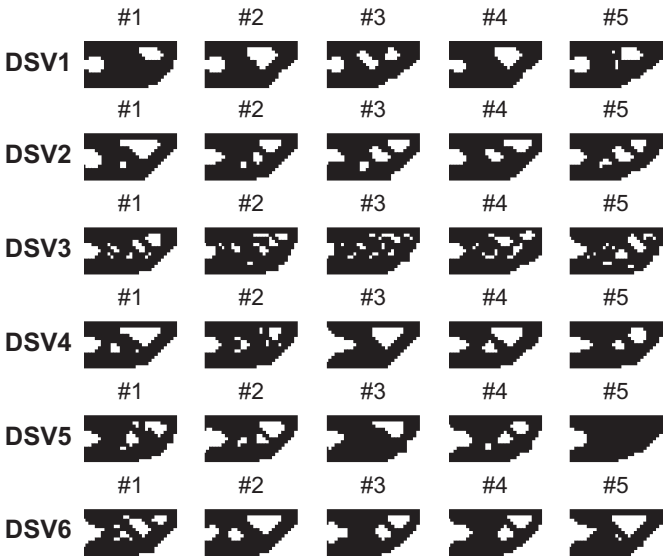

Fig. 15. Optimum topologies of OPT1 obtained from the various SA strategies.

From the primary study, the conditions for using MRDV are assigned as shown in Table 1. The sets of design variables DSV1, DSV2 and DSV3 use single resolution of design variables whereas DSV4, DSV5 and DSV6 use multiple resolution grids of design variables as detailed in the table. The sets of number of iterations assigned for DSV4–6 are obtained from the observation on Figs. 12–14. The SA strategy for the DSV*i* design variables set is termed SA*i* as in the table.

Please cite this article as: S. Bureerat, J. Limtragool, Structural topology optimisation using simulated annealing with multiresolution design variables, Finite Elem. Anal. Des. (2008), doi: 10.1016/j.finel.2008.04.002

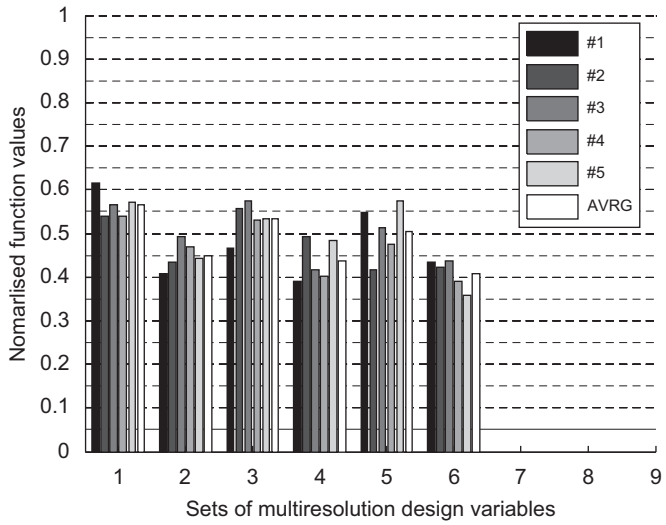

Fig. 16. Comparison of objective function values of OPT1 from the various optimisers.

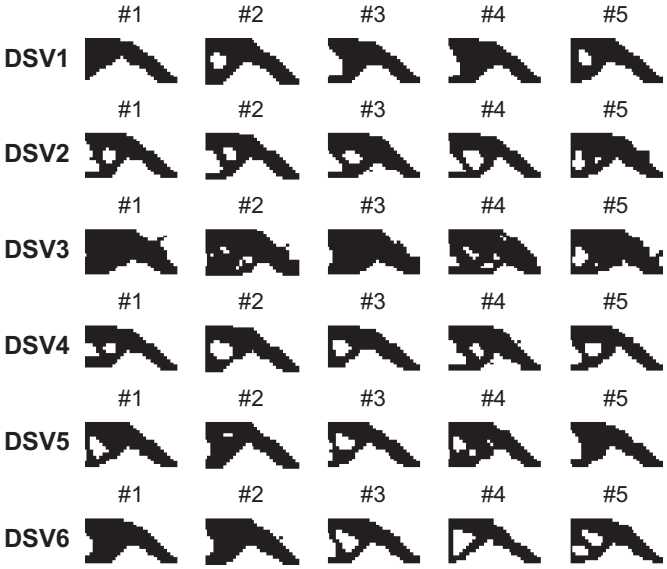

Fig. 18. Optimum topologies of OPT2 obtained from the various SA strategies.

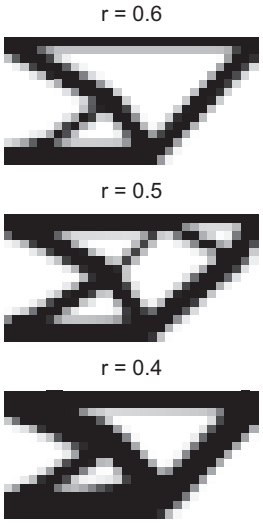

Fig. 17. Optimum topologies of the design domain of OPT1 from using the SIMP approach.

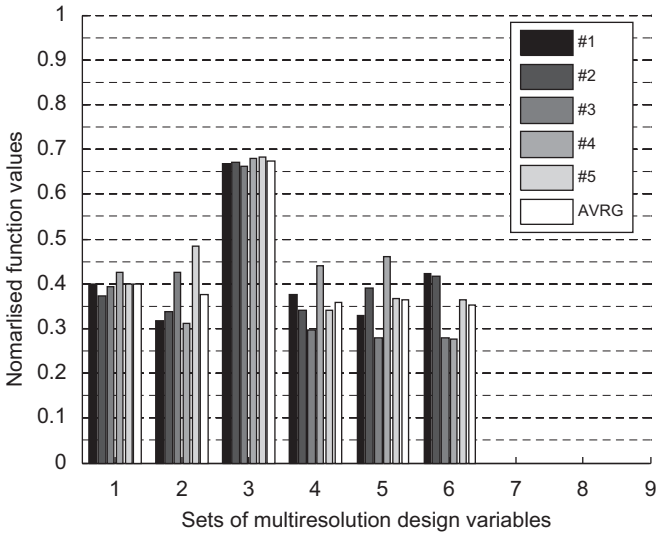

Fig. 19. Comparison of objective function values of OPT2 from the various optimisers.

Each SA strategy is implemented to solve the test problems five optimisation runs so that its convergence rate and consistency can be measured and compared to the other SA search strategies. The population size (the number of children created on each loop) is set to be 10 as five solutions are created from mutating on $\mathbf{x}_{\text{parent}}$ and other five solutions are obtained from mutating on $\mathbf{x}_{\text{best}}$. For each test problem, the six optimisation strategies start with the same initial solution. The solution $\mathbf{x}_{\text{best}}$ obtained at the last iteration is said to be the optimum solution.

5. Optimum results and performance comparison

The optimum topologies of OPT1 obtained from using the various SA strategies are displayed in Fig. 15. Five structural topologies are obtained from each SA strategy as it was operated for five simulation runs. The comparison of the objective function values of the various topologies is given in Fig. 16. In the figure there are six groups of bar charts. In each group the first five bars represent the normalised objective values of the five topologies from five optimisation runs. The sixth (white) bar is the mean value of the five normalised objective values. From the bar chart comparison, SA with DSV6 gives the best results while the second best results are from using SA with DSV4. This implies that the use of multiple resolution grids of design variables improve the search performance of SA. For SA using the single resolution design variables (DSV1–3), SA2 gives the best results while SA1 is the second best. This implies that the predefined 120 iterations and population size 10 are suitable for the DSV2 resolution while the resolution of DSV3 is too high for these design conditions. Fig. 17 displays the topologies obtained from using the gradient-based OCM (the SIMP approach) [5,8] where the ratio of mass reduction is set to be 40%, 50% and 60%. The topologies in Fig. 17, although obtained from different design approaches, look similar to most of the topologies depicted in Fig. 15.

The structural topologies obtained from solving OPT2 using the various SA optimisers are shown in Fig. 18 whereas the bar charts comparing their objective values are given in Fig. 19. According to the comparison, the SA method using DSV6 gives the best results

Please cite this article as: S. Bureerat, J. Limtragool, Structural topology optimisation using simulated annealing with multiresolution design variables, Finite Elem. Anal. Des. (2008), doi: 10.1016/j.finel.2008.04.002

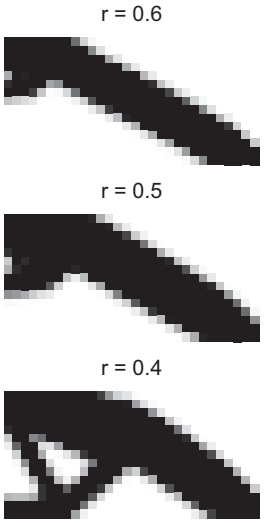

Fig. 20. Optimum topologies of the design domain of OPT2 from using the SIMP approach.

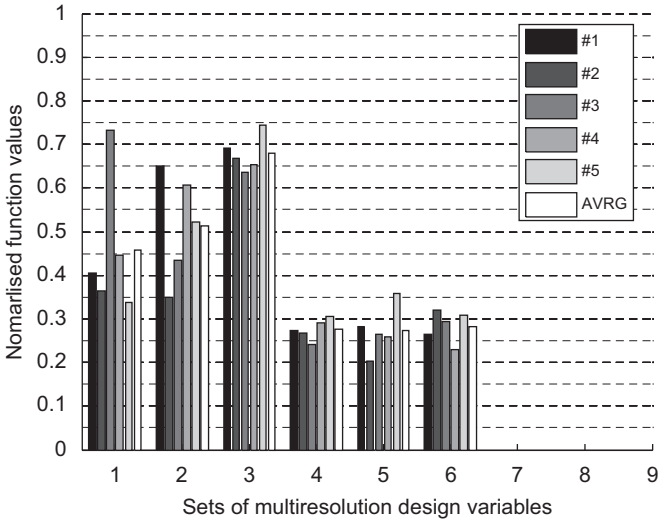

Fig. 22. Comparison of objective function values of OPT3 from the various optimisers.

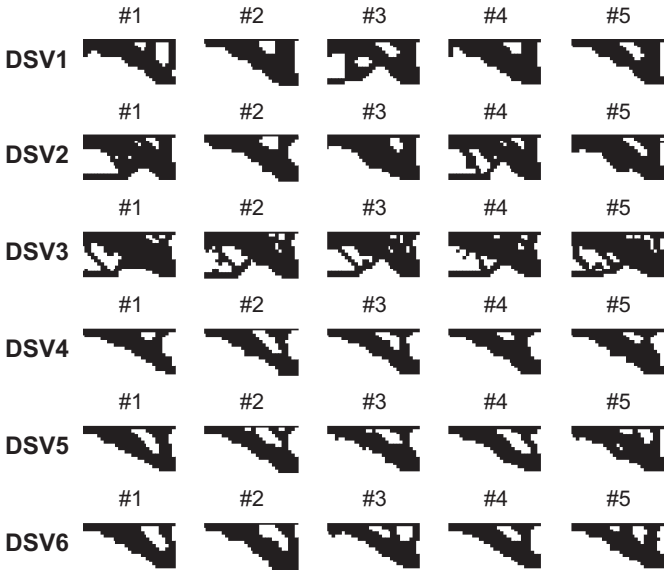

Fig. 21. Optimum topologies of OPT3 obtained from the various SA strategies.

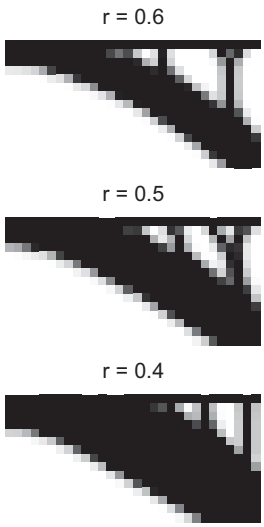

Fig. 23. Optimum topologies of the design domain of OPT3 from using the SIMP approach.

whereas the close second and third best methods are SA4 and SA5, respectively. The design variables grid DSV2 is the best in cases of using a single resolution. The optimum topologies obtained from using OCM with mass reduction ratios of 40%, 50% and 60% are displayed in Fig. 20. It can be observed that the topologies in the figure look similar to those shown in Fig. 18.

The optimum topologies of OPT3 obtained from using the various SA strategies are shown in Fig. 21 while the performance comparison is given in Fig. 22. According to their objective values, the SA method using DSV5 is the best strategy while the very close second and third best strategies are SA with DSV4 and DSV6, respectively. The optimum topologies obtained from using OCM with the mass reduction ratios of 40%, 50% and 60% are displayed in Fig. 23. The topologies in Figs. 21 and 24, although obtained from the different approaches, mostly look similar.

The topologies obtained from solving OPT4 by using the different SA strategies are given in Fig. 24 while the comparison of their objective values is displayed in Fig. 25. According to the performance comparison, the best SA strategy is SA with the use of DSV6 while the second best is SA with DSV4. The optimum topologies obtained from the SIMP approach with the derivative filtering technique are displayed in Fig. 26 where the mass reduction ratio is set to be 40%, 50% and 60%. It can be seen that the topologies obtained from the present approach and from using OCM are slightly different.

The structural topologies obtained from solving OPT5 by using different SA strategies are displayed in Fig. 27 whereas the performance comparison is illustrated in Fig. 28. From the comparison, SA with the use of DSV6 gives the best results while the SA using DSV5 is the second best. The optimum topologies from using OCM with the mass reduction ratio of 40%, 50% and 60% are illustrated in Fig. 29. The topologies from Figs. 27 and 29 are slightly different. In this design problem, the one-node connected part cannot be completely suppressed.

Overall, the best method is SA using DSV6 which uses three resolutions of design variables. The second best method is SA with DSV4 while the third best is SA with the use of DSV5. It can be said that the use of multiple resolutions of design variables help enhancing

Please cite this article as: S. Bureerat, J. Limtragool, Structural topology optimisation using simulated annealing with multiresolution design variables, Finite Elem. Anal. Des. (2008), doi: 10.1016/j.finel.2008.04.002

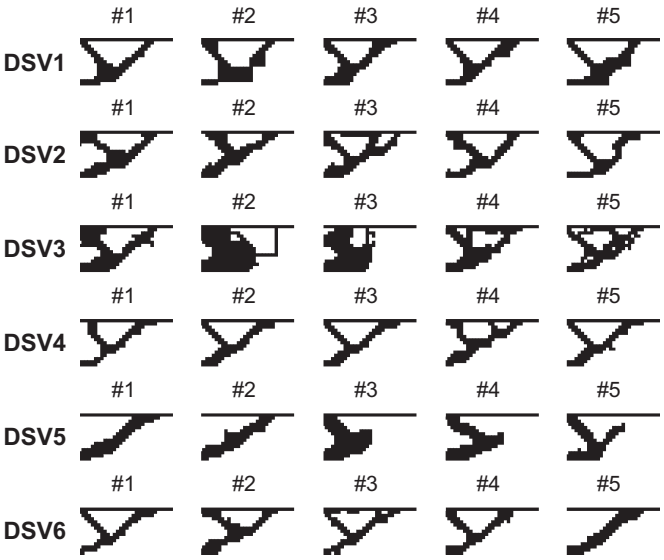

Fig. 24. Optimum topologies of OPT4 obtained from the various SA strategies.

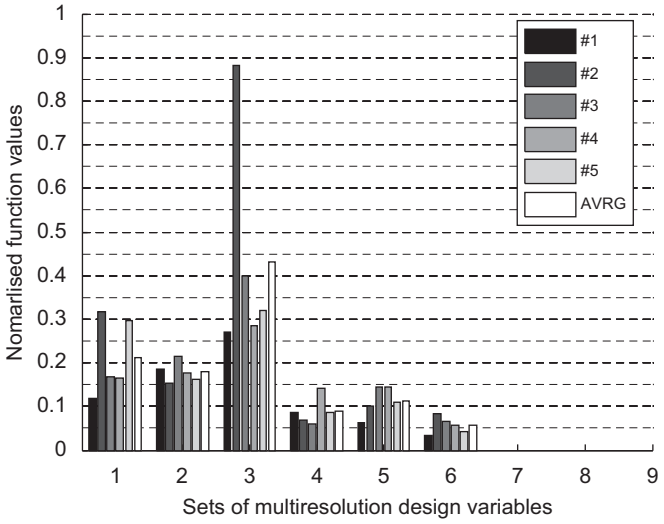

Fig. 25. Comparison of objective function values of OPT4 from the various optimisers.

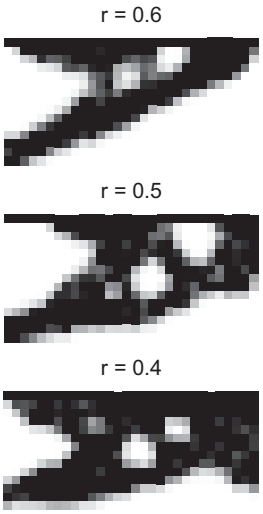

Fig. 26. Optimum topologies of the design domain of OPT4 from using the SIMP approach.

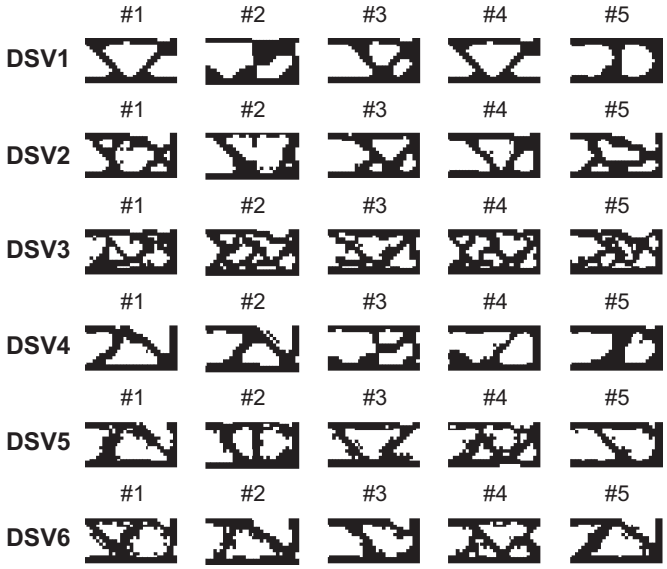

Fig. 27. Optimum topologies of OPT6 obtained from the various SA strategies.

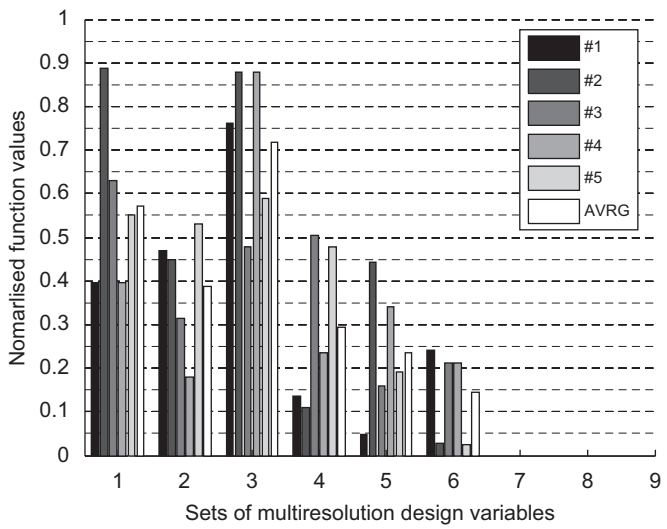

Fig. 28. Comparison of objective function values of OPT6 from the various optimisers.

the searching performance of SA. The more resolutions used leads to the better searching performance if the set of iteration numbers and ADD grids are defined properly. For the SA methods using single design variables grid DSV1–3, the best design variables grid is DSV2 which has 14×7 variables. The second best design variables set is DSV1. The total number of design variables of DSV3 which is 20×10 is too large for the proposed SA method with the given iteration number and population size.

The new design problems combining with the use of MRDV for structural topology optimisation are said to be effective. The approach, however, has some drawbacks, i.e. we need some prior knowledge to specify the degrees of importance used in the objective functions, the design variables resolution and the iteration number for each design variables resolution. Nevertheless, from Figs. 12–14 and the observation on the other design test problems, it can be said that the convergence rate of SA is somewhat related to the number design variables and population size. For example, with 10×5 design variables and population sized 10, the SA method can reach or get close to the optimum approximately within 20 iterations. If

Please cite this article as: S. Bureerat, J. Limtragool, Structural topology optimisation using simulated annealing with multiresolution design variables, Finite Elem. Anal. Des. (2008), doi: 10.1016/j.finel.2008.04.002

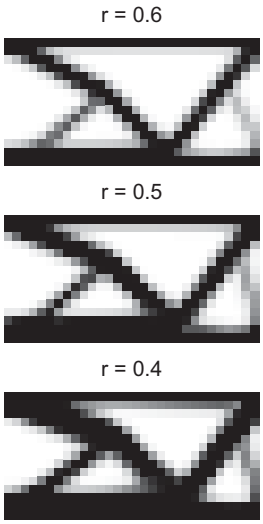

Fig. 29. Optimum topologies of the design domain of OPT6 from using the SIMP approach.

the number of design variables is increased to 14×7 variables, the SA method needs at least 40–80 loops to become close to the optimum topology. With sufficient prior knowledge and experience, the MRDV and the iteration numbers can be set properly.

6. Conclusions and discussion

The algorithm of SA has been detailed and used for structural topology optimisation. The ADD technique is used for checkerboard suppression. MRDV are proposed to be used with SA for solving topological design problems. From the numerical test, it can be concluded that the use of MRDV results in the enhanced performance of the SA optimisation method. The optimum results obtained from using SA are said to be comparable to those obtained from using the classical gradient-based approach. The checkerboard suppression by means of the ADD technique is acceptable although there remain some one-node connected parts on the resulting topologies of OPT5.

Acknowledgements

The authors are grateful for the support from the Thailand Research Fund (TRF).

References

[1] A.R. Yildiz, N. Kaya, F. Ozturk, O. Alanku, Optimal design of vehicle components using topology design and optimization, Int. J. Vehicle Des. 34 (2004) 387–398.
[2] A. Boonapan, S. Bureerat, J. Limtragool, S. Inban, Multi-level design of an automotive part, in: 19th Conference of Mechanical Engineering Network of Thailand, Phuket, Thailand, 2005, pp. 172–177 (in Thai).
[3] S. Bureerat, A. Boonapan, T. Kunakote, J. Limtragool, Design of compliance mechanisms using topology optimisation, in: 19th Conference of Mechanical Engineering Network of Thailand, Phuket, Thailand, 2005, pp. 421–427.
[4] Z. Luo, L. Chen, J. Yang, Y. Zhang, K. Abdel-Malek, Compliance mechanism design using multi-objective topology optimization scheme of continuum structures, Struct. Multidisciplinary Optim. 30 (2005) 142–154.
[5] M.P. Bendsoe, O. Sigmund, Topology Optimization: Theory, Methods and Applications, Springer, Berlin, 2003.
[6] K. Suzuki, N. Kikuchi, A homogenization method for shape and topology optimization, Comput. Methods Appl. Mech. Eng. 93 (1991) 291–318.
[7] Y.M. Xie, G.P. Steven, Evolutionary Structural Optimization, Springer, Berlin, 1997.
[8] O. Sigmund, A 99 line topology optimization code written in MATLAB, Struct. Multidisciplinary Optim. 21 (2001) 120–127.
[9] D. Fujii, N. Kikuchi, Improvement of numerical instabilities in topology optimization using the SLP method, Struct. Multidisciplinary Optim. 19 (2000) 113–121.
[10] C. Kane, F. Jouve, M. Schoenauer, Structural topology optimization in linear and nonlinear elasticity using genetic algorithms, in: 21st ASME Design Automatic Conference, Boston, 1995.
[11] C. Kane, M. Schoenauer, Topological optimum design using genetic algorithms, Control Cybern. 25 (1996) 1059–1088.
[12] S.Y. Wang, K. Tai, Graph representation for structural topology optimization using genetic algorithms, Comput. Struct. 82 (2004) 1609–1622.
[13] M. Jakiela, C. Chapman, J. Duda, A. Adewuya, K. Saitou, Continuum structural topology design with genetic algorithms, J. Comput. Methods Appl. Mech. Eng. 86 (2000) 339–356.
[14] S.Y. Woon, L. Tong, O.M. Querin, G.P. Steven, Effective optimisation of continuum topologies through a multi-GA system, Comput. Methods Appl. Mech. Eng. 194 (2005) 3416–3437.
[15] J.A. Madeiraa, H.C. Rodriguesa, H. Pinam, Multiobjective topology optimization of structures using genetic algorithms with chromosome repairing, Struct. Multidisciplinary Optim. 32 (2006) 31–39.
[16] S. Bureerat, J. Limtragool, Performance enhancement of evolutionary search for topology optimization, Finite Elem. Anal. Des. 42 (2006) 547–566.
[17] S. Bureerat, T. Kunakotem, Topological design of structures using population-based optimization methods, Inverse Probl. Sci. Eng. 14 (2006) 589–607.
[18] Y.S. Patrick, S. Manoochehri, Generating optimal configurations in structural design using simulated annealing, Int. J. Numer. Methods Eng. 40 (1997) 1053–1069.
[19] G.Y. Cui, K. Tai, B.P. Wang, Topology optimization for maximum natural frequency using simulated annealing and morphological representation, AIAA J. 40 (3) (2002) 586–589.
[20] S. Kirkpatrik, C.D. Gelatt Jr., M.P. Vecchi, Optimization by simulated annealing, J. Sci. 220 (1983) 671–680.
[21] A. Suppapitnarm, K.A. Seffen, G.T. Parks, P.J. Clarkson, A simulated annealing algorithm for multiobjective optimization, Eng. Optim. 33 (2000) 59–85.
[22] W.A. Benage, A.K. Dhingra, Single and multiobjective structural optimization in discrete-continuous variables using simulated annealing, Int. J. Numer. Methods Eng. 38 (1994) 2753–2773.

Please cite this article as: S. Bureerat, J. Limtragool, Structural topology optimisation using simulated annealing with multiresolution design variables, Finite Elem. Anal. Des. (2008), doi: 10.1016/j.finel.2008.04.002

Population-Based Incremental Learning for Multiobjective Optimisation

Sujin Bureerat and Krit Sriworamas

Department of Mechanical Engineering, Faculty of Engineering, Khon Kaen University, Thailand, 40002
sujbur@kku.ac.th

Abstract. The work in this paper presents the use of population-based incremental learning (PBIL), one of the classic single-objective population-based optimisation methods, as a tool for multiobjective optimisation. The PBIL method with two different updating schemes of its probability vectors is presented. The performance of the two proposed multiobjective optimisers are measured and compared with four other established multiobjective evolutionary algorithms i.e. niched Pareto genetic algorithm, version 2 of non-dominated sorting genetic algorithm, version 2 of strength Pareto evolutionary algorithm, and Pareto archived evolution strategy. The optimisation methods are implemented to solve 8 bi-objective test problems where design variables are encoded as a binary string. The Pareto optimal solutions obtained from the various methods are compared and discussed. It can be concluded that, with the assigned test problems, the multiobjective PBIL methods are comparable to the previously developed algorithms in terms of convergence rate. The clear advantage in using PBILs is that they can provide considerably better population diversity.

Keywords: Multiobjective Evolutionary Optimisation, Population-Based Incremental Learning, Non-dominated Solutions, Pareto Archive, Performance Comparison.

1 Introduction

In the past, the well-established optimisation methods were mostly developed for single-objective optimisation. They can, however, be employed to solve a multiobjective problem by using numerical strategies such as the weighted-sum technique [14], global criteria method [9] and normalised normal constraint technique [15]. The principle of such numerical strategies is to convert an optimisation problem with multiple design objectives to be a single-objective problem to suit the available optimisers. This means that the optimisation methods need to be performed for as many simulation runs as the number of Pareto optimal points required.

Optimisation methods can be classified as methods with and without using function derivatives. In comparison of EAs, the methods without using derivatives, to the derivative-based methods, the latter are far superior in terms of convergence rate and consistency. Nevertheless, using EAs are advantageous in that they can deal with all kinds of design variables [2], and most importantly the multiobjective evolutionary methods can search for a set of Pareto optimum points within one attempt whereas the

A. Saad et al. (Eds.): Soft Computing in Industrial Applications, ASC 39, pp. 223–232, 2007.
springerlink.com

gradient-based techniques need many operations. Although having such benefits, the evolutionary methods are still not as powerful as expected due to a complete lack of consistency and low convergence rate. Since there is no convergence guaranteed, the results obtained from using an EA are mostly classified as an approximated Pareto front.

In recent years, a number of evolutionary algorithms have been developed as multiobjective optimisers and they are termed multiobjective evolutionary algorithms (MOEAs). In the early days, the well-known methods were, for example, vector evaluation genetic algorithm (VEGA) [16], multiobjective genetic algorithm (MOGA) [7] and none-dominated sorting genetic algorithm (NSGA) [18]. Later, there have been numerous new algorithms developed. Some work on comparing their performance has been made e.g. in [20] and [22]. The development of new approaches, improvement of the existing algorithms, and implementation of the methods on real world applications are still a great challenge.

The work in this paper is aimed at developing population-based incremental learning (PBIL), one of the classical single-objective EAs, as a tool for multiobjective optimisation. The proposed algorithm is said to be a mix of some advantages of the predecessors. Two PBIL algorithms with different probability vector updating procedures are presented: one is modified from that presented in [12] while the other one deals with the weighted-sum technique. The two proposed optimisers along with four recently developed MOEAs including NPGA [4] [10] and [11], NSGAII [6], SPEA2 [21] and PAES [13] are implemented to solve 8 bi-objective test problems. Design variables are encoded as a series of binary strings. The performances of the optimisers are measured, compared and discussed. It can be concluded that, with the given design conditions, the PBILs are said to be as good as some of the existing MOEAs in terms of convergence rate, and superior to them when considering population diversity.

2 Multiobjective Optimisation

A particular multiobjective design problem can be posed as:

Find **x** such that

Min: $\mathbf{f} = \{f_1(\mathbf{x}),\ldots,f_m(\mathbf{x})\}$
Subject to
$g_i(\mathbf{x}) \le 0$
$h_i(\mathbf{x}) = 0$

MOEAs are normally created to deal with unconstrained optimisation; however, they can be applied to constrained problems by using a penalty function technique. Moreover, the non-dominated scheme for constrained optimisation given in reference [5] is found to be greatly efficient and effective. All of the evolutionary methods mentioned in this paper are categorised as Pareto-based methods. The basic concept of exploring Pareto optimum points via such an algorithm is that, on each generation while a new population is created, non-dominated solutions are classified and carried on to the next generation. The term, non-dominated solutions, defines the local Pareto solutions among the members of the current population during evolutionary search.

3 PBIL for Multiobjective Design

The original PBIL algorithm is based upon binary searching space similar to GAs [1]. Later, there has been further development of PBIL for continuous and discrete design spaces [8], [17] and [19]. The method is classified as an estimation of distribution algorithm (EDA) that achieves its search through probability estimation and sampling techniques. The application of PBIL to multiobjective design has been presented in [12] where the approach is named MOSA. The principle of PBIL search can be thought of as iteratively limiting the design space depending on current best design variables and random process. The design space is iteratively narrowed until approaching the optimum. Rather than keeping all binary genes or a population as with GA, the population in PBIL is represented by the probability vector of having '1' at each bit position in the binary strings. For more details, see [1].

Initially, for single objective optimisation, the search procedure starts with the initial probability vector whose elements are full of '0.5'. An initial population corresponding to the probability vector is created. The binary population is decoded and objective values are computed. The best gene, whether it is a minimum or maximum, is chosen to update the next probability vector P_i^{new} using the relation

$$P_i^{new} = P_i^{old}(1 - LR) + b_i LR \tag{1}$$

where $LR \in (0,1)$ is called the learning rate to be defined and b_i is the i^{th} bit of the best binary solution. It is also useful to apply mutation to the probability vector at some predefined probability such that

$$P_i^{new} = P_i^{old}(1 - ms) + \text{rand}(0 \text{ or } 1).ms \tag{2}$$

where ms is the amount of shift used in the mutation. The best solutions are carried over into the next generation ensuring that the best solution during the search is not lost. The probability vector is updated iteratively until convergence is achieved.

When employed as a multiobjective optimiser, more probability vectors should be used in order to obtain a more diverse population; therefore, it is called a probability matrix instead. The search starts with an (empty) external Pareto set and initial probability matrix whose elements are full of '0.5'. Each row of the probability matrix is a probability vector that will be used to create a sub-population. Let N be the number of design solutions in a population, l be the number of probability vectors and n_b be the number of binary bits. The probability matrix, therefore, has the size of $l \times n_b$ where each row of the matrix results in approximately N/l design solutions as one sub-population. Having generated the population and evaluated their corresponding objective values, the non-dominated members sorted from the union set of the current population and the old external Pareto set are taken as a new external Pareto set. If the external Pareto set is full (the number of non-dominated members exceeds the archive size), some solutions are removed from the external Pareto set using the adaptive grid algorithm [13]. The probability matrix and the non-dominated solutions are improved iteratively until some termination criterion is met.

In this paper, two updating schemes for the probability matrix are proposed. The first scheme is quite similar to that presented in [12]. To update a row vector of the probability matrix, $n_0 < N$ binary solutions from the current Pareto archive are

selected at random. The mean value of each i^{th} bit position of the selected binary solutions is computed and used as b_i in equation (1). The mutation (2) is also performed with the given probability.

The second scheme uses the weighted-sum technique. In updating each row of the probability matrix, m weighting factors are generated randomly while the condition $\sum w_i = 1$ is preserved. A binary solution from the union set of the current population and the external Pareto set, which gives the minimum value of the weighted-sum function (3), is chosen to update the row probability vector. The mutation is also allowed to occur by the predefined probability.

$$f_w(\mathbf{b}) = \sum_{i=1}^{m} w_i f_i \tag{3}$$

Selection is performed if the number of non-dominated solutions obtained exceeds the predefined size of the external Pareto set. By using the adaptive grid algorithm, one of the members in the most crowded region is removed from the archive. The crowded regions are updated and the member in the most crowded region is removed iteratively until the number of non-dominated solutions is equal to the size of the archive.

4 Performance Testing

Numerical experiments were made to measure the performances of the proposed PBIL. Six unconstrained bi-objective problems $\mathbf{F}_1$, $\mathbf{F}_2$, $\mathbf{F}_3$, $\mathbf{F}_4$, $\mathbf{F}_5$ and $\mathbf{F}_6$ taken from reference [20] are used to benchmark the presented approaches and the other MOEAs. The optimisation problems are said to cover all aspects of difficulty in approximating a Pareto front via MOEAs [20]. The number of design variables is 30. Two more unconstrained bi-objective test problems, apart from the six test problems previously mentioned, are: $\mathbf{F}_7$ the FON problem in [6], and $\mathbf{F}_8$ the SPH-m problem in [21]. For $\mathbf{F}_8$, the bounds are set to be $x_i \in$ [-5, 5].

The multiobjective evolutionary algorithms i.e. NPGA, NSGAII, SPEA2 and PAES along with PBIL1 and PBIL2 are implemented to solve the bi-objective minimisation problems. The two PBIL strategies are PBIL1 the multiobjective PBIL using the first probability matrix updating scheme, and PBIL2 the multiobjective PBIL using the second probability matrix updating scheme. The algorithms can be categorised as using the crossover-based method (NPGA, NSGA and SPEA), the mutation-based method (PAES) and the estimation of distribution method (PBIL). All of the methods employ a population size of 100 and an iteration number of 100 for every design problem except for the $\mathbf{F}_7$ test-case where the population is sized 30 and the number of iterations is 30. The methods that perform elitism have the archive size of 100. Each design variable is encoded with 30 binary strings unless otherwise specified. Design conditions set for each optimiser are detailed as followed.

NPGA the number of randomly selected individuals for tournament selection is 30, the next generation consists of 50 (15 for $\mathbf{F}_7$) non-dominated solutions and 50 (15 for $\mathbf{F}_7$) members from tournament selection, crossover probability is 1.0 and mutation probability is 0.1.

NSGAII crossover probability is 1.0 and mutation probability is 0.1.
SPEA2 crossover probability is 1.0 and mutation probability is 0.1.
PAES uses (1+1)-PAES and adaptive grid archiving technique.

PBIL1 uses the first probability matrix updating scheme similar to [12], learning rate $LR = 0.5$ (constant), the number of probability vectors $l = 20$, mutation shift $ms = 0.2$ and mutation probability is 0.02.

PBIL2 uses the second probability matrix updating scheme as in equation (3), learning rate $LR = 0.5$ (constant), the number of probability vectors $l = 20$, mutation shift $ms = 0.2$ and mutation probability is 0.02.

Each method is employed to solve each problem over 30 runs while on each operation the non-dominated solutions of the final iteration are taken as the optimal front. The performance assessment is somewhat the same as presented in [20]. Two performance parameters are as follows.

The first indicator is the C value defined as:

$$C(A, B) := \frac{\left|\{\mathbf{b} \in B; \exists\, \mathbf{a} \in A : \mathbf{a} \preceq \mathbf{b}\}\right|}{|B|} \tag{4}$$

From the definition, if $C(A, B) = 1$, all the solutions in B are dominated by or equal to solutions in A whereas $C(A,B) = 0$ implies that none of the solutions in A cover B.

The second criterion is the combination of M_1, M_2 and M_3 whose definitions were given in [20] as

$$M = \frac{M_1}{M_2 + M_3} \tag{5}$$

where M_1 is used to measure the average distance of a set of non-dominated solutions to the true optimal front (lower is better), M_2 is used to measure the front distribution (higher is better), and M_3 is used to measure the extent of the front (higher is better).

Form the relation, a lower value of M means a better Pareto front. Note that the parameter M is proposed as an attempt to have an additional prospective view in evaluating a Pareto front.

The value of the C indicator is used to compare a pair of evolutionary methods. Therefore, there are 6×5 comparisons for a test problem. When solving a test problem, there are 30 M values for each method. The mean value of M is used to interpret the convergence performance.

5 Comparison Results

Fig. 1 (a) displays plots of approximate Pareto fronts of $\mathbf{F}_1$ obtained from the various optimisers. Note that the approximate Pareto front from each method is the best of 30 runs sorted by using C values. Dashed lines are the true optimal Pareto front of $\mathbf{F}_1$. From the figure, the Pareto fronts obtained from PBIL1 and PBIL2 are more evenly distributed than the rest. The Pareto fronts of $\mathbf{F}_2$ from the various methods are shown in Fig. 1 (b). For this design case, the fronts from PBIL1 and PBIL2 are more evenly distributed than those from the other methods. Fig. 2 (a) shows the Pareto fronts of $\mathbf{F}_3$ from the various optimisers. The true optimal front for this problem is

non-contiguous. It is shown that PBIL1 and PBIL2 can explore all the Pareto sub-fronts whereas the fronts obtained from other optimisers cannot cover all sub-fronts.

The Pareto fronts of $\mathbf{F}_4$, multimodal problem, are displayed in Fig. 2 (b). For this test problem, SPEA2 totally outperforms the rest while the second best is PBIL1 and the third best is PBIL2. The fronts from PAES, PBIL1 and PBIL2 are the most evenly distributed. Fig. 3 (a) illustrates the Pareto fronts of the deceptive problem explored by the various optimisers. From the figure, it can be said that using SPEA2 and NSGAII results in better fonts. The approximate Pareto fronts from SPEA2, NSGAII and PAES are the most evenly distributed. Fig. 3 (b) displays the Pareto fronts of $\mathbf{F}_6$ test problem explored by the six algorithms. In this figure, the best Pareto front is that obtained from PBIL1 while the second best is from SPEA2. Fig. 4 (a) displays the Pareto front of $\mathbf{F}_7$ obtained from using the various algorithms. All of the optimisation methods give poor front distribution with PBIL1 being the best. This is caused by the number of iterations and population size being used. The non-dominated fronts of $\mathbf{F}_8$ from using the various optimisers are given in Fig. 4 (b). It can be seen that PBIL2 gives the best front considering the front distribution and the distance from the true optimal front.

The comparison made in the previous two paragraphs is based on observation. The boxplots of C values comparing 6×5 pairs of optimisers are shown in Fig. 5 and 6. From the results, NPGA is less efficient than the others. According to the boxplots, for the first three test problems, all of the methods with the exception of NPGA are said to be equally good. In the $\mathbf{F}_4$ test problem, PBIL1 gives the best results whereas NSGAII and SPEA2 give the best results in the $\mathbf{F}_5$ test problem. NSGAII, SPEA2, PAES and PBIL1 are said to be equally good for the $\mathbf{F}_6$ test problem. SPEA2 is the best method for the case of $\mathbf{F}_7$ while PBIL1 is the close second best. For the $\mathbf{F}_8$ problem, PAES the mutation-based method give the best results whereas PBIL2 is the close second best.

The bar-chart illustration of the M criterion is shown in Fig. 7. A bar graph represents the average of 30 M values obtained from using a particular optimiser for solving a test problem. Based upon this measure, in cases of $\mathbf{F}_1$, $\mathbf{F}_2$ and $\mathbf{F}_3$ the methods that give the best Pareto sets are PBIL1 and PBIL2 whereas PAES is the third best and NPGA has the worst results. In the $\mathbf{F}_4$ case, the best method is PBIL1 but from Fig. 2 the obviously best method is SPEA2. This shows that the population diversity has more weight in the M value. The best results of the problem $\mathbf{F}_5$ are from SPEA2 and NSGAII while the best results of $\mathbf{F}_6$ are from SPEA2, NSGAII, PBIL1 and PBIL2. PBIL2 gives the best M value in the case of $\mathbf{F}_7$ whereas PAES, PBIL1 and PBIL2 are equally good and considered the best for the $\mathbf{F}_8$ problem.

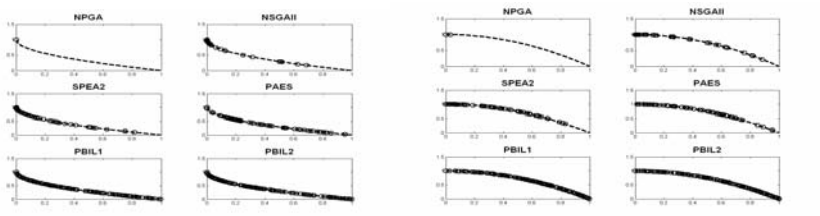

Fig. 1. Pareto front of (a) $\mathbf{F}_1$ and (b) $\mathbf{F}_2$ from the various methods

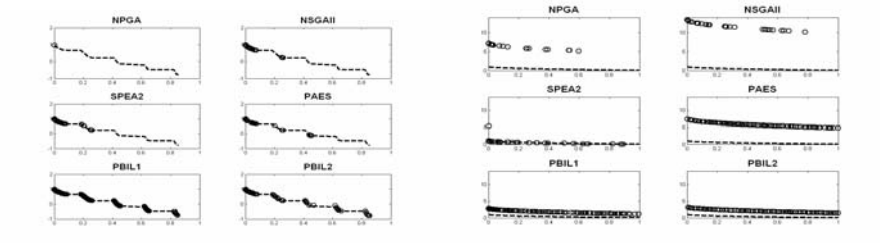

Fig. 2. Pareto front of (a) $\mathbf{F}_3$ and (b) $\mathbf{F}_4$ from the various methods

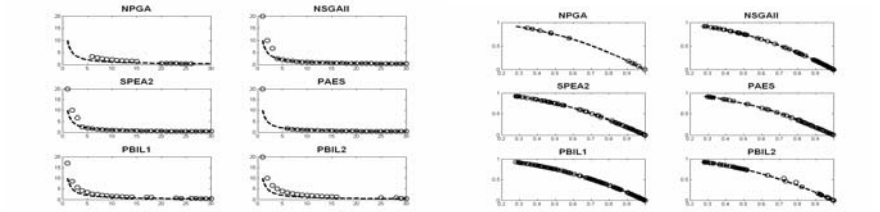

Fig. 3. Pareto front of (a) $\mathbf{F}_5$ and (b) $\mathbf{F}_6$ from the various methods

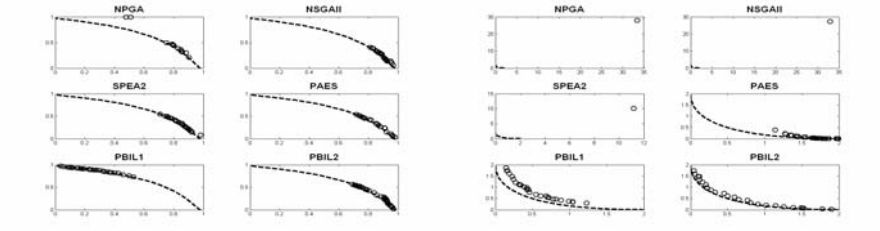

Fig. 4. Pareto front of (a) $\mathbf{F}_7$ and (b) $\mathbf{F}_8$ from the various methods

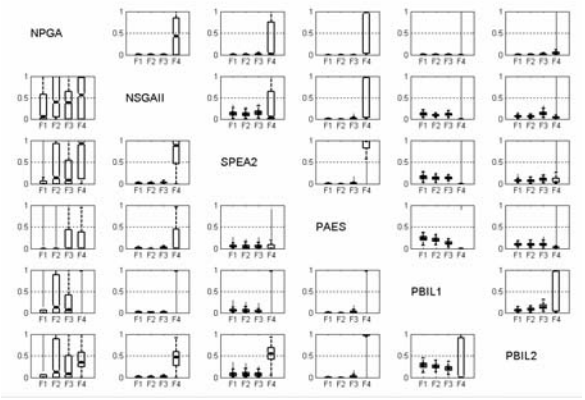

Fig. 5. Boxplot of *C* values $\mathbf{F}_1$ $\mathbf{F}_2$ $\mathbf{F}_3$ & $\mathbf{F}_4$

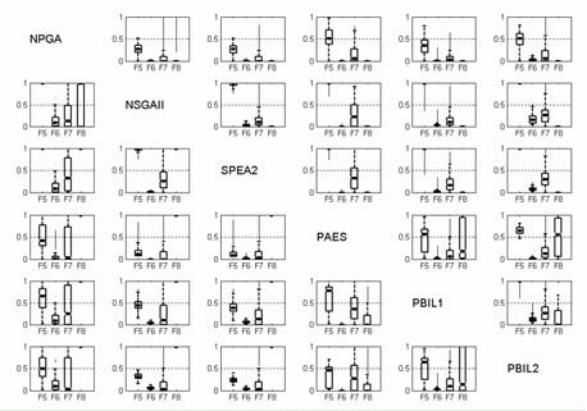

Fig. 6. Boxplot of C values $\mathbf{F}_5$ $\mathbf{F}_6$ $\mathbf{F}_7$ & $\mathbf{F}_8$

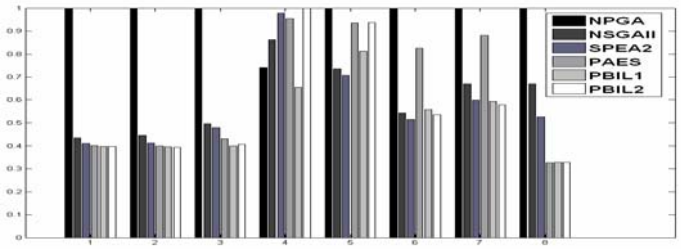

Fig. 7. Comparison of M values

6 Conclusions and Discussion

According to the numerical experiment results and several comparative criteria, it can be said that PBIL is one of the most powerful tools for multiobjective optimisation. The method is overall superior to or as good as the other established multiobjective optimisers in most of the test-cases except for the $\mathbf{F}_4$ and $\mathbf{F}_5$ test problems. It can be concluded that PBIL1 is as good as PBIL2 or vice versa although PBIL1 is better than PBIL2 in terms of front distribution. The most outstanding capability of PBIL is its unmatched ability in providing population diversity.

The conclusions drawn in this paper cannot, nonetheless, be applied to all kinds of optimisation problems as the performance of evolutionary search is rather dependent on the type of design problem. For examples, a crossover-based method is the best for global optimisation whereas a mutation-based method is far superior to others when dealing with some large-scale problem e.g. in references [14] and [3].

The multiobjective PBIL is said to be the simplest form of the estimation of distribution algorithm for multiobjective design. The effect of parameters e.g. the number of probability vectors n_b on the searching performance needs to be investigated. It has

not yet been compared to the more advanced EDAs like the Bayesian network. Furthermore, the test of the presented technique in solving real world problems needs to be proven before being accepted as well-established.

Acknowledgement. The corresponding author is grateful of the support from the Thailand Research Fund (TRF), SIRDC and The Faculty of Engineering, Khon Kaen University.

References

1. Baluja S (1994) Population-based incremental learning: a method for integrating genetic search based function optimization and competitive learning. Technical Report CMU_CS_95_163, Carnegie Mellon University
2. Bureerat S, Cooper JE (1998) Evolutionary methods for the optimisation of engineering systems. In: IEE Colloquium Optimisation in Control: Methods and Applications, IEE, London, Uk, pp 1/1-1/10
3. Bureerat S, Limtragool J (2006) Performance enhancement of evolutionary search for structural topology optimization, Finite Element in Analysis and Design, 42:547-566
4. Coello CC, Romero CEM (2002) Evolutionary algorithms and multiple objective optimization. multicriteria optimization. Ehrgott, Matthias; Gandibleux, Xavier (Eds.), pp 277-331
5. Deb K, Pratap A, Meyarivan T: Constrained test problems for multi-objective evolutionary optimization. KanGAL Report No. 200002, Kanpur Genetic Algorithms Laboraotry (KanGAL), Indian Institute of Technology, Kanpur, India.
6. Deb K, Pratap A, Agarwal S, Meyarivan T (2002) A fast and elitist multiobjective genetic algorithm: NSGAII. IEEE Trans. On Evolutionary Computation 6(2):182-197
7. Fonseca CM, Fleming PJ (1993) Genetic algorithms for multiobjective optimization: formulation, discussion and generalization. In: Proc. of the 5th Inter. Conf. on Gas, pp 416-423
8. Fyfe C (1999) Structured population-based incremental learning. Soft Computing 2(4): 91 – 198
9. Grandhi RV, Bharatram, G (1993) Multiobjective optimization of large-scale structures. AIAA 31(7):1329-1337
10. Horn J, Nafpliotis N (1993) Multiobjective optimization using niched Pareto genetic algorithm. Tech. Report I11iGA1 Report 93005, UIUC
11. Horn J, Nafpliotis N, Goldberg DE (1994) A niched pareto genetic algorithm for multiobjective optimization. In: The 1st IEEE Conf. on Evolutionary Computation, pp 82-87
12. Ivvan S, Pena V, Rionda SB, Aguirre AH (2005) Multiobjective shape optimization using estimation distribution algorithms and correlated information. In: EMO2005, pp 664-676
13. Knowles JD, Corne DW (2000) Approximating the non-dominated front using the Pareto archive evolution strategy. Evolutionary Computation 8(2):149-172.
14. Kunakote T (2004) Topology optimization using evolutionary algorithms: comparison of the evolutionary methods and checkerboard suppression technique. Master thesis, Khon Kaen University
15. Messac A, Ismail-Yahaya A, Mattson CA (2003) The normalized normal constraint method for generating the Pareto frontier. Structural and Multidisciplinary Optimization 25(2):86-98

16. Schaffer JD (1985) Multiobjective optimization with vector evaluated genetic algorithms. In: GAs and their Application: Proc. of 1st Inter Conf. on Gas, pp 93-100
17. Sebag M, Ducoulombier A (1998) Extending population-based incremental learning to continuous search spaces. Lecture Notes in Computer Science 1498: 418
18. Srinivas N, Deb K (1994) Multiobjective optimization using non-dominated genetic algorithms. Evolutionary Computation 2(3):221-248
19. Yuan B, Gallagher M (2003) Playing in continuous spaces: some analysis and extension of population-based incremental learning. In: Proceedings of the 2003 Congress on Evolutionary Computation, IEEE, Canberra, Australia, pp 443-450
20. Zitzler E, Deb K, Thiele L (2000) Comparison of multiobjective evolutionary algorithms: empirical results. Evolutionary Computation 8(2):173-195
21. Zitzler E, Laumanns M, Thiele L (2002) SPEA2: improving the strength Pareto evolutionary algorithm for multiobjective optimization. In: Evolutionary Methods for Design, Optimization and Control, Barcelona, Spain
22. Zitzler E, Thiele L, Laumanns M, Fonseca CM, Fonseca VG (2003) Performance assessment of multiobjective optimizers: an analysis and review. IEEE Trans. on Evolutionary Computation 7(2):117-132

Passive Vibration Suppression of a Walking Tractor Handlebar Structure Using Multiobjective PBIL

Siwadol Kanyakam, and Sujin Bureerat

***Abstract*—This paper is concerned with vibration suppression of a walking tractor handlebar structure using multiobjective population-based incremental learning (PBIL). Two bi-objective optimisation problems are assigned aiming at vibration alleviation as well as structural mass reduction. Design variables are structural shape and sizing parameters whereas the objective functions include structural weight, natural frequencies, and frequency response function. The problems are posed to minimise the objectives whilst meeting structural safety requirement. The PBIL multiobjective optimiser is detailed and implemented to solve the optimization problems. The optimum results obtained are compared, illustrated and discussed. It is shown that a simple but effective passive vibration control of a handlebar structure can be achieved through the implementation of the proposed multiobjective PBIL.**

I. Introduction

A two-wheel ground vehicle called a power tiller or walking tractor, shown in Fig. 1, has long been used in several countries. In Thailand, it has been reported that the number of walking tractors used by Thai farmers is increasing annually. The power tiller consists of approximately five main parts i.e. a single-cylinder engine, tractor frame and wheels, transmission and brake systems, a handlebar system, and an accessory for agricultural or transportation purpose. This kind of tractor has some advantages as it is simple to use and maintain whereas the price is inexpensive. It can be used in a variety of agricultural applications as well as transportation. However, there are some weak points of this vehicle. The user must walk following the tractor in order to use it, which often leads to some foot injuries. It is always dangerous for users who are inexperienced to control it. The power transmission system of Thai power tillers still needs more improvement. Another inevitable problem is the vibration transmission from a reciprocating engine to a user and this can cause some serious cumulative illness. As a result, the vibration transmission from the engine and other external dynamic loads to the user needs to be suppressed.

The work in this paper investigates the use of the PBIL multiobjective algorithm on passive vibration design of the skeleton handlebar structure of a walking tractor. Design function evaluation is carried out by using finite element analysis. Design variables are structural shape and beams cross-sectional areas. The design objectives consist of structural mass, natural frequency, and frequency response function. The design constraint is that the structure must be safe under the applied static loads. The combination of design objective functions leads to 2 bi-objective optimisation problems. The proposed PBIL optimiser is detailed and implemented to solve the 3 design problems. The results obtained from the optimisation method are illustrated, compared and discussed. It is shown that the simple but effective strategy of passive vibration control of the structure can be achieved through multiobjective evolutionary optimisation.

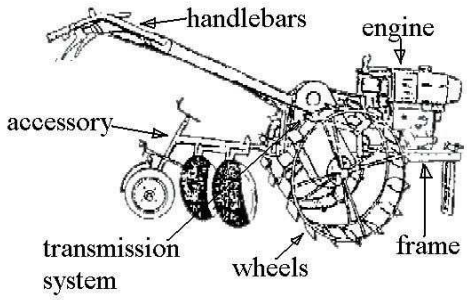

Fig. 1. Walking tractor.

II. Vibration Analysis

A structural dynamic model can be described as a structure being in a dynamic equilibrium state. It is the state at which the system has minimum potential energy (the potential energy herein means the sum of the work done by external, inertial and restoring forces). The equations of motion basically comprise kinetic energy, structural restoration (spring and damping) and external dynamic forces. By using a finite element approach, the structural dynamic model is represented by

$$\mathbf{M}\ddot{\boldsymbol{\delta}} + \mathbf{K}\boldsymbol{\delta} = \mathbf{F}_{ex}(t) \quad (1)$$

where $\boldsymbol{\delta}$ is the vector of structural displacements
$\mathbf{M}$ is a structural mass matrix
$\mathbf{K}$ is a structural stiffness matrix
$\mathbf{F}_{ex}$ is the vector of dynamic forces acting upon the structure.
The computation is traditionally carried out using finite element analysis. With the boundary conditions (say $\boldsymbol{\delta}_b = \mathbf{0}$) being assigned, equation (1) can be partitioned as

S. Kunyakam is with Faculty of Science and Technology, Rajabhat Maha Sarakham University, Maha Sarakham, Thailand, 44000

S. Burerat is with the Department of Mechanical Engineering, Faculty of Engineering, Khon Kaen University, Thailand, 40002 (email: sujbur@kku.ac.th)

1-4244-1340-0/07/$25.00 ©2007 IEEE

$$\begin{bmatrix}\mathbf{M}_{aa} & \mathbf{M}_{ab}\\ \mathbf{M}_{ba} & \mathbf{M}_{bb}\end{bmatrix}\begin{bmatrix}\ddot{\boldsymbol{\delta}}_a\\ \ddot{\boldsymbol{\delta}}_b\end{bmatrix}+\begin{bmatrix}\mathbf{K}_{aa} & \mathbf{K}_{ab}\\ \mathbf{K}_{ba} & \mathbf{K}_{bb}\end{bmatrix}\begin{bmatrix}\boldsymbol{\delta}_a\\ \boldsymbol{\delta}_b\end{bmatrix}=\begin{bmatrix}\mathbf{F}_a\\ \mathbf{F}_b\end{bmatrix} \quad (2)$$

where the subscript *b* indicates the known displacements and unknown reactions, and the subscript *a* denotes the unknown displacements and predefined external forces.

Equation (1) can be rearranged leading to 2 systems of equations

$$\mathbf{M}_{aa}\ddot{\boldsymbol{\delta}}_a+\mathbf{K}_{aa}\boldsymbol{\delta}_a=\mathbf{F}_a \quad (3)$$

and

$$\mathbf{M}_{ba}\ddot{\boldsymbol{\delta}}_a+\mathbf{K}_{ba}\boldsymbol{\delta}_a=\mathbf{F}_b. \quad (4)$$

When damping is introduced to the system, a damping matrix can be included into (3) yielding

$$\mathbf{M}_{aa}\ddot{\boldsymbol{\delta}}_a+\mathbf{C}_{aa}\dot{\boldsymbol{\delta}}_a+\mathbf{K}_{aa}\boldsymbol{\delta}_a=\mathbf{F}_a. \quad (5)$$

Rayleigh damping or proportional damping is used in this work. By letting

$$\mathbf{z}=\begin{bmatrix}\boldsymbol{\delta}\\ \dot{\boldsymbol{\delta}}\end{bmatrix},$$

equation (5) can be formed as a state-space model

$$\dot{\mathbf{z}}=\mathbf{A}\mathbf{z}+\mathbf{F} \quad (6)$$

where

$$\mathbf{A}=\begin{bmatrix}\mathbf{0} & \mathbf{I}\\ -\mathbf{M}_{aa}^{-1}\mathbf{K}_{aa} & -\mathbf{M}_{aa}^{-1}\mathbf{K}_{aa}\end{bmatrix}$$ is a state matrix

and

$$\mathbf{F}=\begin{bmatrix}\mathbf{0}\\ \mathbf{M}_{aa}^{-1}\mathbf{F}_a\end{bmatrix}.$$

Frequency Response Function (FRF) is defined as the ratio of steady-state harmonic output to steady-state harmonic input at any given frequency. The FRF here is the ratio of displacement response to input force or *receptance.* From (7), it can be determined using the relation [1]

$$\mathbf{H}(i\omega)=\mathbf{U}_{upper}\left[diag\left(\frac{1}{i\omega-\lambda_j}\right)\right]\mathbf{U}_{right}^{-1}\mathbf{M}^{-1} \quad (7)$$

where ω is the frequency of the input forces and displacements.

The relation between displacement response and input force is

$$\bar{\boldsymbol{\delta}}_a=\mathbf{H}(i\omega)\bar{\mathbf{F}}_a \text{ or } \boldsymbol{\delta}_a=\bar{\boldsymbol{\delta}}_a e^{i\omega t}=\mathbf{H}(i\omega)\bar{\mathbf{F}}_a e^{i\omega t}. \quad (8)$$

U is the matrix of the eigenvectors and λ_js are the eigenvalues of the state-space matrix **A**. $\mathbf{U}_{upper}$ can be computed from

$$\mathbf{U}=\begin{bmatrix}\mathbf{U}_{upper}\\ \mathbf{U}_{lower}\end{bmatrix}=\begin{bmatrix}\mathbf{U}_{upper}\\ \mathbf{U}_{upper}[diag(\lambda_j)]\end{bmatrix} \quad (9)$$

and the inverse of $\mathbf{U}_{right}$ is partitioned from

$$\mathbf{U}^{-1}=[\mathbf{U}_{left}^{-1}\quad \mathbf{U}_{right}^{-1}]. \quad (10)$$

Note that there are several ways to compute the FRF values other than using (8). Fig. 2 illustrates how to measure $H(r,s)$ which represents the ratio of displacement response at the r^{th} degree of freedom to harmonic excitation at the s^{th} degree of freedom at the same frequency.

Apart from FRF, by defining force transmissibility $\mathbf{T}(i\omega)$ as the ratio of output harmonic reaction forces to the input external harmonic forces, it can be written as

$$\bar{\mathbf{F}}_b=\mathbf{T}(i\omega)\bar{\mathbf{F}}_a \text{ or } \mathbf{F}_b=\bar{\mathbf{F}}_b e^{i\omega t}=\mathbf{T}(i\omega)\bar{\mathbf{F}}_a e^{i\omega t}. \quad (11)$$

Substituting (12) and (9) into (4), the force transmissibility (FT) can be obtained as

$$\mathbf{T}(i\omega)=\left(-\omega^2\mathbf{M}_{ba}+\mathbf{K}_{ba}\right)\mathbf{H}. \quad (12)$$

Some research work on passive vibration control of skeleton structures using genetic algorithms has been made [2-5]. In structural vibration design, FRF and FT determine structural merit. Lower magnitude of FRF or FT at a particular frequency means better structural vibration design. Therefore, the design objective can be assigned in such a way that the values of FRF or FT at a frequency range of interest are minimised. Moreover, maximising structural natural frequency is an alternative criterion for the design of structures under dynamic loadings.

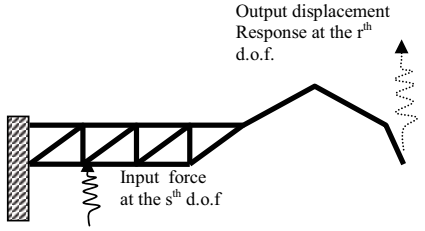

Fig. 2. Harmonic response.

III. PBIL MULTIOBJECTIVE OPTIMISER

A particular multiobjective design problem can be defined as:

Find **x** such that

Min: $\mathbf{f}=\{f_1(\mathbf{x}),\ldots,f_m(\mathbf{x})\}$ (13)

Subject to

$g_i(\mathbf{x})\le 0$

$h_i(\mathbf{x})=0$

where **x** is the vector of *n* design variables

f_i are the *m* objective functions

g_i are inequality constraints

and h_i are equality constraints.

In the past, most optimisers were developed to deal with a single objective problem. They can however be modified to use in multiobjective design by introducing additional numerical schemes that can convert the multiobjective problem to be a single objective case. The disadvantage in using such strategies is that the optimisation method needs to be performed as many times as the number of Pareto points required. This inferiority can be sorted out by the use of MOEAs, which can explore a Pareto front within a single run of the algorithms. Furthermore, using MOEAs is advantageous as they can deal with all kinds of design variables and functions without the requirement of functional derivatives in searching. They however have a complete lack of consistency and low convergence rate. Thus, the non-dominated front obtained from using these methods is often classified as an approximate Pareto front.

The basic concept of exploring Pareto optimum points via MOEA search is that, at each generation while a new population is created, non-dominated solutions are classified

and carried on to the next generation. The term non-dominated solutions define the local Pareto solutions among the members in the current population during evolutionary search. The non-dominated solutions obtained at each generation are saved to the external Pareto archive.

The multiobjective evolutionary optimiser used in this paper is the multiobjective version of PBIL. The PBIL method is probably the simplest form of the estimation of distribution methods (EDM) [6]. The PBIL algorithm proposed for multiobjective optimisation here is a modification from [7]. The PBIL search procedure is based upon binary searching space, and can be thought of as iteratively limiting the design spaces depending on the current non-dominated solutions and randomisation. Rather than keeping all binary solutions or a population as with genetic algorithms, the population in PBIL is represented by the probability vector of having '1' of each bit position of the binary strings. Fig. 3 shows three probability vectors producing three binary populations where each row vector of the populations represents a design solution. It is shown that one probability vector can form a variety of populations. A probability of 1 indicates that all the bits in its corresponding column of the population are '1' whereas a probability of '0' means that the column is full of zeros.

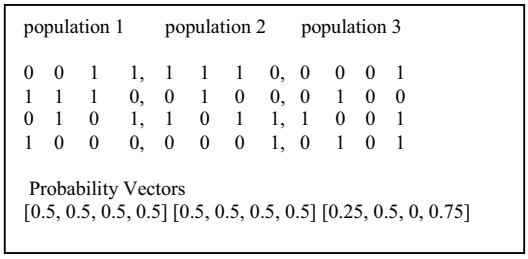

Fig. 3. PBIL probability vectors and corresponding populations.

When employed in multiobjective optimisation, more probability vectors should be used in order to obtain the more diverse population; therefore, it is called a probability matrix instead. The PBIL search starts with an (empty) external Pareto archive and initial probability matrix whose elements are full of '0.5'. Each row of the matrix is a probability vector used to create a sub-population. Let N_P be the number of design solutions in a population, l be the predefined number of probability vectors, and n_b be the number of binary bits for each solution. The probability matrix, therefore, has the size of $l \times n_b$ where each row produces N_P/l design solutions as one sub-population. Each design variable is represented by a binary string with n_b/n elements.

Having generated the current population and evaluated their corresponding objective values, the external Pareto archive is replaced by the non-dominated members of the union set of the current population and the old external Pareto archive. If the number of non-dominated members obtained is larger than the predefined archive size, some solutions are removed from the new external Pareto archive and here the use of a Pareto archiving technique is required.

The probability matrix is updated in such a way that $n_0 < N_a$ binary solutions are randomly selected from the current Pareto archive to modify the i^{th} row of the probability matrix. Note that N_a is the number of solutions in the current external archive. The i^{th} row of the probability matrix is updated using the relation

$$P_{i,j}^{new} = P_{i,j}^{old}(1 - LR) + \bar{b}_j LR \tag{14}$$

where LR is called the learning rate, and $\bar{b}_j$ is the mean value of the j^{th} column of the n_0 selected binary solutions. In this paper the learning rate is set as

$$LR = 0.5 + rand \cdot (+0.1 \text{ or } -0.1) \tag{15}$$

where $rand \in [0,1]$ is a uniform random number. It is also useful to, afterwards, apply mutation to the i^{th} row of the probability matrix at some predefined probability such that

$$P_{i,j}^{new} = P_{i,j}^{old}(1 - ms) + \text{rand}(0 \text{ or } 1).ms \tag{16}$$

where ms is the amount of shift used in the mutation.

The updating process is completed when all rows of the probability matrix are changed. The probability matrix is updated and the external Pareto archive is improved iteratively until convergence is achieved.

As previously mentioned, in cases where the total number of the non-dominated solutions is greater than the archive size, the archiving operator is activated to remove some solutions from the archive. The archiving technique presented here is called the normal line method which borrows some concepts from the so-called normalised normal constraint technique [7]. It should be noted that the proposed normal line archiving technique is not the same thing as the normalised normal constraint technique but they share some ideas and some technical terms. Let N be the total number of the current non-dominated solutions (which exceeds the archive size) and all of them are normalised as:

$$u_i = \frac{(f_i - f_i^{\min})}{(f_i^{\max} - f_i^{\min})} \tag{17}$$

where $f_i^{\min}$ are the minimum values of the i^{th} objective function sorted from the current non-dominated solutions, and $f_i^{\max}$ are the maximum values of the i^{th} objective function.

The numerical procedure in cases of bi-objective optimisation is displayed in Fig. 4. The points that give the minimum values of each objective are taken as the anchor points [7]. The line connecting between the two anchor points is called the Utopia line while N_a reference points are evenly spaced on the Utopia line. The normal lines are the lines that are normal to the Utopia line, and pass the reference points as shown. A non-dominated point is archived if it is the closest point to a particular normal line. The non-dominated point is iteratively selected until the external Pareto set is full. Six selected non-dominated points are bounded by a dashed rectangle as shown in Fig. 4. The computational steps can be given as:

1. Normalise the objective values of all the non-dominated solutions
2. Find N_a reference points
3. For $i = 1$ to N_a
4. Compute the distances of the non-dominated solutions to the i^{th} normal line
5. Find the solution having minimum distance to the i^{th} line
6. Save the solution to the archive
7. Remove the selected solution from the selecting pool
8. Next i

Note that the normal line method may look similar to the strip method presented in [7] but they are two different approaches and the obtained results are different.

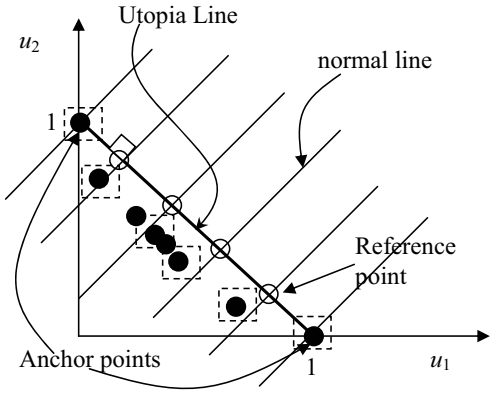

Fig. 4. Normal line archiving method.

IV. Design Problems

A walking tractor handlebar taken from the local manufactory is displayed in Fig. 5 and named as **Structure0**. The structure is stiffened to be **Structure1** as shown in Fig. 6. The structure is stiffened by adding to it some beam elements so as to have a better design. The simple finite element model of Structure1 is shown in Fig. 7. It consists of 16 nodes and 27 elements with four nodes being fixed. The 2-node 3-dimensional 12 d.o.f. beam element is employed. The structure is subjected to two static load cases, one is the load for turning the tractor and the other is the load for balancing and controlling the tractor. The design objectives are

FUN1: structural mass

FUN2: $1/(\omega_1 + \omega_2 + \omega_3)$

FUN3: the mean value of FRF crest parameters at ω_1, ω_2 and ω_3.

ω_i denotes the i^{th} natural frequency of the structure. All of the objective functions are treated for minimisation. Minimising FUN1 is somewhat proportional to structural cost reduction. Fig. 8 depicts a particular FRF plot. In this paper, the crest parameter at a natural frequency ω_i is the average of H_{rs} magnitudes in the frequency interval $[\omega_i - \Delta, \omega_i + \Delta]$. The objective FUN3 is set to reduce the z-direction *point* FRF at the tip of the handlebar structure. The optimisation problem is to minimise the design objectives while the design constraint is that the structure under static loading has to meet safety requirements. The design variables are nodal positions of some selected nodes and beam cross-sectional areas of some selected elements. This implies that the design variables determine structural shape and element diameters simultaneously. Two bi-objective design problems which yield the minimisation of mass and vibration in three different ways are assigned as:

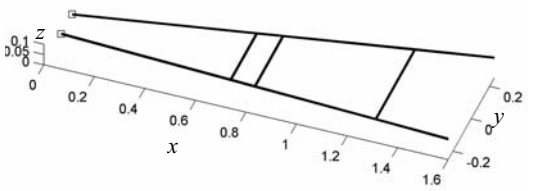

Fig. 5. Structure0: original structure from the local manufactory.

OPT1

Min: [FUN1, FUN2]

Subject to $\sigma_i \le \sigma_{\text{allowable}}$

OPT2

Min: [FUN1, FUN3]

Subject to $\sigma_i \le \sigma_{\text{allowable}}$

The PBIL optimiser is implemented to solve the design problems where N_b/n is set to be 10. The number of search iterations is set to be 150. The population size is 100 while the Pareto archive size is 100. Each design variable is encoded by 10 binary bits. The non-dominated sorting proposed in [8] is applied for dealing with the constraints.

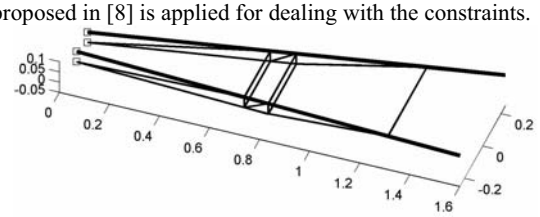

Fig. 6. Structure1: stiffened structure.

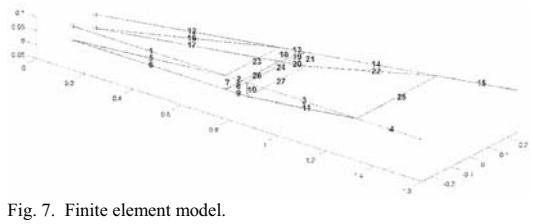

Fig. 7. Finite element model.

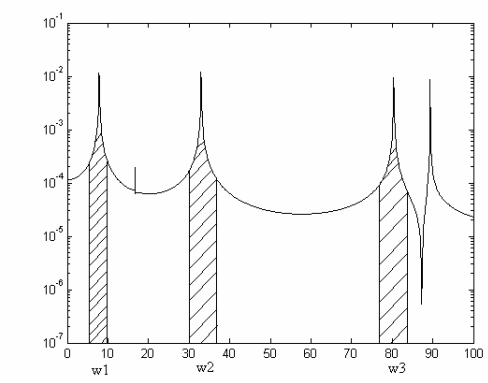

Fig. 8. FRF crest parameters.

V. Design Results

Apart from the use of PBIL, other well-established multiobjective evolutionary algorithms i.e. version 2 of Non-dominated Sorting Genetic Algorithm (NSGA) [10], Pareto Archive Evolution Strategy (PAES) [11-12] and version 2 of Strength Pareto Evolutionary Algorithm (SPEA) [13] are employed so as to measure the performance of multiobjective PBIL. All of the method use binary strings for encoding the design variables and they are employed to solve the optimisation problems 5 simulation runs with the same population size and total number of iterations as used by PBIL. It should be noted that the main work in this paper is not comparative performance of MOEAs but it is concerned with the use of multiobjective PBIL for vibration suppression. The comparison results are presented merely to show that the PBIL method is sufficiently powerful for solving the design problems.

Fig. 9 displays the approximate Pareto fronts of OPT1 obtained from using the various optimisers. Each non-dominated front is the best obtained from 5 runs of each method. It is shown that the front obtained from PBIL is the best front.

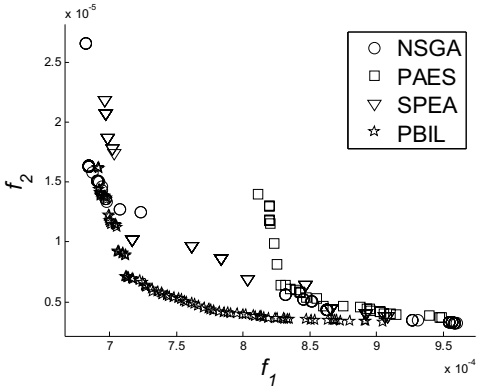

Fig. 9. Pareto fronts of OPT1 from the various MOEAs.

Fig. 10 shows the approximate Pareto fronts of OPT2 obtained from using the various optimisers. It is shown that the front obtained from PBIL is also the best for the design case.

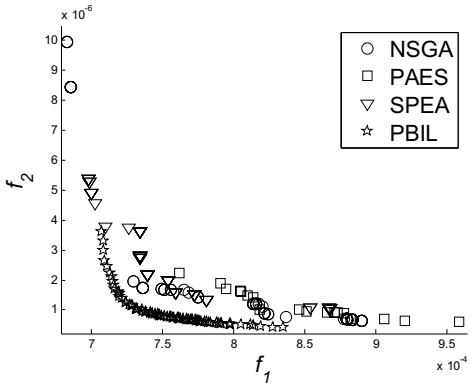

Fig. 10. Pareto fronts of OPT2 from the various MOEAs.

The box-plots of *C*-indicators [14] comparing the non-dominated fronts from the various optimisation methods are given in Fig. 11. From *C*-comparison, it is shown that PBIL is the best multiobjective optimiser for the proposed design problems.

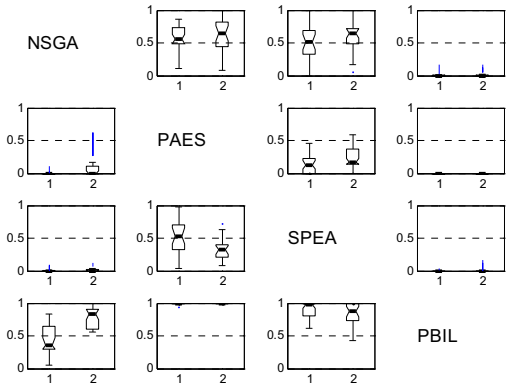

Fig. 11. *C*-comparison of the MOEAs for OPT1 and OPT2.

The optimum results in solving OPT1 are illustrated in Fig. 12-14. In Fig. 12, the approximate Pareto front obtained from performing the PBIL multiobjective optimiser is displayed along with the objective values of Structure0 and Structure1. The diamond and pentagram markers represent Structuct0 and Structure1 respectively. It can be seen that the weight of Structure0 is lighter than that of the stiffened structure, Structure1, while the vibration merit of Structure1 is superior. The two solutions are totally dominated by all of the solutions obtained from the optimisation process. This implies that, with the use of the multiobjective evolutionary algorithm, the better passive design of a structure is achievable. Fig. 13 displays the front where 6 design points are selected. The handlebar structures corresponding to those design points are shown in Fig. 14. It can be seen that the structures have various shapes and sizes.

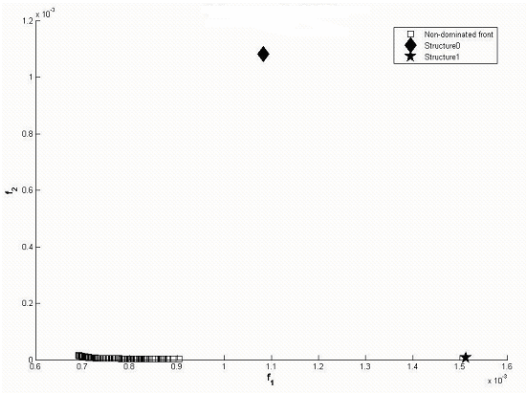

Fig. 12. Approximate Pareto front of OPT1 from PBIL.

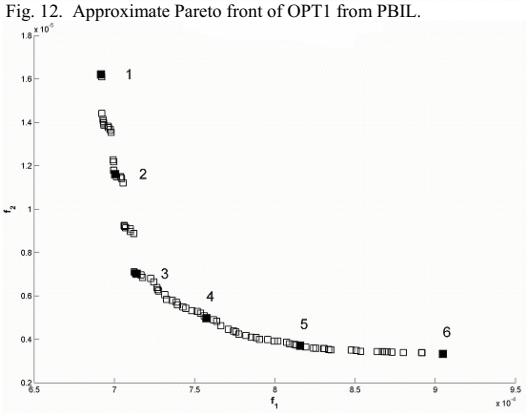

Fig. 13. Approximate Pareto front of OPT1 with 6 selected design points.

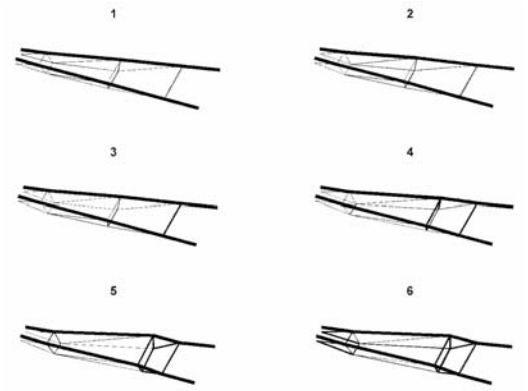

Fig. 14. Corresponding structures of the point in Fig.13.

The Pareto optimal solutions of the second design problem obtained from using the PBIL optimiser along with the design points of Structure0 and Structure1 are illustrated in Fig. 15. Similarly to the OPT1 problem, Structuct1 has better vibration merit than Structure0. Both of them are totally dominated by all of the non-dominated solutions obtained from the optimisation process. The approximate Pareto front of the second design case is displayed in Fig. 16 where 6 design points are selected. The handlebar structures corresponding to the selected design points are displayed in Fig. 17. It can be seen that the 6 structures have various shapes and sizes.

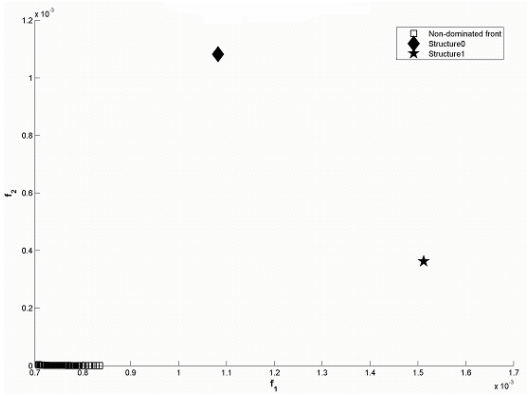

Fig. 15. Approximate Pareto front of OPT2.

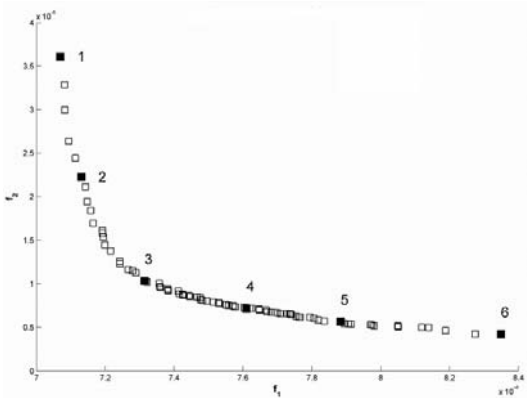

Fig. 16. Approximate Pareto front of OPT2 with 6 selected design points.

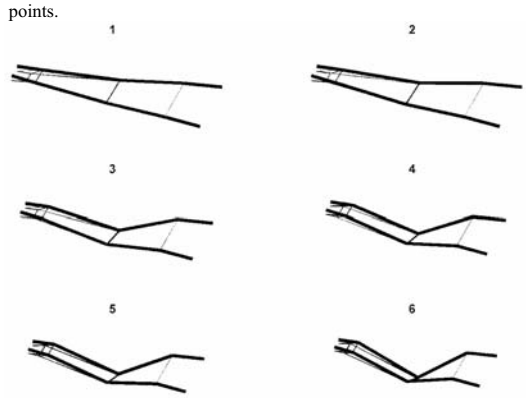

Fig. 17. Corresponding structures.of the points in Fig 16

Fig. 18 displays the FRF of Structue1 as well as the 1st and 6th design points of OPT1, which are said to be the anchor points of the obtained Pareto front. The FRF of Structure1 and the 1st and 6th design solutions of OPT2 are shown in Fig 19. It can be seen that the FRF of the optimum solutions are far superior to the FRF of Structure1 if the lower FRF

magnitude means the better design. In comparing the structures from OPT1 and OPT2, the first three natural frequencies of the structures from OPT1 are overall higher than the natural frequencies of the two structures form OPT2. However, based on the magnitude of the point FRF, the structures from OPT2 are superior to the structures from OPT1. The preference between OPT1 and OPT2 is dependent on the designer's objective. For example, if minimising the magnitude of vibration response due to a harmonic external force is more important than maximising natural frequencies, OPT2 is chosen.

Fig. 20 shows the FT of Structure1, and the 1st and 6th design points of OPT1. The FT here is the force transmissibility from the grips to the fixed points at the tractor frame. The FT graphs of Structure1 and the 1st and 6th structures of OPT2 are given in Fig. 21. Similarly to the FRF plots, the FT graphs of the structures obtained from the optimisation processes are far superior to Structure1. In comparing the structures from the two design problems based on FT, the structures from OPT1 are slightly better than the structures from OPT2. However, it should be noted that the magnitude of FT can also be assigned as an objective function. Therefore, if structures with minimised FT magnitude are required, the new optimisation problem with FT crest parameter being one of the objective functions should be used rather than using OPT1 or OPT2.

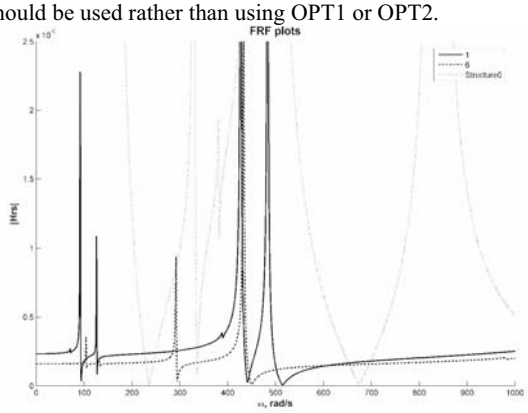

Fig. 18. FRF of Structure1 & the 1st and 6th design points of OPT2

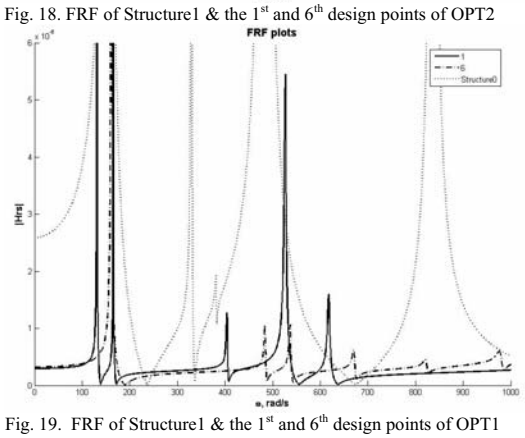

Fig. 19. FRF of Structure1 & the 1st and 6th design points of OPT1

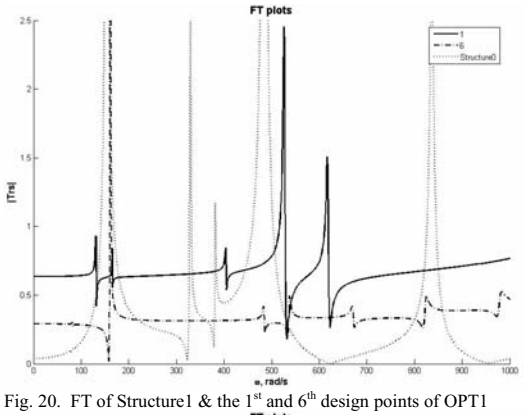

Fig. 20. FT of Structure1 & the 1st and 6th design points of OPT1

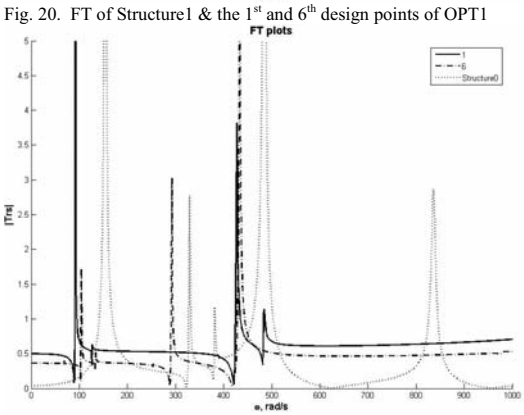

Fig. 21. FT of Structure1 & the 1st and 6th design points of OPT2

VI. Conclusions

The proposed multiobjective PBIL is a powerful tool for passive vibration alleviation of a walking tractor handle bar structure. The design approaches presented in this paper can be applied to passive vibration control of skeleton-type structures. The searching performance of the proposed multiobjective PBIL should be compared to other established multiobjective evolutionary algorithms.

Acknowledgment

The authors are grateful for the support from the Coordinating Centre for Thai Government Science and Technology Scholarship Students, Sustainable Infrastructure Research and Development Centre, the Faculty of Engineering, Khon Kaen University, and Rajabhat Maha Sarakham University.

References

[1] D. E. Newland, *Mechanical Vibration Analysis and Computation.* Longman Scientific & Technical, 1994, ch. 8

[2] M. Moshrefi-Torbati, A. J. Keane, J. Elliott, M. J. Brennan and E. Rogers, "Passive Vibration Control of a Satellite Boom Structure by Geometric Optimization using Genetic Algorithm," *J. of Sound and Vibration*, vol. 276, 2003, pp. 879-892.

[3] W. H. Tong, J. S. Jiang and G. R. Liu, "Dynamic Design of Structures under Random Excitation," *Computational Mechanics*, vol. 22, 1998, pp. 388-394.

[4] A. J. Keane, “Passive Vibration Control via Unusual Geometries: The Applications of Genetic Algorithm Optimization to Structural Design,” *J. of Sound and Vibration*, vol. 185, no.30, 1995, pp. 441-453.
[5] R. Alkhatib, G. N. Jazar and M. F. Golnaraghi, “Optimal Design of Passive Linear Suspension using Genetic Algorithm,” *J. of Sound and Vibration*, vol. 275, 2004, pp. 665-691.
[6] Baluja, S.: Population-Based Incremental Learning: A Method for Integrating Genetic Search Based Function Optimization and Competitive Learning. CMU_CS_163, (1994)
[7] S. Bureerat and K. Sriworamas, “Population-Based Incremental Learning for Multiobjective Optimisation,” *Advances in Soft Computing*, vol. 39, 2007, pp. 223-232
[8] A. Messac, A. Ismail-Yahaya and C. A. Mattson, “The Normalized Normal Constraint Method for Generating the Pareto Frontier,” *Structural and Multidisciplinary Optimization*, vol. 25, no.2, 2003, pp. 86-98.
[9] K. Deb, A. Pratap and T. Meyarivan, *Constrained Test Problems for Multi-Objective Evolutionary Optimization*. KanGAL Report No. 200002, Kanpur Genetic Algorithms Laboraotry (KanGAL), Indian Institute of Technology, Kanpur, India
[10] K. Deb, A. Pratap, S. Agarwal and T., Meyarivan, “A Fast and Elitist Multiobjective Genetic Algorithm: NSGAII,” *IEEE Trans. On Evolutionary Computation*, vol. 6, no. 2, 2002, pp. 182-197.
[11] J. Knowles and D., Corne, “The Pareto Archived Evolution Strategy: a New Baseline Algorithm for Pareto Multiobjective Optimization,” In: Congress on Evolutionary Computation, 1999.
[12] J. D. Knowles and D.W., Corne, “Approximating the Non-Dominated Front Using the Pareto Archive Evolution Strategy,” *Evolutionary Computation*, vol. 8, no. 2, 2000, pp. 149-172.
[13] E. Zitzler, M., Laumanns and L., Thiele, “SPEA2: Improving the Strength Pareto Evolutionary Algorithm for Multiobjective Optimization,” In: Evolutionary Methods for Design, Optimization and Control, Barcelona, Spain, 2002
[14] E. Zitzler and L., Thiele, “Multiobjective Evolutionary Algorithms: A Comparative Case Study and the Strength Pareto Approach,” *IEEE Trans. On Evolutionary Computation*, vol. 3, no. 4, 1999, pp. 257-271.

Technology and Innovation for Sustainable Development Conference (TISD2008)
Faculty of Engineering, Khon Kaen University, Thailand
28-29 January 2008

Topology Optimisation of a Plate Structure Using Multiobjective Population-Based Incremental Learning

Tawatchai Kunakote and Sujin Bureerat*
Department of Mechanical Engineering, Faculty of Engineering, Khon Kaen University,
Khon Kaen 40002
E-mail: sujbur@kku.ac.th*

Abstract

In this paper, an unconventional topological design problem was posed to find structural topologies of a cantilever plate while design objectives are weight and compliance with stress and displacement constraints. Multiobjective population-based incremental learning (MOPBIL) in combining with an approximate density distribution technique is employed to explore a Pareto optimal front of the design problem. The design results show that MOPBIL is a powerful tool for multiobjective topology optimisation although its convergence rate is not as good as the gradient-based optimality criteria method. With the use of MOPBIL, multiple structural configurations can be obtained within one optimisation run, and any unconventional design problem can be dealt with.

Keywords: Multiobjective Population-Based Incremental Learning, Evolutionary Algorithms, Pareto Front, Approximate Density Distribution, Topology Optimisation

1. Introduction

Topology optimisation is regarded as one of the most effective and powerful tools for the conceptual design of several engineering systems. This design technology has been significantly developed in the past two decades. The design strategy for structural conceptual design can be thought of as how to make the best use of material available while achieving the optimum design objective. A topological design process can be carried out by using finite element analysis for function evaluation and an optimisation method for searching the optimum solution. The topological design problem is usually a simplified constrained optimisation problem. The most preferable optimiser for such a design problem is the optimality criteria method (OCM) [6], [14]. Some other gradient-based optimisation method such as sequential linear programming (SLP) [3] and the method of moving asymptotes (MMA) [14] have also been implemented successfully. The applications of population-based optimisers or evolutionary algorithms, however, are said to be ineffective for this type of design problem due to a considerably large number of topological design variables [2], [4], [11].

Nevertheless, the use of evolutionary algorithms for topology optimisation is still attractive to engineering designers since the methods can deal with almost all kinds of design objective functions and constraints. There recently has been some research work on how to improve the searching performance of the evolutionary algorithms. The use of graph representation approach was proposed by Wang and Kang [8]. S. Bureerat and J. Lintragool [1] presented the design strategy employing a numerical technique called approximate density distribution (ADD), which can improve the search performance of several evolutionary algorithms as well as can suppress checkerboard formation on the resulting topologies. The use of multiobjective evolutionary algorithm for a topology design problem was proposed in [5] where the design problem has two objective functions and one equality constraint. The numerical scheme named chromosome repairing was proposed in the work to repair a design solution such that it results in a better. The results in this work show that the use of multiobjective evolutionary algorithms for structural topology optimisation is advantageous since many topologies can be obtained within one optimisation run.

This article demonstrates the application of a multiobjective evolutionary algorithm for structural topology optimisation. An unconventional topological design problem was posed to find structural topologies of a cantilever plate while design objectives are weight and compliance with stress and displacement constraints. Multiobjective population-based incremental learning (MOPBIL) [7], [9] one of the most powerful and robust multiobjective evolutionary algorithms (MOEAs) is employed to explore a Pareto optimal front of the design problem. The design results show that MOPBIL is a powerful tool for multiobjective topology optimisation although its convergence rate is not as good as OCM. With the use of MOPBIL, an unconventional design problem can be dealt with.

2. Topology Optimisation

A structure achieved by means of topology optimisation is the best structural layout that optimises a predefined objective function while meeting all design constraints. The traditionally used objective functions are weight, system compliance, deflection and natural frequency while design constraint is a mass or volume constraint. Stress constraint is not added to a design problem because it results in some difficulties in finding the optimum solution. It is usually considered in the later stage of a deign process.

Figure 1 illustrates the concept of topology optimisation. The design process is initialised with a predefined design domain and what application a designer needs to use the structure for. The optimum structural configuration is defined in the design domain. In practice, a topological design process can be carried out by using finite element analysis in combining with a numerical optimisation method. For plate structure, the design domain is discretised into a number of finite elements as many as possible. Topological design variables are the thicknesses of the elements. It can be said that the distribution of elements' thicknesses determines a structural topology. Having obtained the optimum solution, the elements with nearly zero thicknesses represent holes or voids on the structure whereas other elements indicate the existence of the structural material as shown in Figure 2.

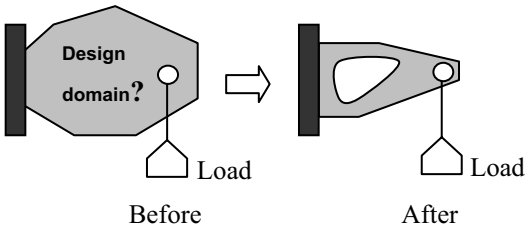

Figure 1. Topology optimisation

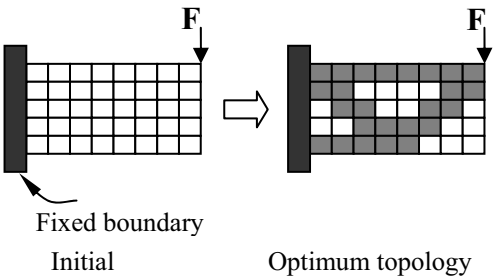

Figure 2. Topology design using finite element analysis

The design problem used in this study can be expressed as:

$$\text{min: } \mathbf{f}(\boldsymbol{\rho}) = \{w, \boldsymbol{c}\}^T \quad (1)$$

subject to

$$\sigma_i(\boldsymbol{\rho}) \le \sigma_a$$
$$\delta \le \delta_a$$
$$\rho_i \in \{\rho_i^{\min}, \rho_i^{\max}\}$$

where $\mathbf{KU} = \mathbf{F}$

$c = \mathbf{U}^T\mathbf{KU}$

$\boldsymbol{\rho}$ is a vector of topological design variables, which herein are the finite elements' thicknesses

w is structural weight

c is structural compliance

$\mathbf{U}$ is the vector of nodal displacements of a structure due to applied forces $\mathbf{F}$

$\mathbf{K}$ is a structural stiffness matrix

σ_i is the equivalent stress on the i^{th} element

σ_a is an allowable stress

δ is a maximum deflection

δ_a is an allowable deflection

$\rho_i^{\min}$ is the lower bound of the i^{th} design variable and $\rho_i^{\max}$ is the plate thickness at the i^{th} element.

The design problem is said to be unconventional since stress and deflection constraints are added to the problem. When using a lower order finite element formulation, checkerboard formation can occur on the resulting topology due to numerical instability. It is also found that, with a grate number of finite elements, an evolutionary algorithm always has an unacceptable convergence rate and complete lack of consistency. In this paper, we use the ADD technique [1] (also known as a ground element filtering technique, GEF [12]) to reduce the total number of design variables to a reasonable amount that the evolutionary algorithm can cope with. The technique can also suppress checkerboard patterns as the secondary advantage. The design problem with the use of ADD technique therefore becomes

$$\min_{\boldsymbol{\rho}^{ADD}} : \{\, c(\boldsymbol{\rho}^{ADD}),\ w(\boldsymbol{\rho}^{ADD}) \,\} \quad (2)$$

subject to

$$\sigma_i(\boldsymbol{\rho}) \le \sigma_a$$
$$\delta \le \delta_a$$
$$\rho_i \in \{0, 1\}$$

where $\boldsymbol{\rho}^{ADD}$ is the vector of new design variables being either 0 or 1. The transformation between $\boldsymbol{\rho}$ and can be expressed as:

$$\boldsymbol{\rho} = \mathbf{T}\boldsymbol{\rho}^{ADD}.$$

In cases that we need to use the ADD technique to suppress checkerboard pattern, the transformation needs to be modified leading to

$$\boldsymbol{\rho} = round(\mathbf{T}\boldsymbol{\rho}^{ADD} + \boldsymbol{\rho}^0)$$

where $\boldsymbol{\rho}^0$ is a constant vector needs to be specified. For more details of the ADD technique, see references [1] and [12].

3. Multiobjective Population-Based Incremental Learning

Population-based incremental learning (PBIL) is a simple version of the estimation of distribution algorithm (EDA). The method was first proposed by Beluja [13] for single objective optimisation. It has been developed as one of the MOEAs as presented in [7] and [10]. It has been found that the multiobjective version of PBIL is among the most powerful MOEAs using binary string as design variables.

For MOPBIL, the search procedure starts with an initial probability matrix and an empty external Pareto archive. A binary population is then generated according to the current probability matrix. The non-dominated solutions of the population are then sorted and put into an external Pareto archive. The probability matrix is updated based upon the non-dominated binary solutions in the Pareto archive and a new population according to the updated probability matrix is then created. The external Pareto archive is updated by replacing the members in the archive with the non-dominated solutions sorted from the combination of the new population and the members in the previous archive. In cases that the number of non-dominate solutions in the archive exceeds the predefined archive size, the normal line technique is activated to remove some of the members from the archive while maintaining population diversity. The computational steps are repeated until the termination criterion is met. For more details of MOPBIL, see [7] and [10].

4. Design Test-Case

A cantilever plate is used for a design case study. Figure 3 illustrates the design domain of the cantilever plate while a point load is applied at the top right-hand corner of the plate. All details of the material properties that are used to solve the problem are as follows:

- The structure is made of material with 205×10^9 N/m^2 young's modulus and 0.3 Poisson's ratio.
- The structure has the dimensions of L = 0.3 m and H = 0.1 m.
- The yield stress is set to be 250×10^6 N/m^2 and 0.005 m deflection.
- The structure is meshed to have 38 ×12 finite elements while the ADD design variables have 19×6 elements.
- The finite element domain and the ADD or design variables grids are shown in Figure 4.
- The values of $\rho_i^{\min}$ and $\rho_i^{\max}$ are set to be 0.000001 m and 0.015 m respectively.

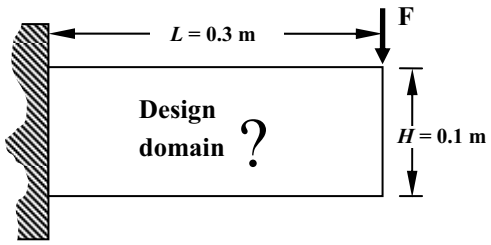

Figure 3. Design domain of a cantilever plate

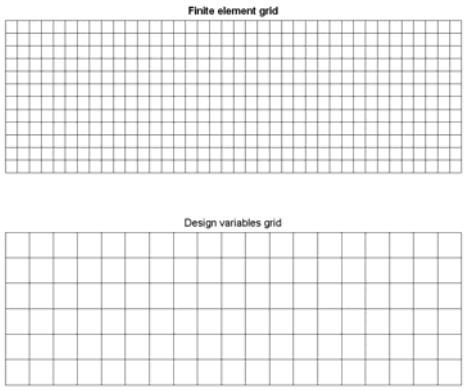

Figure 4. Finite element and design variable grids

5. Design Results

The effect of generation number and population size on the searching performance of MOPBIL is investigated. Note that the archive size is set to be100 for all simulation runs. Figure 5 shows the structural topologies of some selected non-dominated solutions where the number of generations is set to be 50 and the population size is 50. It can be observed that the obtained non-dominated front is still far from the real Pareto optimum front. The non-dominated topologies obtained from setting the iteration number as 50 with the population sizes of 100 and 150 are illustrated in Figures 6 and 7 respectively. The optimum topology obtained from using the solid isotropic material with penalisation (SIMP) approach and OCM [14] is illustrated in Figure 8. It can be seen that the bigger population size results in the better non-dominated front. However, the obtained results from running MOPBIL are still far from practicality compared to that obtained from OCM.

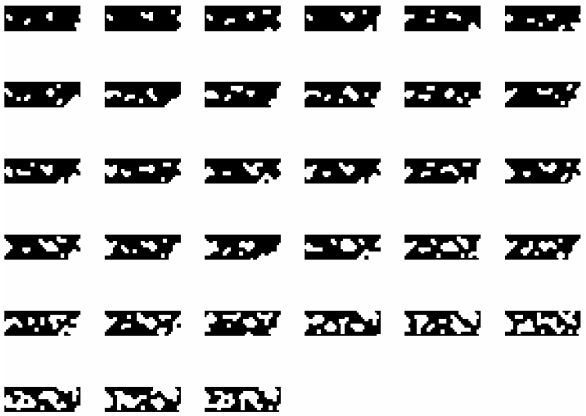

Figure 5. Topology results: 50 generations and 50 population size

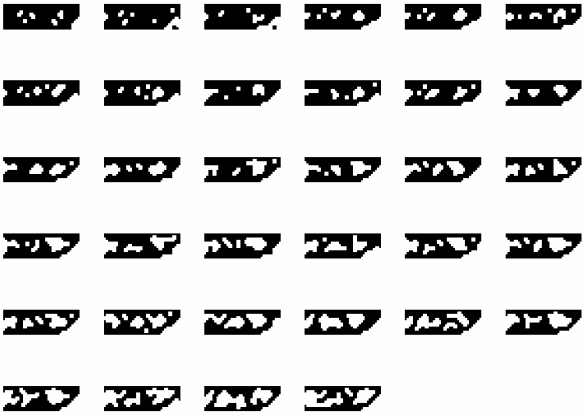

Figure 6. Topology results: 50 generations and 100 population size

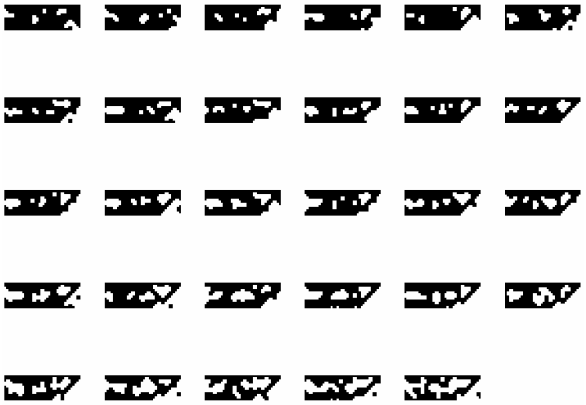

Figure 7. Topology results: 50 generations and 150 population size

Figure 8. Topology structure from OCM

Figure 9 displays the approximate Pareto front obtained from using MOPBIL where the population size is set to be 100 and the generation number is set to be 50, 100, 150, 200, 250 and 300. The non-dominated topologies from using the generation numbers of 50, 100, 150, 200,250 and 300 are displayed in Figures 10, 11, 12, 13, 14 and 15 respectively. It can be seen that, with the same population size, the larger number of generations leads to the better Pareto front. The results obtained from MOPBIL with more than 100 generations are said to be comparable to the topology obtained from using OCM. Nevertheless, it should be note that the topologies obtained from using MOPBIL and OCM are the design solutions the different optimisation problems.

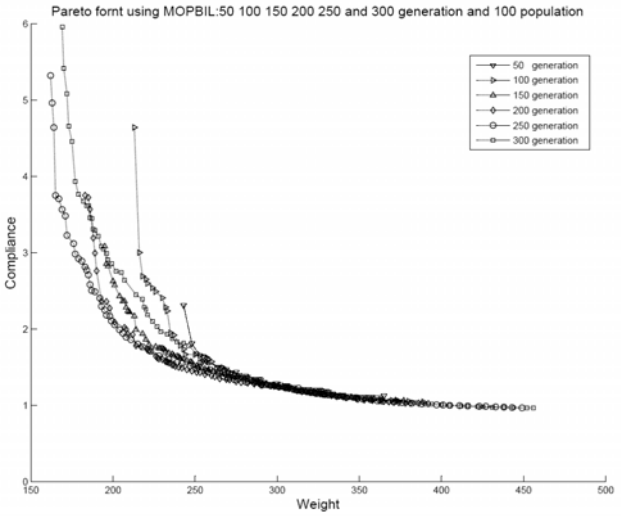

Figure 9. Pareto fronts at 50, 100, 150, 200, 250 and 300 generations with 100 population size

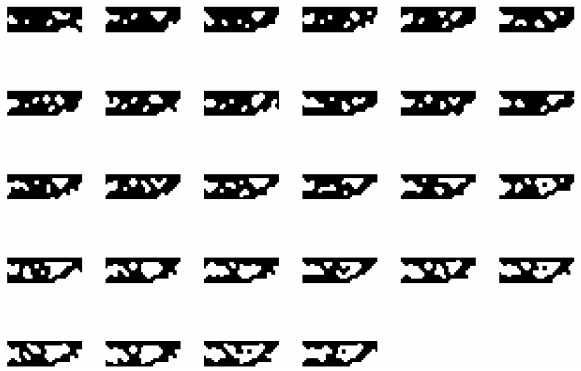

Figure 10. Topology results: 50 generations and 100 population size

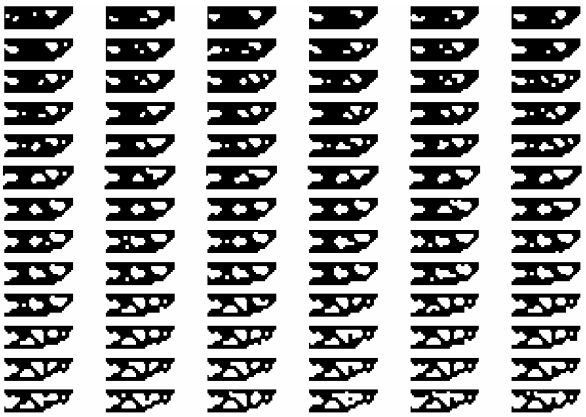

Figure 11. Topology results: 100 generations and 100 population size

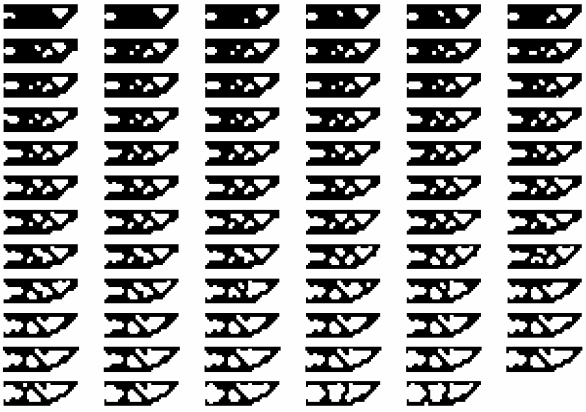

Figure 12. Topology results: 150 generations and 100 population size

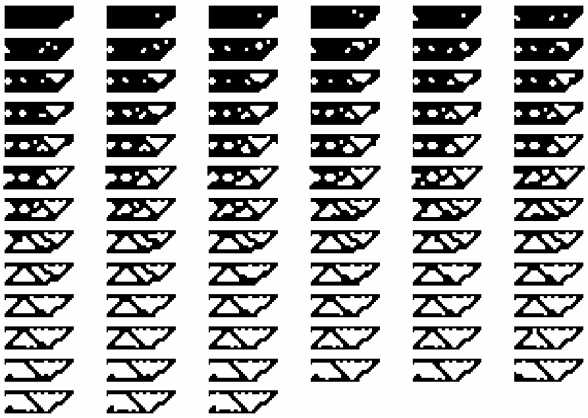

Figure 13. Topology results: 200 generations and 100 population size

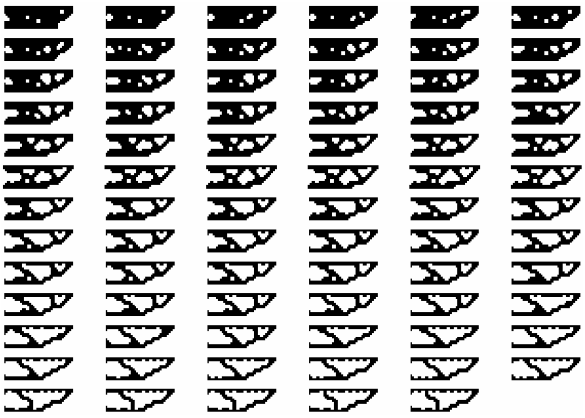

Figure 14. Topology results: 250 generations and 100 population size

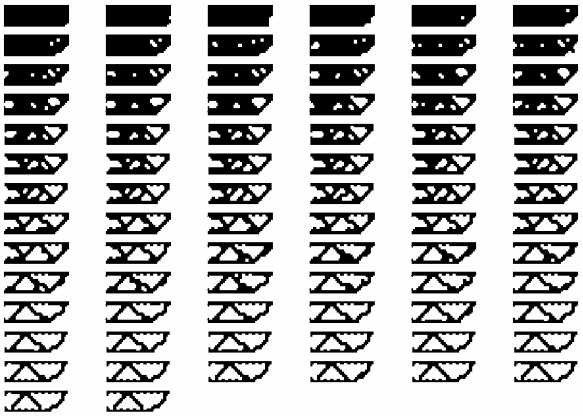

Figure 15. Topology results: 300 generations and 100 population size

The test in measuring the consistency of MOPBIL is made by running the optimisation method three times with the number of iterations being 250 and population sized 100. The approximate Pareto fronts from the three runs are plotted in Figure 16. The structural topologies corresponding to the fronts from the first, second and third runs are illustrated in Figures 17, 18 and 19 respectively. It can be observed that the MOPBIL search is somewhat inconsistent as we obtain three different Pareto fronts from three runs. All of the fronts however have reasonable and realisable topologies.

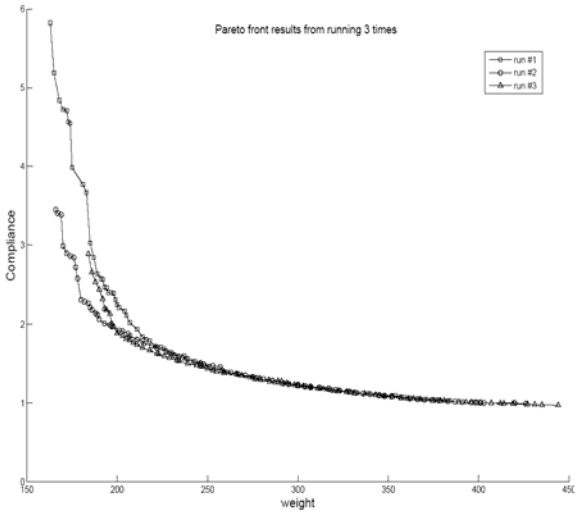

Figure 16. Pareto fronts from running MOPBIL 3 times

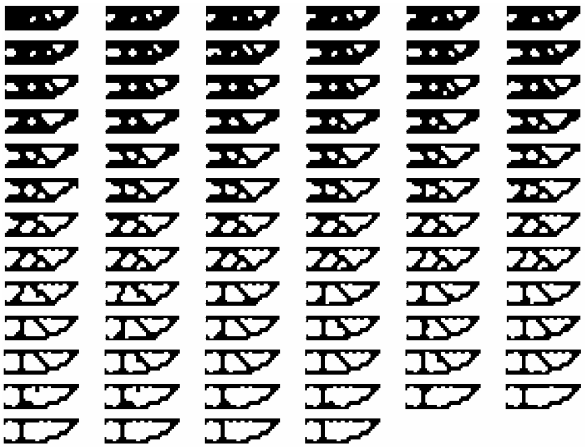

Figure 17. Results from the first running

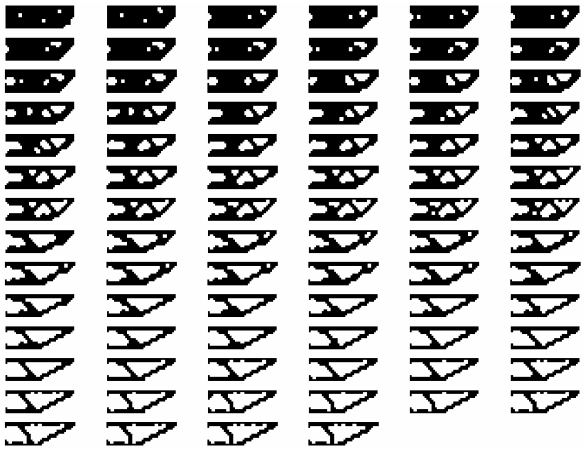

Figure 18. Results from the second running

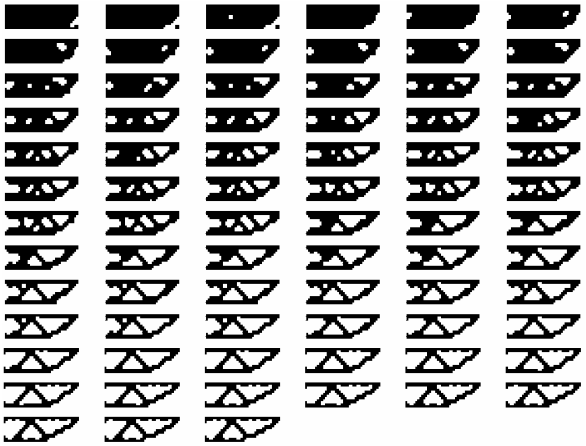

19 Results from the third running

From the results, it can be said that the effective conceptual design of a cantilever plate can be obtain by the use of MOPBIL. Pareto optimal solutions can be obtained within one optimisation run. The structures from using MOPBIL are almost ready to be manufactured since the safety constraints have been added to the design problem during the topology optimisation process.

6. Conclusions

The multiobjective optimisation problem of the topology design for cantilever plate is introduced. MOPBIL is implemented for solving the compliance and structural weight minimisation problem. The element stresses and system defection of the structure are used to the constraints where design variables represent a structural topology. The topology optimisation results of the structure show that MOPBIL is effective and powerful for this problem. Multiple structural topologies can be obtained within one optimisation run and the method can deal with an unconventional topology optimisation problem. However, it is considerably time-consuming compared to OCM. As a result, MOPBIL searching performance should be enhanced so that it can be used for the real-world applications.

Acknowledgments

This research was financially supported by Commission on Higher Education and the Faculty of Engineering, Khon Kaen University.

References

Journal

[1] Bureerat, S. and Limtragul, J. 2006. Performance Enhancement for Evolutionary Search for Structural Toplogy Optimisation. Finite Element in Analysis and Design, 42: 547-566.

[2] S. Bureerat and T. Kunakote. 2006. Topological design of structures using population-based optimisation methods. Inverse Problems in Science and Engineering, 14:589-607.

[3] Fujii D, Kikuchi N. Improvement of numerical instabilities in topology optimization using the SLP method. Structural and Multidisciplinary Optimization 2000; 19:113-121.

[4] Kane C, Schoenauer M. Topological optimum design using genetic algorithms. Control & Cybernetics 1996; 25:1059-1088.

[5] Madeiraa JA, Rodriguesa HC, Pina H. 2006 Multiobjective topology optimization of structures using genetic algorithms with chromosome repairing. Struct Multidisc Optim., 32:31–39.

[6] O. Simund. 2001. A 99 Line topology optimization code written in MATLAB. J. Struct. Multidiscip. Optim, 21:120–127.

[7] S. Bureerat and K. Sriworamas. 2007. Population-Based Incremental Learning for Multiobjective Optimisation. Advances in Soft Computing, 39:223-232.

[8] Wang SY, Tai K. 2004. Graph representation for structural topology optimization using genetic algorithms. Computers and Structures, 82:1609-1622.

Conference
[9] Bureerat, S., Kunakote T., and Limtragool, J. 2006. Structural Topology Optimization Using Design Variable Filtering. TISD2006, Khon Kaen, Thailand, January.
[10] Siwadol Kanyakam and Sujin Bureerat 2007 Passive Vibration Suppression of a Walking Tractor Handlebar Structure Using Multiobjective PBIL, CEC 2007, Singapore, pp. 4162-4169
[11] Kane C, Jouve F, Schoenauer M. Structural topology optimization in linear and nonlinear elasticity using genetic algorithms. 21st ASME Design Automatic Conf., Boston, 1995
[12] T. Kunakote and S. Bureerat. 2006. Topological Design of Structures with Stress Constraints. The 20th Conference of Mechanical Engineering Network of Thailand, October.
Book
[13] Baluja, S. 1994. Population-Based Incremental Learning: A Method for Integrating Genetic Search Based Function Optimization and Competitive Learning. CMU_CS_163.
[14] M.P. BensZe, O. Sigmund, 2003. Topology Optimization Theory, Method and Applications, Springer, Berlin, Heidelberg.